Dynamics of ataxin-1 in spinocerebellar ataxia type 1

Hilde A. G. Krol

voor mijn ouders

ISBN: 978-94-9037102-9

The studies described in this thesis were performed at the Department of Cell Biology and Histology of the Academic Medical Center, University of Amsterdam, The Netherlands.
The printing of this thesis was financially supported by the University of Amsterdam, J. E. Jurriaanse Stichting and Leica Microsystems.

Cover design, layout and production by Off Page

DYNAMICS OF ATAXIN-1 IN SPINOCEREBELLAR ATAXIA TYPE 1

ACADEMISCH PROEFSCHRIFT

ter verkrijging van de graad van doctor
aan de Universiteit van Amsterdam
op gezag van de Rector Magnificus
prof.dr. D.C. van den Boom
ten overstaan van een door het college voor promoties ingestelde
commissie, in het openbaar te verdedigen in de Agnietenkapel
op donderdag 10 september 2009, te 12:00 uur

door

Hilde Aagje Gerbrich Krol

geboren te Leeuwarden

Promotiecommissie:

Promotor:	Prof. dr. C.J.F. Van Noorden
Co-promotores:	Dr. E.A. Reits Dr. E.M. Hol
Overige leden:	Dr. J.A. Aten Prof. dr. F. Baas Prof. dr. H.H. Kampinga Prof. dr. H.P.H. Kremer Dr. P.J. Verschure Prof. dr. M. De Visser

Faculteit der Geneeskunde

Contents:

Chapter 1

General introduction

General introduction

Spinocerebellar ataxias

The spinocerebellar ataxias (SCAs) are diseases characterized by progressive neurodegeneration of the cerebellum. The clinical symptoms reflect cerebellar dysfunction, such as problems with the coordination of gait and movements of hands and eyes. Typically, a person with SCA remains cognitively intact, but progressively loose control over muscle movements (Soong and Paulson, 2006). To date, the SCAs are a group of 30 neurodegenerative disorders, that are caused by different types of autosomal dominant mutations in various genes such as coding polyglutamine (CAG) (polyQ) repeat expansions, non-coding (CTG, CAG) repeat expansions or missense or deletion mutations in the coding regions of SCA genes (Duenas et al., 2006). These mutations lead to dysfunction and degeneration of mainly the Purkinje cells in the cerebellum, although other brain areas can also be affected which may contribute to differences between the various SCA types.

The SCA genes play a role in a broad range of cellular processes. Recent studies that focused on the physiologic (wildtype) and pathogenic (mutant) functions of these genes led to the identification of some shared pathways underlying ataxia, such as dysfunctions in gene transcription, synaptic transmission and intracellular signaling pathways such as calcium or glutamate signaling (Carlson et al., 2008; Lim et al., 2006; Seeley et al., 2009). **The first question addressed in this thesis is how mutations in different proteins lead to a similar disease phenotype.** The common neuropathological and clinical characteristics imply that the biological pathways underlying SCAs are interconnected. Interactions have been found between some of the ataxia proteins (Lim et al., 2006), which strengthens the hypothesis that shared pathways underly ataxia. Understanding of these pathways will allow better understanding of the different mutated proteins that cause similar diseases. This will not only contribute to the understanding of SCAs and neurodegenerative disease in general but will also pave the way to the design of new effective therapies for SCAs. Currently, such therapies are not available.

This thesis focuses on ataxin-1 which is the protein mutated in SCA1, a relatively rare disorder with a prevalence of approximately 1-2 in 100,000 (Mittal et al., 2005). The disease becomes manifest around the 4th decade of life causing death within 15 years. The clinical symptoms of SCA1 vary depending on the length of the polyQ repeat and the stage of the disease. Besides ataxia, these symptoms include dysarthria and swallowing and breathing problems. SCA1 is caused by a CAG repeat expansion mutation in the SCA1 gene, resulting in an ataxin-1 protein with an extended polyQ stretch. This mutation is dominantly inherited and was first discovered in 1993 (Banfi et al., 1994; Chung et al., 1993; Orr et al., 1993; Quan et al., 1995; Ranum et al., 1994).

Therefore, the second question of this thesis is how does polyQ expansion in ataxin-1 induce SCA1? The third question is whether ataxin-1 accumulations present in SCA1 represent polyQ aggregates? It has been shown that the nuclear localization, and not the formation of nuclear inclusions is crucial for the pathogenesis (Cummings et al., 1999; Emamian et al., 2003; Klement et al., 1998). We show that both wildtype and

polyQ-expanded ataxin-1 form multiple nuclear inclusions *in vitro*, which are dynamic. The observed inclusions do not represent irreversible sequestered aggregates, but represent functional protein complexes with ataxin-1 as one of the components. Therefore, these inclusions should be redefined as nuclear bodies (Chapter 2; Krol et al., 2008).

The aim of this thesis is to unravel the effect of the polyQ expansion on the intracellular function of ataxin-1 and how this can lead to SCA1. Furthermore, we investigate whether there are common pathways for SCAs by studying interactions between SCA1 and SCA14. To address these questions, we applied advanced microscopy on cell models, and biochemistry and histology on mouse SCA1 material.

Outline of the thesis

In **chapter 2** of this thesis, we study the dynamics of ataxin-1 nuclear bodies in living cells and show that these structures are fundamentally different from polyQ aggregates. Subsequently, we investigate in **chapter 3** whether these nuclear bodies are also present *in vivo*, using a SCA1 mouse model. Furthermore, we investigated whether the localization and dynamics of three allegedly ataxin-1 interacting proteins, LANP, PQBP-1 and RBM17, are altered when they are co-expressed with mutant ataxin-1. In **chapter 4**, we search for a common pathway of ataxin-1 and PKCγ (the protein mutated in SCA14) by studying interactions between the two proteins. We also study the effects of PKCγ on ataxin-1 nuclear body formation and dynamics, and vice versa the effects of mutant ataxin-1 on the distribution of PKCγ in SCA1 mouse. In **chapter 5**, we discuss the different molecular and cellular levels at which mutant ataxin-1 can initiate toxicity. Here, we start in the nucleus and travel towards the cell periphery to discuss normal and toxic functions of ataxin-1 in each cellular compartment.

PolyQ proteins are being degraded by proteases like the proteasome. In the last part of this thesis, **chapter 6**, we mimic generation of polyQ fragments by the proteasome and examine whether these fragments are degradation-resistant and sufficient to initiate aggregation.

References

Banfi S, Servadio A, Chung MY, Kwiatkowski TJ Jr, McCall AE, Duvick LA, Shen Y, Roth EJ, Orr HT and Zoghbi HY (1994) Identification and characterization of the gene causing type 1 spinocerebellar ataxia. *Nat Genet* 7: 513-20.

Burright EN, Clark HB, Servadio A, Matilla T, Feddersen RM, Yunis WS, Duvick LA, Zoghbi HY and Orr HT (1995) SCA1 transgenic mice: a model for neurodegeneration caused by an expanded CAG trinucleotide repeat. *Cell* 82: 937-48.

Carlson KM, Melcher L, Lai S, Zoghbi HY, Brent Clark H and Orr HT (2008) Characterization of the Zebrafish atxn1/axh Gene Family. *J Neurogenet*, epub ahead of print.

Chung MY, Ranum LP, Duvick LA, Servadio A, Zoghbi HY and Orr HT (1993) Evidence for a mechanism predisposing to intergenerational CAG repeat instability in spinocerebellar ataxia type I. *Nat Genet* 5: 254-8.

Cummings CJ, Reinstein E, Sun Y, Antalffy B, Jiang Y, Ciechanover A, Orr HT, Beaudet AL and Zoghbi HY (1999) Mutation of the E6-AP ubiquitin ligase reduces nuclear inclusion frequency while accelerating polyglutamine-induced pathology in SCA1 mice. *Neuron* 24, 879-92.

Duenas AM, Goold R and Giunti P (2006) Molecular pathogenesis of spinocerebellar ataxias. *Brain* 129: 1357-70.

Emamian ES, Kaytor MD, Duvick LA, Zu T, Tousey SK, Zoghbi HY, Clark HB and Orr HT (2003) Serine 776

of ataxin-1 is critical for polyglutamine-induced disease in SCA1 transgenic mice. *Neuron* 38: 375-87.

Klement IA, Skinner PJ, Kaytor MD, Yi H, Hersch SM, Clark HB, Zoghbi HY and Orr HT (1998) Ataxin-1 nuclear localization and aggregation: role in polyglutamine-induced disease in SCA1 transgenic mice. *Cell* 95: 41-53.

Krol HA, Krawczyk PM, Bosch KS, Aten JA, Hol EM and Reits EA (2008). Polyglutamine expansion accelerates the dynamics of ataxin-1 and does not result in aggregate formation. *PLoS ONE* 3: e1503.

Lim J, Hao T, Shaw C, Patel AJ, Szabo G, Rual JF, Fisk CJ, Li N, Smolyar A, Hill DE et al. (2006) A protein-protein interaction network for human inherited ataxias and disorders of Purkinje cell degeneration. *Cell* 125: 801-14.

Matilla A, Roberson ED, Banfi S, Morales J, Armstrong DL, Burright EN, Orr HT, Sweatt JD, Zoghbi HY and Matzuk MM (1998). Mice lacking ataxin-1 display learning deficits and decreased hippocampal paired-pulse facilitation. *J Neurosci* 18: 5508-16.

Mittal U, Sharma S, Chopra R, Dheeraj K, Pal PK, Srivastava AK and Mukerji M (2005) Insights into the mutational history and prevalence of SCA1 in the Indian population through anchored polymorphisms. *Hum Genet* 118: 107-14.

Orr HT, Chung MY, Banfi S, Kwiatkowski TJ Jr, Servadio A, Beaudet AL, McCall AE, Duvick LA, Ranum LP and Zoghbi HY (1993) Expansion of an unstable trinucleotide CAG repeat in spinocerebellar ataxia type 1. *Nat Genet* 4: 221-6.

Quan F, Janas J and Popovich BW (1995) A novel CAG repeat configuration in the SCA1 gene: implications for the molecular diagnostics of spinocerebellar ataxia type 1. *Hum Mol Genet* 4: 2411-3.

Ranum LP, Chung MY, Banfi S, Bryer A, Schut LJ, Ramesar R, Duvick LA, McCall A, Subramony SH, Goldfarb L et al. (1994) Molecular and clinical correlations in spinocerebellar ataxia type I: evidence for familial effects on the age at onset. *Am J Hum Genet* 55: 244-52.

Seeley WW, Crawford RK, Zhou J, Miller BL and Greicius MD (2009) Neurodegenerative diseases target large-scale human brain networks. *Neuron* 62: 42-52.

Skinner PJ, Koshy BT, Cummings CJ, Klement IA, Helin K, Servadio A, Zoghbi HY and Orr HT (1997) Ataxin-1 with an expanded glutamine tract alters nuclear matrix-associated structures. *Nature* 389: 971-4.

Soong BW and Paulson HL (2007) Spinocerebellar ataxias: an update. *Curr Opin Neurol* 20: 438-46.

Chapter 2

Polyglutamine expansion accelerates the dynamics of ataxin-1 and does not result in aggregate formation

PLoS One. 2008 Jan 30; 3 (1): e 1503

Polyglutamine expansion accelerates the dynamics of ataxin-1 and does not result in aggregate formation

Hilde A Krol[1], Przemek M Krawczyk[1], Klazien S Bosch[1], Jacob A Aten[1], Elly M Hol[2] and Eric A Reits[1]*

[1] Department of Cell Biology and Histology, Academic Medical Centre, University of Amsterdam, The Netherlands; [2] Netherlands Institute for Neuroscience, an institute of the Royal Netherlands Academy of Arts and Sciences, Amsterdam, The Netherlands

* Corresponding author

Address of Correspondence: Eric Reits, PhD, Research Group Protein Degradation and Aggregation, M3-107 Department of Cell Biology and Histology, Academic Medical Center, University of Amsterdam, Meibergdreef 15, 1105 AZ Amsterdam, The Netherlands, tel: 0031 20 5666259, fax: 0031 20 6974156, email: e.a.reits@amc.uva.nl

Abstract

Background. Polyglutamine expansion disorders are caused by an expansion of the polyglutamine (polyQ) tract in the disease related protein, leading to severe neurodegeneration. All polyQ disorders are hallmarked by the presence of intracellular aggregates containing the expanded protein in affected neurons. The polyQ disorder SpinoCerebellar Ataxia 1 (SCA1) is caused by a polyQ-expansion in the ataxin-1 protein, which is thought to lead to nuclear aggregates. Methodology/Principal Findings. Using advanced live cell fluorescence microscopy and a filter retardation assay we show that nuclear accumulations formed by polyQ-expanded ataxin-1 do not resemble aggregates of other polyQ-expanded proteins. Instead of being static, insoluble aggregates, nuclear accumulations formed by the polyQ-expanded ataxin-1 showed enhanced intracellular kinetics as compared to wild-type ataxin-1. During mitosis, ataxin-1 accumulations redistributed equally among daughter cells, in contrast to polyQ aggregates. Interestingly, polyQ expansion did not affect the nuclear-cytoplasmic shuttling of ataxin-1 as proposed before. Conclusions/Significance. These results indicate that polyQ expansion does not necessarily lead to aggregate formation, and that the enhanced kinetics may affect the nuclear function of ataxin-1. The unexpected findings for a polyQ-expanded protein and their consequences for ongoing SCA1 research are discussed.

Introduction

Polyglutamine (polyQ) expansion disorders include diseases such as Huntington's disease (HD), dentatorubropallidoluysian atrophy (DRPLA), spinobulbar muscle atrophy (SBMA) and the spinocerebellar ataxias (SCA) type 1, 2, 3, 6, 7 and 17. These polyQ disorders are caused by an expansion of the CAG-trinucleotide repeat region in the

respective disease-related genes. Although the different polyQ proteins are widely expressed in cells throughout the brain, there is a high variability in the cell type loss in different brain areas. In most polyQ disorders the disease becomes manifested when the polyQ expansion exceeds 36-40 glutamines. The length of the polyQ expansion is inversely correlated with the age of onset of the disease. All polyQ disorders are dominantly inherited and the general concept is that the disease is caused by a toxic gain of function of the polyQ-expanded protein. Furthermore, commonly for all polyQ disorders, the affected cells show intracellular aggregates containing the polyQ-expanded protein. This aggregation is a result of the extended polyQ stretch in the proteins. It is still unclear whether the aggregates are toxic for cells, as a protective role has also been suggested [1-4].

SCA1 is a polyQ disorder caused by a glutamine expansion in the protein ataxin-1, which results in selective loss of Purkinje cells in the cerebellum, atrophy of specific brain stem neurons and extensive loss of motor neurons in the spinal cord [5]. Patients suffer from progressive loss of motor coordination, speech impairment and problems with swallowing. In healthy individuals the levels of ataxin-1 expression in the central nervous system is two to four-fold of that in peripheral tissues [6]. The function of ataxin-1 is still elusive. Wild-type ataxin-1 is a nuclear protein that can shuttle between the nucleus and the cytoplasm [7]. In the Purkinje cells and brain stem neurons, ataxin-1 is mainly present in the nucleus and only to some extent in the cytoplasm. This is in contrast with the localization of the protein in non-neuronal tissues, where ataxin-1 is mainly in the cytoplasm [6, 8-10]. This suggests that the nuclear localization of ataxin-1 in Purkinje cells may contribute to the selectivity of the disorder. Indeed, transgenic mice expressing polyQ-expanded ataxin-1 with a mutated nuclear localization signal did not develop the disease, demonstrating that nuclear localization is critical for the pathogenesis [3].

While the function of ataxin-1 is still elusive, it has been suggested that ataxin-1 is involved in gene expression regulation, as it can bind to RNA and interact with various transcription factors [11-16]. Ataxin-1 contains an AXH (Ataxin-1 and HMG-box protein 1) domain that has been shown to interact with other proteins and RNA and that has been implicated to play a role in transcriptional repression [12, 16-20]. In addition, ataxin-1 has a self associating region spanning the amino acids 570 to 605 of the wild-type protein. This region overlaps partly with the AXH domain [19]. The presence of nuclear aggregates in the cerebellum of SCA1 patients has led to the assumption that the polyQ-expansion causes ataxin-1 to misfold and form intranuclear aggregates. Not only may these aggregates lead to neuronal toxicity, polyQ-expansion may also alter the normal function of ataxin-1, or lead to the loss of nucleocytoplasmic shuttling ability. While aggregates composed of polyQ-expanded proteins are generally static structures comprised of tightly aggregated proteins, we state that this assumption needs to be reevaluated in the case of SCA1.

Here we show that the kinetics of nuclear polyQ-expanded ataxin-1 accumulations are very different from other polyQ proteins. Both wildtype (Atx1[Q2]GFP) and polyQ-expanded (Atx1[85Q]GFP) accumulations turned out to be soluble, whereas other polyQ-GFP aggregates form insoluble structures. In addition, mitotic cells redistributed the nuclear accumulations of polyQ-expanded ataxin-1 proteins to both daughter

cells, whereas 'true' polyQ aggregates were all trans-located to one daughter cell. In contrast to an earlier report [7], the polyQ-expansion did not affect shuttling of ataxin-1 between the nucleus and cytoplasm. Surprisingly, a longer polyQ-expansion led to an increase in speed of exchange of ataxin-1 between the nuclear accumulations and the free nuclear pool. In addition, we observed that the ataxin-1 accumulations were mobile and frequently fused with each other, and polyQ-expansion led to an increase in both mobility and fusion of the nuclear accumulations.

Results

PolyQ-expanded ataxin-1 does not form insoluble aggregates. PolyQ disorders show accumulation of polyQ-expanded proteins into a single cytoplasmic or nuclear aggregate. In agreement with data published previously [13, 21] our experiments demonstrated that ataxin-1 is mostly accumulating into multiple nuclear accumulations and this process is independent of the length of the polyQ expansion (Fig 1A). To compare the distribution and aggregate formation of ataxin-1 to a variety of different polyQ-expanded proteins we transfected Cos-7 cells with different polyQ proteins tagged with green fluorescent protein (GFP), to enable visualization in living cells. Cos-7 cells were chosen since they have a low expression level of endogenous ataxin-1 [8]. This minimizes interactions between the transfected ataxin-1 fusion proteins and the endogenous wild-type ataxin-1, thereby preventing any additional effect on the attaxin-1 aggregate formation. Next to the wildtype ataxin-1 (Atx1[2Q]GFP) and the polyQ-expanded ataxin-1 (Atx1[85Q]GFP), two disease-related polyQ-expanded fusion proteins were used, i.e. the truncated androgen receptor (AR[Q112]GFP) and huntingtin exon1 (Htt[Q103]GFP) which are both aggregation-prone (Fig 1A). We also expressed a pure polyQ-tract fused to GFP (Q65-GFP) and a polyQ-GFP fused to a nuclear localization signal (NLS[Q64]GFP). These fusion proteins are also aggregation-prone due to a similar polyQ-expansion. The NLS signal targets the protein to the nucleus, which mimics ataxin-1 polyQ localization. When cells were analyzed by Confocal Laser Scanning Microscopy, all polyQ-expanded proteins formed irregularly shaped intracellular aggregates within 24 hours after transfection, with exception of Atx1[85Q]GFP and Atx1[2Q]GFP which formed multiple nuclear accumulations (Fig 1A). The formation of multiple nuclear accumulations of Atx1[2Q]GFP has been described before [13, 21]. The distinct pattern of the formation of multiple nuclear accumulations is probably due to features of the ataxin-1 protein, since nuclear polyQ-expanded GFP (NLS[Q64]GFP) resulted in a single nuclear aggregate which increased in size in time due to sequestering of newly synthesized polyQ-GFP proteins, similar as observed with other polyQ-expanded proteins. This main difference between Atx1[85Q]GFP and NLS[Q64]GFP was maintained up to 72 hours after transfection.

As polyQ-protein aggregates form insoluble inclusions we examined whether the distinct difference in distribution between ataxin-1 and other polyQ proteins is also reflected by a difference in the solubility of the aggregates. By using a filter retardation assay, SDS-insoluble aggregates can be detected and quantified on a membrane while the remaining cell lysate passes through [22]. The solubility of both the Atx1[Q2]GFP and Atx1[85Q]GFP ataxin-1 was compared to NLS[Q64]GFP at three different time points after transfection (24, 48 and 72 hours, Fig 1B). At these timepoints most cells con-

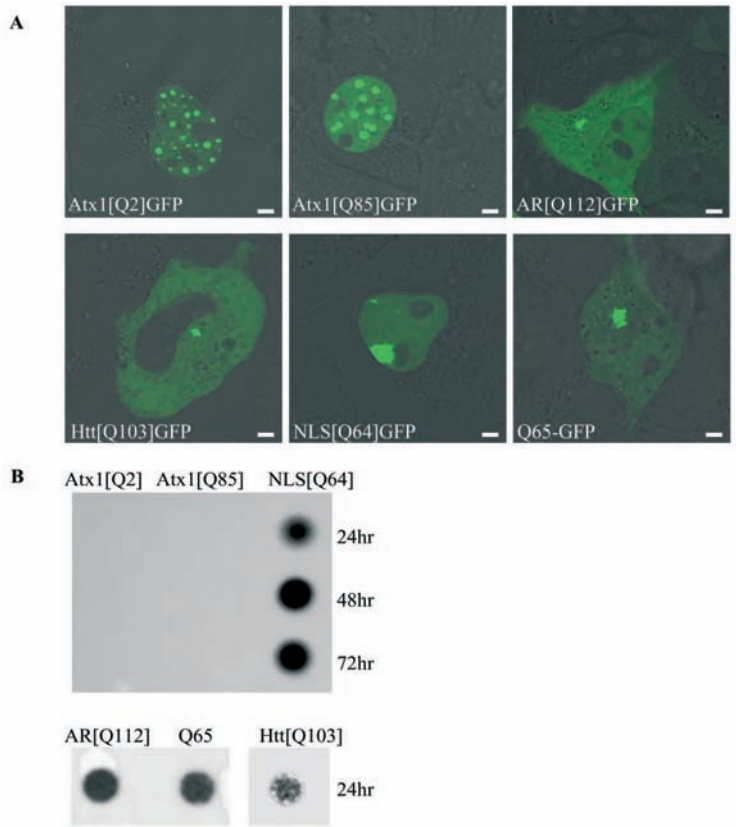

Figure 1. Nuclear ataxin-1 accumulations do not resemble aggregates formed by other disease-related polyglutamine-expanded proteins. **(A).** Live cell images of wild-type and polyQ-expanded ataxin-1 (Atx1[Q2]GFP and Atx1[Q85]GFP) and polyglutamine-expanded proteins androgen receptor (AR[Q112]GFP), huntingtin exon-1 (Htt[Q103]GFP), NLS[Q64]GFP and Q65-GPF in Cos7 cells. **(B).** Filtertrap assay of celllysates of Cos7 cells expressing Atx1[Q2]GFP, Atx1[Q85]GFP and NLS[Q64]GFP, 24, 48 and 72 hr after transfection (upper panel) and of Cos7 cells expressing AR[Q112]GFP, Q65-GFP and Htt[Q103]GFP 24 hours after transfection (lower panel). Sizebar = 1 μm.

tained both small and large accumulations of Atx1[2Q]GFP, Atx1[85Q]GFP and NLS[Q64]GFP. Aggregates formed by the truncated androgen receptor (AR[Q112]GFP), Q65-GFP and huntingtin exon-1 (Htt[Q103]GFP) were already present after 24 hours and also varied in size from small to large. Figure 1B clearly shows that the ataxin-1 accumulations are soluble, whereas all other polyQ aggregates were trapped on the filter. This suggests that nuclear accumulations consisting of polyQ-expanded ataxin-1 cannot be defined as aggregates, as ataxin-1 accumulations are soluble and not sequestered into a single aggregate as generally observed in polyQ disorders. Instead of calling them aggregates, the term nuclear accumulations will now be used for these soluble structures.

PolyQ expansion increases nuclear dynamics of ataxin-1. Since polyQ aggregates are generally static structures characterized by a low on/off rate of the aggregated proteins, we next examined whether the length of the polyQ-expansion would

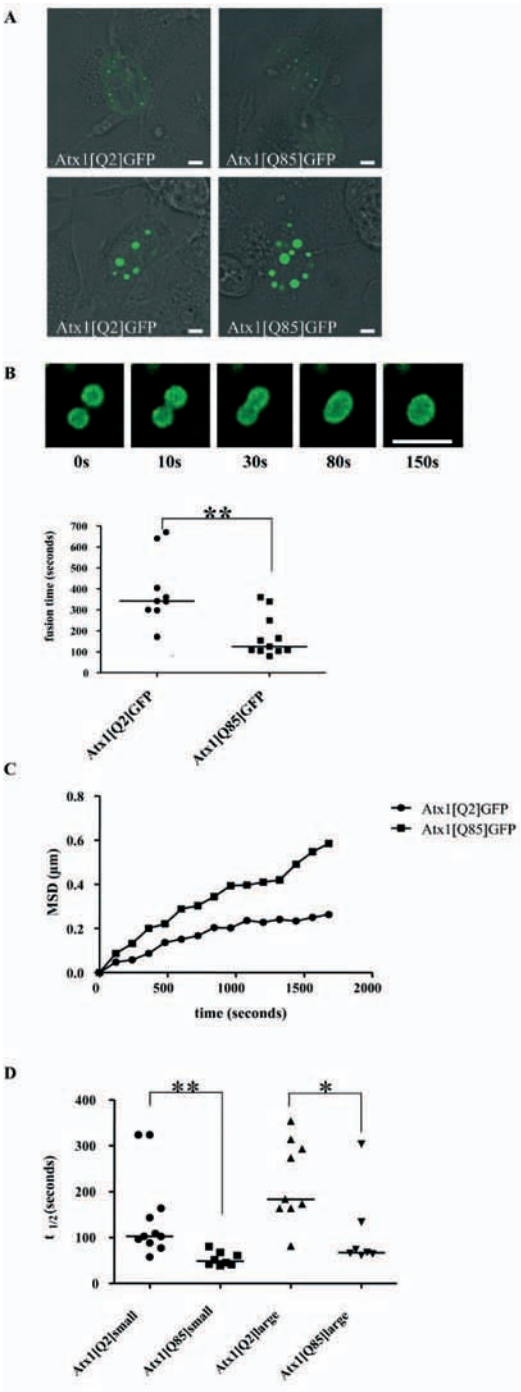

Figure 2. Polyglutamine expansion accelerates ataxin-1 dynamics. **(A).** Atx1[Q2]GFP and Atx1[Q85]GFP form similarly sized nuclear accumulations including small nuclear accumulations (upper panel) and large nuclear accumulations (lower panel). **(B)**. PolyQ expansion enhances ataxin-1 nuclear accumulation fusion speed. Pictures 1-5 show fusion of two Atx1[Q85]GFP nuclear accumulations within 150 seconds. The fusion speed of Atx1[85Q]GFP nuclear accumulations is faster than of similarly sized Atx1[Q2]GFP nuclear accumulations (lower panel, n = 9 resp. 11). Data have been tested non-parametrically (**P<0.005). **(C).** Increased mobility of Atx1[Q85]GFP over Atx1[Q2]GFP nuclear accumulations 24 hours after transfection. The Y-axis depicts the average mean square displacement (MSD) of 93 Atx1[Q2]GFP nuclear accumulations and 128 similarly sized Atx1[Q85]GFP nuclear accumulations. **(D).** Atx1[Q85]GFP nuclear accumulations have a higher on/off rate than Atx1[Q2]GFP nuclear accumulations. FRAP live cell experiments were performed 24 hr after transfection. Small and large nuclear accumulations have been analyzed separately. Half-time recovery data have been tested non-parametrically (**P< 0.005, *P<0.05). Sizebar = 1 μm.

affect the kinetics of the nuclear ataxin-1 accumulations. To compare the kinetics in a background of low endogenous ataxin-1 levels we transfected both Atx1[Q2]GFP and Atx1[Q85]GFP into Cos-7 cells and analyzed formed nuclear accumulations by confocal microscopy. Both Atx1[Q2]GFP and Atx1[Q85]GFP formed nuclear accumulations of various sizes, and we observed movement and fusion of all types of nuclear accumulations in time (Fig 2A, supplementary movie 1). We next investigated whether the polyQ length might affect the duration of the fusion in the cell nucleus by determining the time needed for a complete fusion event. Time-lapse imaging monitored the fusion process of similarly sized nuclear ataxin-1 accumulations. As shown in Figure 2B and Movie 1 in the supplementary material, the fusion of two nuclear Atx1[Q85]GFP accumulations is faster than of two similarly sized Atx1[Q2]GFP accumulations (p = 0.0019).

We analyzed respectively 9 and 11 fusion events for Atx1[Q2]GFP and Atx1[Q85]GFP in individual cells and we observed that the fusion of the nuclear Atx1[Q2]GFP accumulations was finished in a time between 172 and 670 seconds (median = 342 seconds) and of the Atx1[Q85]GFP accumulations between 80 and 340 seconds (median = 125 seconds). This suggests that the nuclear accumulations of Atx1[Q85]GFP are more dynamic then Atx1[Q2]GFP, and that polyQ expansion accelerates the fusion between nuclear ataxin-1 accumulations. In addition we studied whether the Atx1[Q2]GFP and Atx1[Q85]GFP accumulations have different mobilities in the nucleus. We compared the mobility of equally sized accumulations of Atx1[Q2]GFP or Atx1[Q85]GFP in the nucleus 24 hours after transfection. The mobility of 93 nuclear Atx1[Q2]GFP accumulations, measured in 12 individual cells, was compared to 128 Atx1[Q85]GFP accumulations in 16 individual cells. The mean square displacement of these accumulations has been calculated after each time point. The presence of a polyQ expansion resulted in an increased mobility of the nuclear accumulations in the nucleus (Fig 2C). The accelerated fusion speed and mobility of Atx1[Q85]GFP contrasts with the general view that polyQ aggregates are static, immobile structures composed of irreversibly trapped polyQ proteins.

To examine the on/off rate of nuclear ataxin-1 accumulations we performed Fluorescence Recovery after Photobleaching (FRAP) experiments to determine the exchange of ataxin-1 present between accumulations and the nuclear environment. Using FRAP, irreversible photobleaching leads to permanent loss of the fluorescence of the selected nuclear ataxin-1 accumulation, and fluorescence recovery can only occur when bleached ataxin-1 is replaced by fluorescent ataxin-1 from other nuclear accumulations or the free pool. The time needed for the recovery of fluorescence is therefore representative for the rate of exchange between the bleached nuclear accumulation, the surrounding Atx1-GFP fluorescent accumulations and the nuclear pool of Atx1-GFP. Surprisingly, when measuring the $t_{1/2}$ (which is the time point where the fluorescence has recovered to 50% of its original fluorescence intensity level), we found that fluorescence of the Atx1[Q85]GFP accumulations recovered much faster than Atx1[Q2]GFP (Fig 2D). In addition, we measured differences in the recovery of the small and large nuclear accumulations, since we anticipated that larger accumulations would show a lower exchange due to the reduction in surface/volume ratio. The $t_{1/2}$ of small Atx1[Q85]GFP accumulations (median = 48 seconds) was significantly lower than the $t_{1/2}$ of small Atx1[Q2]GFP accumulations (median = 102.4 seconds, $p = 0.001$), measured in respectively 8 and 11 bleaching experiments in individual cells. In addition, the $t_{1/2}$ of large Atx1[Q85]GFP accumulations (median = 67.2 seconds) was also significantly lower than Atx1[Q2]GFP accumulations (median = 183.6 seconds, $p = 0.013$), measured in respectively 7 and 9 experiments. We observed no difference in size between the immobile fractions of the nuclear accumulations formed by either Atx1[Q2]GFP or Atx1[Q85]GFP (data not shown). These data indicate that polyQ-expansion enhances the kinetics of ataxin-1, leading to less stable structures, which is also suggested by the accelerated fusion speed.

Nuclear ataxin-1 accumulations separate symmetrically during cell division. Cells containing polyglutamine aggregates are still able to enter mitosis [23] (and unpublished observation). Interestingly, when cells contained multiple aggregates, these

aggregates were always distributed to only one of the daughter cells, whereas the other daughter cell was free of any aggregate. We therefore examined whether polyQ-expanded ataxin-1 accumulations are also asymmetrically divided during mitosis, by following the nuclear accumulations in mitotic cells that expressed either Q65-GFP, Atx1[Q2]GFP or Atx1[Q85]GFP, using automated time-lapse fluorescence imaging. Indeed, mitotic cells containing multiple polyQ nuclear aggregates formed by Q65-GFP showed asymmetrical separation of aggregates to only one daughter cell (Fig 3A). In contrast, cells containing multiple nuclear accumulations formed by either Atx1[Q2]GFP or Atx1[Q85]GFP distributed ataxin-1 to both daughter cells, regardless of polyQ expansion (Fig 3B,C). Note that most nuclear accumulations fuse into large accumulations shortly before entering mitosis, while right after cell division, both daughter cells again contain multiple small nuclear accumulations.

PolyQ expansion does not affect ataxin-1 nuclear shuttling. As wild-type ataxin-1 can shuttle between the nucleus and the cytoplasm of a cell, it has been suggested that ataxin-1 is involved in RNA binding and transport to the cellular periphery [7]. This transport may be abolished in SCA1, as polyQ expansion hampers the nuclear export of ataxin-1 [7]. It should however be noted that in this study small wild-type ataxin-1 nuclear accumulations were compared to large polyQ-expanded ataxin-1 nuclear accumulations. As we showed that large accumulations of both polyQ-expanded Atx1[Q85]GFP and wildtype Atx1[Q2]GFP have a lower recovery rate when compared to small accumulations this might have limited the exit of free ataxin-1 from the nucleus. We also observed that Cos-7 cells expressing either Atx1[Q2]GFP or Atx1[Q85]GFP showed cytoplasmic presence of the protein, either diffuse or in body-like structures, independent of the length of the polyQ expansion (Fig 4A). The presence of cytoplasmic polyQ-expanded ataxin-1 is not limited to Cos-7 cells, as cultured neuroblastoma cells such as SH-SY5Y and N2A neuroblastoma cells (Fig 4A) as well as U343MG astrocytoma cells (data not shown) showed cytoplasmic presence and movement of ataxin-1 accumulations. The cytoplasmic presence may reflect the suggested role of ataxin-1 in RNA binding and shuttling to cytoplasmic domains [7]. To test whether polyQ-expansion limits the nuclear-cytoplasmic shuttling of ataxin-1, we performed a nucleocytoplasmic shuttling assay with Atx1[Q2]GFP and Atx1[Q85]GFP transfected in Cos-7 cells. To measure the nuclear shuttling, we performed FRAP analysis on cells containing two nuclei (bikaryons) by photobleaching all fluorescence except for one ataxin-1 nucleus and visualized the exchange and shuttling of GFP-tagged ataxin-1 by imaging the increase of fluorescence in the bleached nucleus. These experiments were performed in the presence of the translation inhibitor cycloheximide to prevent fluorescence recovery due to de novo synthesis of ataxin-1. We distinguished between cells having either only small or large nuclear ataxin-1 accumulations. Cells having only free nuclear ataxin-1 distribution or ataxin-1 present in small nuclear accumulations showed recovery of fluorescence in the bleached nucleus within 30 minutes after bleaching, independent of the length of a polyQ expansion (Fig 4B,C, upper panel). However, the bikaryons with large nuclear ataxin-1 accumulations did not show any recovery within this time span. This observation was independent of the length of the polyQ tract (Fig 4B,C lower panel). Taken together, these data show that the shuttling of ataxin-1 only occurs when

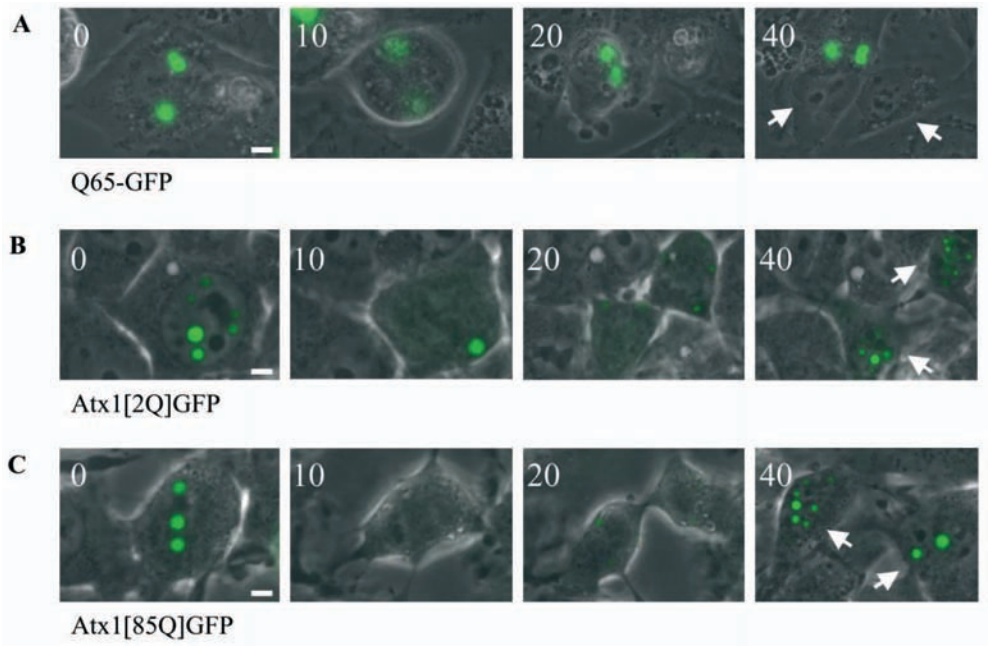

Figure 3. Nuclear ataxin-1 accumulations distribute symmetrically to daughter cells during cell division. Representative series of images showing cell division of a cell containing fluorescent aggregates or nuclear accumulations. **(A).** Asymmetric distribution of Q65-GFP aggregates in time. Arrows indicate the two daughter cells. **(B).** Symmetric distribution of Atx1[Q2]GFP nuclear accumulations during cell division. Nuclear accumulations fuse prior to division. After division both daughter cells contain cytoplasmic accumulations and later nuclear accumulations. **(C).** Symmetric distribution of Atx1[Q85]GFP nuclear accumulations during cell division. Time is indicated in minutes. Sizebar = 1 μm.

the protein is diffusely dispersed in the nucleoplasm or when the protein is present in small nuclear accumulations. More importantly, the ability of ataxin-1 to shuttle from the nucleus is not affected by the length of the polyQ expansion.

Discussion

PolyQ disorders are characterized by the presence of insoluble, intracellular aggregates initiated by the respective polyQ-expanded proteins, and these aggregates are also present when the polyQ expansion is fused to non disease-related proteins (e.g. Q65-GFP). Nuclear aggregates are present in neurons of several brain areas in transgenic mice expressing an expansion of 146 glutamines fused to a non disease-related protein [24]. While processes like autophagy may clear the cytoplasm from polyQ aggregates, the nucleus seems particularly sensitive since in all polyQ diseases the aggregates have been primarily found in the nuclei of patient material tissue [25]. It is therefore not surprising that SCA1 is often categorized as one of the polyQ disorders due to the presence of nuclear aggregates. However, various reports have shown that polyQ expansion is not the only domain which can induce ataxin-1 accumulation as the self associating region and two other domains seem to be involved

in ataxin-1 self-association [12,19]. Accordingly, wild-type ataxin-1 can also form similar nuclear structures, and deletion of the self associating region prevents nuclear accumulation of polyQ-expanded ataxin-1 in COS cells and transgenic mice [3,10]. This is in contradiction with findings showing that polyQ expansion leads to inclusion formation in SCA1.

We observed that nuclear polyQ-expanded ataxin-1 accumulations could not be detected by a filter retardation essay, whereas

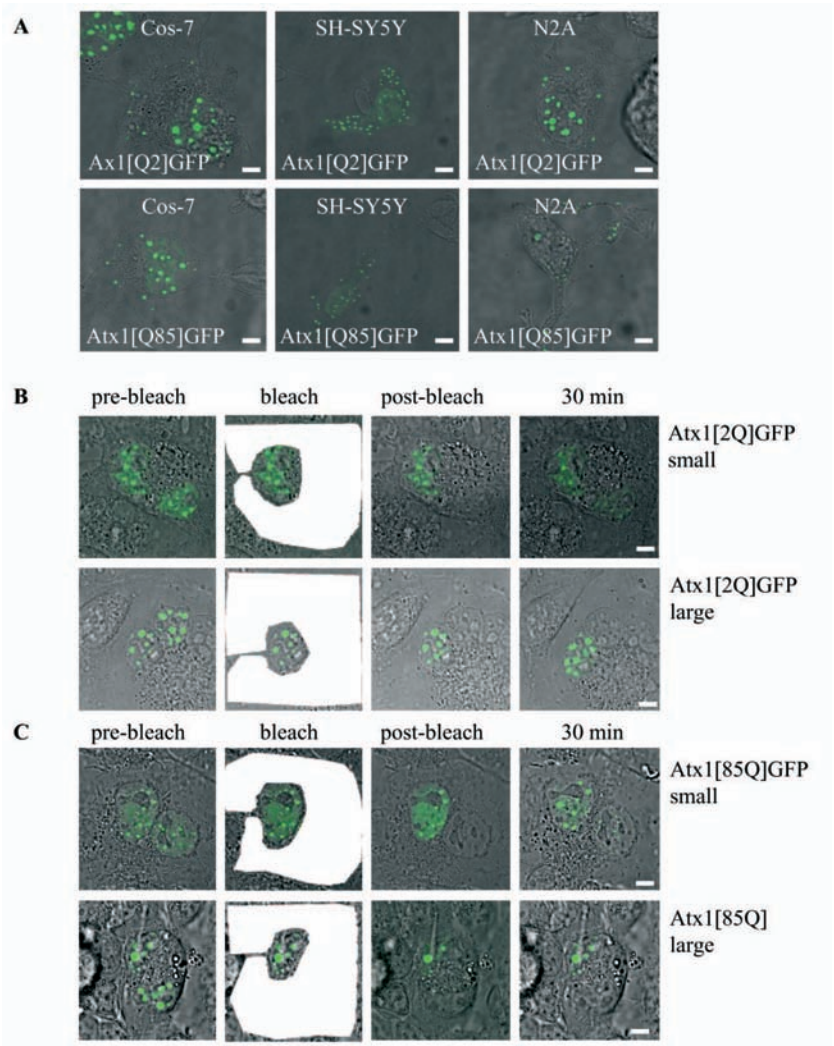

Figure 4. Polyglutamine expansion does not affect ataxin-1 shuttling between the nucleus and the cytoplasm. **(A).** Cos-7 cells and N2A and differentiated SH-SY5Y neuronal cells contain cytoplasmic accumulations of both Atx1[Q2]GFP and Atx1[Q85]GFP. **(B).** Representative nucleocytoplasmic shuttling assay in a Cos-7 bikaryon with small and large Atx1[Q2]GFP nuclear accumulations. Shuttling to the bleached nucleus is only observed when small nuclear accumulations are present. **(C)**. Atx1[Q85]GFP can shuttle between nucleus and cytoplasm when bikaryons of Cos-7 cell contain small nuclear accumulations. When large nuclear accumulations are present there is no nucleocytoplasmic shuttling of either Atx1[Q2]GFP or Atx1[Q85]GFP. The bleached region is indicated in white. Sizebar = 1 μm.

other polyglutamine aggregating proteins where clearly insoluble (including nuclear polyQ-GFP proteins). The non-static behavior of nuclear Atx1[Q85]GFP accumulations was also shown by their ability to move and fuse within the nucleus, with a surprising increase in the fusion speed and on/off rates as compared to wild-type nuclear ataxin-1 (Atx1[Q2]GFP) accumulations. The enhanced fusion could also result in a slightly higher amount of large nuclear accumulations in time in Atx1[Q85]GFP cells [21]. The enhanced on/off rate of polyQ-expanded ataxin-1 is different from earlier observations by Stenoien and colleagues, who showed that polyQ expansion of ataxin-1 leads to reduced exchange within nuclear accumulations [21]. Since ataxin-1 has been shown to associate with the nuclear matrix [8], structures incorporating polyQ-expanded ataxin-1 may be less stably associated with the matrix then the wild-type ataxin-1, which might in turn lead to an increase of their mobility. However the nuclear matrix is a structure that is not clearly defined and it might be more appropriate to suggest that ataxin-1 associates with the nuclear scaffold. It has been suggested that ataxin-1 is present in a transcription/RNA processing complex [7,18] whose functionality is lost upon transcription inhibition. An example is the known complex of ataxin-1, RORα, a transcription factor critical for cerebellar development, and tip60, a co-activator of RORα [26,27]. The polyglutamine expansion might not only affect the self-association of ataxin-1, but may also disturb the interaction with proteins such as RORα and tip60, resulting in alteration of transcriptional activity of several proteins and downregulation of important proteins [28]. The observed decrease in stable complex interactions of polyQ-expanded ataxin-1 containing nuclear accumulations might therefore affect its regulatory function.

Besides enhanced kinetics and solubility, a third major difference between polyQ-expanded ataxin-1 and other polyQ proteins was the separation of aggregates during cell division. Cells containing multiple polyQ aggregates are viable enough to enter mitosis, and by yet undefined mechanism all aggregates segregate into one daughter cell. While it is attractive to think that this might be a mechanism allowing separation of harmful proteins into one cell and leaving the other free of aggregates, it is of less importance for neurons, most of which are post-mitotic. In contrast to the asymmetrically dividing polyQ aggregates, nuclear polyQ ataxin-1 accumulations are redistributed equally among the daughter cells. They fuse into large accumulations prior to the actual M phase, and during the actual division the accumulations rapidly dissociate into a diffuse nuclear distribution. As the appearance of small accumulations can be observed soon after cell division, this mechanism may guarantee equal distribution of these proteins to both daughter cells. This phenomenon also occurs in case of specific cytoplasmic organelles but also the nucleoli (which also has a function in local transcription and RNA binding), resulting in equal redistribution to both daughter cells [29]. It also supports our model that nuclear accumulations formed by ataxin-1 resemble functional complexes and not aggregates. Therefore we suggest that ataxin-1 nuclear bodies should be a better definition than aggregates, inclusion bodies or accumulations.

Shortly after mitosis we observed a rapid re-formation of multiple ataxin-1 nuclear bodies that subsequently localize to the newly formed nucleus. The rapid ataxin-1 dynamics and redistribution underscores our hypothesis that polyQ-expanded atax-

in-1 is able to shuttle through the nuclear pore complex and is in contrast by findings from Irwin and collegues [7]. In this study the nucleocytoplasmic shuttling capability of wild type ataxin-1 in cells containing small nuclear bodies was compared with cells containing only large polyQ-expanded ataxin-1 nuclear bodies. Since the size of the nuclear bodies affects on/off ratios and therefore the amount of free ataxin-1, we compared similarly-sized nuclear bodies between Atx1[Q2]GFP and Atx1]Q85]GFP expressing cells. Interestingly, if only large nuclear bodies are present there is no nucleocytoplasmic shuttling of either ataxin-1 protein. In the case of free nucleoplasmic distribution or only small nuclear bodies, shuttling is not impaired by polyQ expansion. To unravel SCA1 disease it will be important to understand the nature of these nuclear bodies and to examine their composition and function in both the nucleus and cytoplasm But if the polyQ expansion does not induce aggregation or impair nuclear shuttling, what may be affected in SCA1? Ataxin-1 is involved in multiple pathways as suggested previously and each of these might contribute to SCA1 pathogenesis [26]. PolyQ-expanded ataxin-1 might play its role at the transcriptional level and alter the transcription of genes important for Purkinje cells [11,26,28]. In addition polyQ-expanded ataxin-1 could be involved in post-transcriptional processes such as mRNA splicing through its interaction with polyglutamine-tract-binding protein 1 (PQBP1) [14], a protein that has been shown to interact with the splicing factor SIPP1 [30]. PolyQ expansion of ataxin-1 also influences its binding to RNA [18] and in this manner could alter its suggested role in nucleocytoplasmic shuttling of mRNA [7], a process that is very important for local translation of proteins in neurons.

Materials and Methods

DNA constructs. Q65-GFP was generated using Ub-M-GFP-Q65 as a template (kindly provided by Nico Dantuma, Stockholm, Sweden) using primers flanking the polyQ stretch (forward: CCGGAATTCACCATGGAGTACACACCTCCCGGCGCCAGTTT with EcoRI site and reverse: GGATCCCGGGCCCCTCCTGGGGCTAGTCTCTTGCTG with ApaI site) and subsequent ligation into EGFP-N3 vector (Clontech, Palo Alto, CA). Htt[Q103]GFP was kindly provided by Ron Kopito, Stanford, California. AR[Q112]GFP contains a truncated version of the androgen receptor tagged with GFP (kindly provided by Paul Taylor, Philadelphia, Pennsylvania). The NLS[Q64]GFP contains a nuclear localization signal (NLS) to target the protein to the nucleus (kindly provided by Itaru Toyoshima, Akita, Japan). Atx1Q2]GFP and Atx1[Q85]GFP contain full length ataxin-1 cloned into a pEGFP-C2 vector (kindly provided by Huda Zoghbi, Houston, Texas).

Cell culture and transfection. Cos7, SH-SY5Y and N2A cells were cultured in Dulbecco's Modified Eagle Medium (DMEM) supplemented with 10% fetal bovine serum and 5% penicillin (100U/ml), streptomycin (100mg/ml) and glutamine (100mg/ml). U343MG astrocytomas cells were cultured in DMEM (high glucose) and HAM F10 (1:1) supplemented with 10% fetal bovine serum, 5% penicillin and 100U/ml streptomycin. Cells were maintained at 37°C in an atmosphere of 5% CO_2. For live cell microscopy 0.2 x10^{-6} cells were plated on glass coverslips (24mm; Fisher Scientific, Germany) in a 6-well plate and transfected with DNA plasmids after 24 hours using Lipofectamine 2000 transfection reagent according to manufacturer's instructions (Invitrogen, The Netherlands) for Cos-7, N2A and U343MG astrocytoma cells. SH-SY5Y cells were transfected using dreamfect gold (OZ Biosciences, France). Retinoic acid (Sigma R 2625, final concentration 10μM) was added to the SH-SY5Y culture medium for 3 days to differentiate them. For fixation 4% paraformaldehyde in PBS was used.

Filter retardation assay. Filter retarda-

tion assay was performed as described before [22]. Briefly, cell lysates were incubated for 30 minutes on ice and centrifuged at 14,000 rpm for 15 minutes at 4°C. Pellets containing the insoluble material and aggregates were resuspended in benzonase buffer (1mM $MgCl_2$, 50mM Tris-HCl; pH 8.0) and incubated for 1 hour at 37°C with 1µl benzonase (100,000 units/vial (Merck; Darmstadt, Germany). Incubations were terminated by adding 100µl 2x termination buffer (40mM EDTA, 4% SDS, 100mM DTT). Equal amounts of protein extracts were diluted in 200µl 2% SDS and filtered on a dot-blot filtration unit through a cellulose acetate membrane (Schleicher and Schuell, 0.2-µm pore size) that has been pre-equilibrated with 2% SDS. Filters were washed twice with 200µl 0.1%SDS and GFP fluorescence was measured by using the LAS-3000 (Fujifilm).

Confocal laser scanning microscopy (CLSM) and fluorescence recovery after photobleaching (FRAP) analysis. Transfected cells were categorized by the size of the nuclear accumulations: small (≤1µm diameter) and large (≥2.5µm size). FRAP analysis was performed using a Leica Sp2 CLSM adapted for living cell analysis using a 63x oil immersion objective. A selected ataxin-1 accumulation was repeatedly bleached in 10 frames at maximum laser power, resulting in a reduction of fluorescence to less than 10% of the initial value. Fluorescence recovery was measured by time-lapse imaging for 10 minutes post bleaching. Intranuclear mobility of the nuclear accumulations in time was corrected for overall movement of the nucleus by a custom-written software based on Matlab (Mathworks, Inc., USA) DipImage and IterativeClosest Point algorithm [31].

Nucleocytoplasmic transport assay. Cells were incubated with cycloheximide (final concentration 200 mM) for 15 minutes prior to cell fusion, which was performed by washing the cells with PBS, incubating them in 50% (w/v) polyethylene glycol 1500 (Roche Molecular Biochemicals) for 2 min, and rinsing with PBS. Cells were then incubated for 20 minutes in the cell culture medium containing 100µg/ml cycloheximide before analysis by CLSM. During the experiment the cells were incubated in the same cell culture medium including cycloheximide. FRAP was performed on a laser scanning confocal microscope (Leica Sp2 CLSM) by photobleaching a region surrounding the bikaryon but one nucleus. Recovery of fluorescence in the bleached nucleus was monitored in time and compared to the fluorescence intensity of the second nucleus in the bikaryon.

Life cell imaging. Time lapse movies were performed using a Leica (DM-IRBE) inverted microscope and a 63x oil immersion objective enclosed in a 37°C incubator with atmosphere of 5% CO_2. Images were created using a GFP filter set (Leica c1) for GFP excitation. For the analysis of accumulation behavior during cell division fluorescent and phase contrast images have been taken every 10 minutes. For the analysis of accumulation mobility, 3-D, time-lapse movies of nuclear ataxin-1 accumulations, acquired every 2 min have been deconvolved and corrected for cell mobility during the experiment. Next, mean squared displacement (MSD) of the nuclear accumulations during 30 minutes was calculated. For the analysis of accumulation fusion, 2-D images were acquired every 2 seconds. Fusion was calculated as a time between touching of two fusing nuclear accumulations and rounding of the resulting accumulation.

Abbreviation list

Atx1: Ataxin-1
FRAP: Fluorescent recovery after photobleaching
PC: Purkinje cell
PolyQ: Poly glutamine
SCA: Spinocerebellar ataxia

Acknowledgements

We would like to thank Nico Dantuma, Ron Kopito, Paul Taylor, Itaru Toyoshima and Huda Zoghbi for providing us with constructs used in this research.

References

1. Slow EJ, Graham RK, Osmand AP, Devon RS, Lu G, et al. (2005) Absence of behavioral abnormalities and neurodegeneration *in vivo* despite widespread neuronal huntingtin inclusions. *Proc Natl Acad Sci USA* 102: 11402-7.
2. Cummings CJ, Reinstein E, Sun Y, Antalffy B, Jiang Y, et al. (1999) Mutation of the E6-AP ubiquitin ligase reduces nuclear inclusion frequency while accelerating polyglutamine-induced pathology in SCA1 mice. *Neuron* 24: 879-92.
3. Klement IA, Skinner PJ, Kaytor MD, Yi H, Hersch SM, et al. (1998) Ataxin-1 nuclear localization and aggregation: role in polyglutamine-induced disease in SCA1 transgenic mice. *Cell* 95: 41-53.
4. Saudou F, Finkbeiner S, Devys D, Greenberg ME (1998) Huntingtin acts in the nucleus to induce apoptosis but death does not correlate with the formation of intranuclear inclusions. *Cell* 95: 55-66.
5. Robitaille Y, Schut L, Kish SJ (1995) Structural and immunocytochemical features of olivopontocerebellar atrophy caused by the spinocerebellar ataxia type 1 (SCA-1) mutation define a unique phenotype. *Acta Neuropathol* 90: 572-81.
6. Servadio A, Koshy B, Armstrong D, Antalffy B, Orr HT, et al. (1995) Expression analysis of the ataxin-1 protein in tissues from normal and spinocerebellar ataxia type 1 individuals. *Nat Genet* 10: 94-98.
7. Irwin S, Vandelft M, Pinchev D, Howell JL, Graczyk J, et al. (2005) RNA association and nucleocytoplasmic shuttling by ataxin-1. *J Cell Sci* 118: 233-42.
8. Skinner PJ, Koshy BT, Cummings CJ, Klement IA, Helin K, et al. (1997) Ataxin-1 with an expanded glutamine tract alters nuclear matrix-associated structures. *Nature* 389: 971-74.
9. Cummings CJ, Mancini MA, Antalffy B, DeFranco DB, Orr HT, et al. (1998) Chaperone suppression of aggregation and altered subcellular proteasome localization imply protein misfolding in SCA1. *Nat Genet* 19: 148-154.
10. Koshy BT, Matilla A, Zoghbi HY (1998) Clues about the pathogenesis of SCA1: from biochemical and molecular studies of ataxin-1. In: *Genetic Instabilities and Hereditary Neurological disorders*. Wells RD, Warren ST (eds). Academic Press, San Diego, CA, pp 241-8.
11. Lam YC, Bowman AB, Jafar-Nejad P, Lim J, Richman R, et al. (2006) ATAXIN-1 interacts with the repressor Capicua in its native complex to cause SCA1 neuropathology. *Cell* 127: 1335-47.
12. Mizutani A, Wang L, Rajan H, Vig PJ, Alaynick WA, et al. (2005) Boat, an AXH domain protein, suppresses the cytotoxicity of mutant ataxin-1. *Embo J* 24: 3339-51.
13. Tsai CC, Kao HY, Mitzutani A, Banayo E, Rajan H, et al. (2004) Ataxin 1, a SCA1 neurodegenerative disorder protein, is functionally linked to the silencing mediator of retinoid and thyroid hormone receptors. *Proc Natl Acad Sci USA* 101: 4047-52.
14. Okazawa H, Rich T, Chang A, Lin X, Waragai M, et al. (2002) Interaction between mutant ataxin-1 and PQBP-1 affects transcription and cell death. *Neuron* 34: 701-13.
15. Matilla A, Koshy BT, Cummings CJ, Isobe T, Orr HT, et al. (1997) The cerebellar leucine-rich acidic nuclear protein interacts with ataxin-1. *Nature* 389: 974-8.
16. Tsuda H, Jafar-Nejad H, Patel AJ, Sun Y, Chen HK, et al. (2005) The AXH domain of Ataxin-1 mediates neurodegeneration through its interaction with Gfi-1/Senseless proteins. *Cell* 122: 633-44.
17. De Chiara C, Menon RP, Dal Piaz F, Calder L, Pastore A (2005) Polyglutamine is not all: the functional role of the AXH domain in the ataxin-1 protein. *J Mol Biol* 354: 883-93.
18. Yue S, Serra HG, Zoghbi HY, Orr HT (2001) The spinocerebellar ataxia type 1 protein, ataxin-1, has RNA-binding activity that is inversely affected by the length of its polyglutamine tract. *Hum Mol Genet* 10: 25-30.
19. Burright EN, Davidson JD, Duvick LA, Koshy B, Zoghbi HY, et al. (1997) Identification of a self-association region within the SCA1 gene product, ataxin-1. *Hum Mol Genet* 6: 513-8.
20. Matilla-Duenas A, Goold R, Giunti P (2008) Clinical, genetic, molecular, and pathophysiological insights into spinocerebellar ataxia type 1. *Cerebellum* 7:106-14.
21. Stenoien DL, Mielke M, Mancini MA (2002) Intranuclear ataxin1 inclusions contain both fast- and slow-exchanging components. *Nat Cell Biol* 4: 806-10.

22. Wanker EE, Scherzinger E, Heiser V, Sittler A, Eickhoff H, et al. (1999) Membrane filter assay for detection of amyloid-like polyglutamine-containing protein aggregates. *Methods Enzymol* 309: 375-86.

23. Rujano MA, Bosveld F, Salomons FA, Dijk F, van Waarde MA, et al. (2006) Polarised asymmetric inheritance of accumulated protein damage in higher eukaryotes. *PLoS Biol* 4: e417.

24. Ordway JM, Tallaksen-Greene S, Gutekunst CA, Bernstein EM, Cearley JA, et al. (1997) Ectopically expressed CAG repeats cause intranuclear inclusions and a progressive late onset neurological phenotype in the mouse. *Cell* 91: 753-63.

25. Cummings CJ, Zoghbi HY (2000) Trinucleotide repeats: mechanisms and pathophysiology. *Annu Rev Genomics Hum Genet* 1: 281-328.

26. Serra HG, Duvick L, Zu T, Carlson K, Stevens S, et al. (2006) RORalpha-mediated Purkinje cell development determines disease severity in adult SCA1 mice. *Cell* 127: 697-708.

27. Gold DA, Baek SH, Schork NJ, Rose DW, Larsen DD, et al. (2003) RORalpha coordinates reciprocal signaling in cerebellar development through sonic hedgehog and calcium-dependent pathways. *Neuron* 40: 1119-31.

28. Serra HG, Byam CE, Lande JD, Tousey SK, Zoghbi HY, et al. (2004) Gene profiling links SCA1 pathophysiology to glutamate signaling in Purkinje cells of transgenic mice. *Hum Mol Genet* 13: 2535-43.

29. Hobdy-Henderson KC, Hales CM, Lapierre LA, Cheney RE, Goldenring JR (2003) Dynamics of the apical plasma membrane recycling system during cell division. *Traffic* 4: 681-93.

30. Llorian M, Beullens M, Lesage B, Nicolaescu E, Beke L, et al. (2005) Nucleocytoplasmic shuttling of the splicing factor SIPP1. *J Biol Chem* 280: 38862-9.

Chapter 3

PolyQ expansion in ataxin-1 does not affect intracellular dynamics of ataxin-1-interacting proteins LANP, PQBP-1 or RBM17

Manuscript in preparation

PolyQ expansion in ataxin-1 does not affect intracellular dynamics of ataxin-1-interacting proteins LANP, PQBP-1 or RBM17

Hilde A Krol[1], Klazien S Bosch[1], Elly M Hol[2] and Eric A Reits[1]

[1] Department of Cell Biology and Histology, Academic Medical Center, University of Amsterdam, The Netherlands; [2] Netherlands Institute for Neuroscience, an institute of the Royal Netherlands Academy of Arts and Sciences, Amsterdam, The Netherlands

Abstract

Spinocerebellar ataxia type 1 (SCA1) is one of nine neurodegenerative disorders that are caused by a dominantly inherited polyglutamine (polyQ) repeat expansion in the disease-related protein ataxin-1. The exact function of ataxin-1 is unknown, but interacting proteins have been identified that point towards a function in transcriptional regulation or RNA metabolism. SCA1 differs from the other polyQ disorders since expression of polyQ-expanded, but also wildtype ataxin-1 results in formation of dynamic nuclear bodies instead of static intracellular aggregates. These nuclear bodies likely represent functional protein complexes rather than toxic nuclear aggregates. We showed previously that polyQ expansion in mutant ataxin-1 increases the dynamics of ataxin-1 suggesting that the polyQ repeat alters protein-protein interactions inside and between nuclear bodies. Here, we explored the dynamics of the nuclear proteins LANP, PQBP-1 and RBM17 that have been reported to interact with ataxin-1 in a polyQ-dependent fashion. We investigated whether these proteins are recruited into ataxin-1 nuclear bodies using life cell imaging, and studied the nuclear-cytoplasmic shuttling and intranuclear dynamics of these proteins. Despite the reported polyQ-dependency of interactions, none of the allegedly interacting proteins co-localized in ataxin-1 nuclear bodies, since we show that the dynamics of all three proteins were not or only marginally affected by the polyQ repeat length of ataxin-1.

Introduction

Polyglutamine (polyQ) expansion disorders is a group of disorders that includes nine different diseases such as Huntington's disease and the spinocerebellar ataxias (SCAs) type 1, 2, 3, 6, 7 and 17. The polyQ disorders have as a common molecular background the expansion of the CAG-trinucleotide repeat region in the respective disease-related genes. In the normal situation, the polyQ-rich region can be up to 36-40 amino acids long. The disease becomes manifest when the polyQ stretch exceeds this thresh-

old, with the length of the polyQ inversely related to the age of onset of the disease. SCA6 is an exception since a repeat of 20-33 amino acids is enough to trigger disease (Riess et al., 1997; Zhuchenko et al., 1997). However, sequences outside of the polyQ tract also play a critical role, which may explain the preferential loss of specific subsets of neurons by the different polyQ-expanded proteins (de Chiara et al., 2005; Orr, 2001).

SCA1 is a polyQ disorder that is caused by a glutamine expansion in the protein ataxin-1. This disease mainly affects Purkinje cells of the cerebellum although atrophy of specific brain stem neurons and extensive loss of motor neurons in the spinal cord have also been described (Robitaille et al., 1995). Patients suffer from clinical features including slurred speech, swallowing difficulty, spasticity, and cognitive impairments. A pathological hallmark of polyQ disorders is the presence of inclusion bodies containing the aggregated polyQ-expanded protein, components of the ubiquitin-proteasome system and chaperones (Cummings et al., 1998; Raspe et.al., 2009). However, a number of studies cast doubt on the assumption that inclusion bodies in SCA1 are pathogenic, as the nuclear localisation and not the formation of nuclear inclusions is crucial for disease-related pathology (Cummings et al., 1999; Emamian et al., 2003; Klement et al., 1998). Remarkably, both mutant and wild-type ataxin-1 proteins expressed in tissue culture models show multiple nuclear inclusions that are dynamic (Irwin et al., 2005; Stenoien et al., 2002). Therefore inclusions do not represent irreversible aggregates but represent protein complexes including ataxin-1 and should be defined as nuclear bodies (Krol et al., 2008). In addition, Purkinje cells of mice expressing ataxin-1 under a Purkinje cell-specific promoter showed similar nuclear bodies (Koshy B.T., 1998) suggesting that these accumulations do not represent polyQ aggregates.

We recently showed that the polyQ expansion increases the dynamics of ataxin-1, as the mutated ataxin-1 shows even a higher on/off rate with its surrounding ataxin-1 proteins than wildtype ataxin-1. Furthermore, mutant ataxin-1 nuclear bodies are more dynamic as these structures fuse faster and have a higher mobility within the nucleus (Krol et al., 2008). It was initially suggested that the polyQ expansion prevented nuclear-cytoplasmic shuttling of ataxin-1 (Irwin et al., 2005) but we showed recently that nuclear import and export is not affected by polyQ expansions (Krol et al., 2008). Since polyQ expansions did not induce aggregation, and also did not affect intracellular ataxin-1 localization, we reasoned that an alternative pathway leading to SCA1 might be due to altered protein-protein interactions between ataxin-1 and associating proteins. Indeed, several proteins are known to interact with ataxin-1 in a polyQ-dependent fashion. Therefore, we hypothesized that their intracellular dynamics and functions may be altered due to increased affinity with the polyQ-expanded ataxin-1. Many of these interacting proteins play a role in transcriptional regulation or RNA metabolism and processing such as polyglutamine binding protein 1(PQBP-1), leucine-rich acidic nuclear protein (LANP) and the RNA binding motif protein 17 (RBM17; also known as spf45). The interactions between these proteins and ataxin-1 is affected by the AXH domain (which is also important for interactions with RNA) as well as the phosphorylation status of ataxin-1. Phosphorylation of ataxin-1 at Ser776 is essential for both the interaction with other proteins and toxicity of the mutant ataxin-1, as prevention of phosphorylation of this resi-

due abolishes the toxicity of polyQ-expanded ataxin-1 (Emamian et al., 2003). In addition, phosphorylation of ataxin-1 at Ser776 aggravates interactions between ataxin-1 and 14-3-3 and RBM17 (Chen et al., 2003; Lim et al., 2008). Interactions of RBM17 and ataxin-1 also depend on the polyQ expansion as RBM17 ataxin-1 interactions are stronger when the polyQ expansion mutation is present (Lim et al., 2008). Similarly, the protein regions responsible for LANP-ataxin-1 interactions is dependent on the length of the polyQ expansion as well (Matilla et al., 1997; Mizutani et al., 2005), and PQBP-1 binds with an increased affinity to polyQ-expanded ataxin-1 (Okazawa et al., 2002). Interestingly, overexpression of PQBP-1 in cultured cells results in accumulation of nuclear bodies, reminiscent of the ataxin-1 nuclear bodies (Enokido et al., 2002; Okazawa et al., 2001; Waragai et al., 1999). Moreover, PQBP-1 and LANP but not RBM17 have previously been described to colocalize within ataxin-1 nuclear bodies (Matilla et al., 1997; Okazawa et al., 2002).

To study whether polyQ expansion of ataxin-1 affects localization and intracellular kinetics of ataxin-1-interacting proteins, we visualized the dynamics of LANP, PQBP-1 and RBM17 in living cells that express either wildtype or polyQ-expanded ataxin-1. Here, we show that polyQ expansion of ataxin-1 did not lead to recruitment of LANP, PQBP-1 and RBM17 into ataxin-1 containing nuclear bodies. Also no changes in the kinetics of these three interacting proteins were observed. Although both wildtype and mutant ataxin-1 form nuclear bodies in cultured cells and in Purkinje cells of mice overexpressing ataxin-1, none of the studied proteins colocalized with the ataxin-1 nuclear bodies, which is in contrast with the previously reported interactions between these proteins detected *in vitro*. We conclude that the localization and dynamics of ataxin-1-associating proteins are not affected by mutations in ataxin-1. Therefore, it is likely that the localization and dynamics of these proteins remains unaltered in SCA1.

Materials and Methods

DNA constructs. FLAG-Atx1[30Q], FLAG-Atx1[82Q], GFP-Atx1[2Q] and GFP-Atx1[85Q] were kindly provided by Dr. Huda Zoghbi (Houston, Texas, US). PQBP-1-GFP was kindly provided by Dr. Hitoshi Okazawa (Tokyo, Japan) and was constructed as described previously (Waragai et al., 2000). GFP-LANP was kindly provided by Dr. Kerstin Danker (Berlin, Germany) (Mutz et al., 2006) and GFP-RMB17 (also known as GFP-spf45) was kindly provided by Dr. Angus Lamond (Dundee, UK) (Neubauer et al., 1998).

Cell culture and transfection. COS7 cells were cultured in Dulbecco's Modified Eagle Medium supplemented with 10% fetal bovine serum and penicillin (100 U/ml), streptomycin (100 mg/ml) and glutamine (100 mg/ml). Cells were maintained at 37°C in an a humidified atmosphere of 5% CO2. For live cell microscopy, 2 x106 cells were plated on glass coverslips (24 mm; Fisher, Braunschweig, Germany) in a 6-well plate and transfected with DNA plasmids using Lipofectamine 2000 transfection reagent (Invitrogen, Carlsbad, CA) according to manufacturer's instructions at 24 after plating. A freshly-prepared solution containing 2% paraformaldehyde in phosphate-buffered saline (PBS) was used for fixation of the cells.

Confocal laser scanning microscopy (CLSM), fluorescence recovery after photobleaching (FRAP) and fluorescence loss in photobleaching (FLIP) analysis. Cells were transfected with FLAG-Atx1[30Q/82Q] in combination with either PQBP-1-GFP, GFP-LANP or GFP-RBM17 in a plasmid DNA ratio of 2:1 to ensure proper co-expression of ataxin-1. As a control GFP-LANP/PQBP-1-GFP/GFP-RBM17 were transfected with an empty vector in the same

plasmid DNA ratio. Cells transfected with PQBP-1-GFP were selected on the basis of nuclear and cytoplasmic fluorescence and the presence of nuclear bodies. GFP-LANP-, PQBP-1-GFP- and GFP-RBM17-transfected cells were selected on the basis of nuclear and cytoplasmic fluorescence. FRAP analysis was performed using an Sp2 CLSM adapted for live cell analysis using a 63x oil immersion objective (Leica, Mannheim, Germany). At 24 h after transfection PQBP-1-GFP-, GFP-RBM17- or GFP-LANP-expressing cells were rapidly photo-bleached in 4 frames at maximum laser power, resulting in a reduction of fluorescence to less than 10% of the initial level. Fluorescence recovery was measured by time-lapse imaging post bleaching until recovery.

For FLIP analysis, cells were selected on the basis of similar features. However, we made a distinction between cells that formed PQBP-1 nuclear bodies and cells that had PQBP-1 free in the nucleoplasm. Most of the cytoplasm was bleached in 50 frames at maximum laser power, while loss of fluorescence of the nuclear fraction was simultaneously measured. Since PQBP-1 forms nuclear bodies, we also studied the dynamics of a single nuclear body by performing FLIP analysis on PQBP-1 where the complete nucleus was bleached in 50 frames of 1.6 seconds at maximum laser power with exception of one selected PQBP-1 nuclear body.

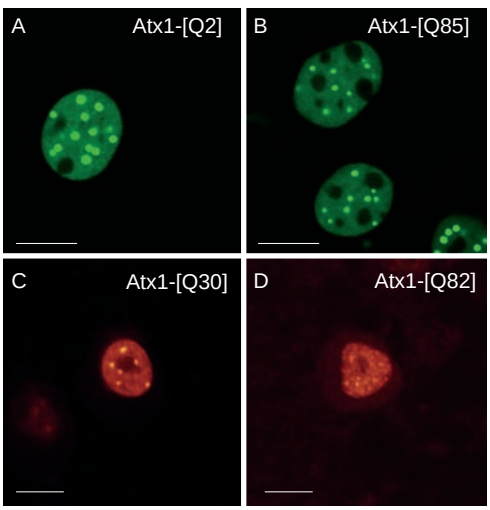

Figure 1. Ataxin-1 forms nuclear bodies both *in vitro* and *in vivo*. (**A, B**) Both GFP-Atx1[Q2] and GFP-Atx1[Q85] ataxin-1 form nuclear bodies when expressed in COS cells. (**C, D**) Purkinje cells expressing Atx1[Q30] form similar nuclear bodies as COS cells but cells expressing mutant Atx1[Q82] contain nuclear bodies that are diminished in size. Scale bar ~ 5 µm.

Immunocytochemical staining. Cells on coverslips were fixed in 2% paraformaldehyde in PBS for 15 min and were washed three times with PBS followed by permeabilisation in PBS containing 0.2% Triton-X100 for 30 min. Subsequently, cells were incubated in the presence of 5% fetal calf serum (FCS) in PBS for 1 h to block aspecific staining, washed three times in PBS and then incubated with an antibody against ataxin-1 (11750V; kindly provided by Dr. Huda Zoghbi, Houston, TX, in a dilution of 1:3500 in PBS) overnight at room temp. After washing three times with PBS, cells were incubated for 1 h with the secondary goat anti-rabbit Cy3 antibody (Jackson dilution 1:100 in PBS + 1% FCS) followed by washing three times in PBS. Cells were embedded in Vectashield (Vector, Burlingame, CA).

Brains of wildtype and mutant mice expressing respectively Atx1[Q30] and Atx1[Q82] under a Purkinje cell specific promoter were kindly provided by Dr. Harry Orr (University of Minnesota, Minneapolis, MA) (Burright et al., 1995). The brains of the sacrificed mice were frozen in liquid nitrogen, stored at -80°C. Sections (10 µm thick) were cut on a cryostat. Sections were mounted on glass slides, post-fixed in 4% buffered paraformaldehyde for 10 min and blocked in 10% normal goat serum and 0.4% Triton-X100 in 0.05 M phosphate buffer (pH 7.4) for 1 h at room temp. For immunostaining of the sections, we used a dilution of 1:8000 of the anti-ataxin-1 11750V antibody. Sections were incubated overnight at 4°C in PBS containing the primary antibody, 0.1% Triton and 1% FCS (pH 7.4) followed by an incubation in PBS containing the secondary goat anti-rabbit Cy3 (Jackson) in a dilution of 1:100 in PBS in the presence of 1% FCS for 60 min at room temp. Then, sections were washed in PBS and embedded in Vectashield.

Results

Ataxin-1 forms nuclear bodies both *in vivo* and *in vitro*. To examine whether kinetics and intracellular distribution of ataxin-1-interacting proteins are altered in SCA1, we first examined whether ataxin-1 distribution was altered upon polyQ expansion. While the formation of multiple nuclear ataxin-1 bodies has been described before (Krol et al., 2008; Stenoien et al., 2002; Tsai et al., 2004) these studies were performed in *in vitro* cell culture systems following overexpression of ataxin-1. To investigate whether ataxin-1 formed comparable nuclear bodies both in cell culture and in mouse neurons, we compared COS cells expressing ataxin-1 tagged with GFP with mouse cerebellum of SCA1 mice. These mice expressed either the human wildtype (Q30) or mutant (Q82) ataxin-1 protein driven by a Purkinje cell-specific promoter (Burright et al., 1995).

Upon expression of GFP-Atx1[Q2] or GFP-Atx1[Q82] in COS cells, nuclear bodies were present in both wildtype and polyQ-expanded ataxin-1-expressing cells (Fig. 1A,B). In both cases, ataxin-1 was also present diffusely throughout the nucleus. Similar ataxin-1 nuclear bodies were also present in Purkinje cells of SCA1 mice, especially in the Atx1[Q30] mice (Fig. 1C). Whereas the nuclear bodies in Atx1[Q30] mice closely

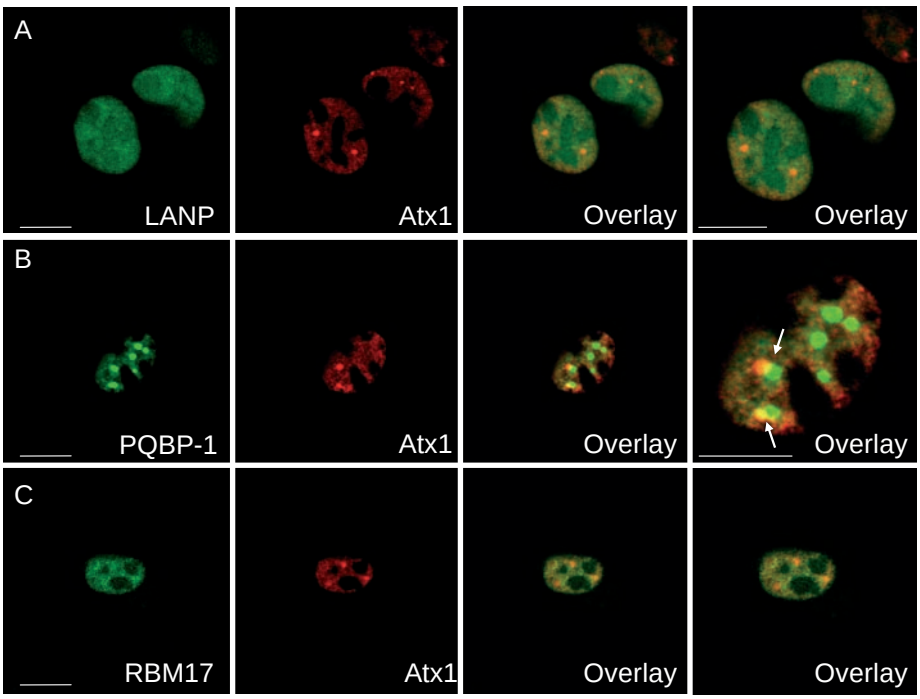

Figure 2. LANP, RBM17 and PQBP-1 do not colocalize with ataxin-1 nuclear bodies. COS cells transfected with GFP-tagged LANP, PQBP-1 or RBM17 (green) together with FLAG-tagged Atx1[Q30] (red) were analysed by CLSM. **(A).** LANP was predominantly localized in the nucleoplasm without colocalizing with ataxin-1 nuclear bodies. **(B)** PQBP-1 was present in similarly-sized nuclear bodies as ataxin-1 bodies, but the structures did not colocalize (arrows). **(C)** RBM17 is expressed throughout the nucleoplasm but does not colocalize with ataxin-1 nuclear bodies. Scale bar ~5 μm.

resembled the nuclear bodies in cell culture. The Atx1[Q82] mouse showed fewer neurons with nuclear bodies, and most structures seemed to be smaller in size (Fig. 1D). The nuclear staining of ataxin-1 in these Purkinje cells is strong compared to the cytoplasmic staining. It remains to be established why nuclear bodies were smaller in size in polyQ ataxin-1 mice, but the redistribution resembled ataxin-1 nuclear bodies that decrease in size upon transcription inhibition *in vitro* (unpublished observation; Irwin et al., 2005).

LANP, RBM17 and PQBP-1 are not recruited into ataxin-1 nuclear bodies. Several proteins have been described to interact with ataxin-1 on the basis of co-immunoprecipitation studies and yeast two-hybrid screens (Lim et al., 2006; Matilla-Duenas et al., 2008). For LANP, PQBP-1 and RMB17 it has also been suggested that the polyQ expansion in ataxin-1 alters the interactions with these proteins (Lim et al., 2008; Matilla-Duenas et al., 2008). For LANP, PQBP-1 and RMB17 it has also been suggested that the polyQ expansion in ataxin-1 alters the interactions with these proteins (Lim et al., 2008; Matilla et al., 1997; Okazawa et al., 2002). To examine whether these proteins interact and colocalize with ataxin-1 in nuclear bodies, we co-expressed FLAG-tagged Atx1[30Q/82Q] with PQBP-1-GFP, GFP-LANP or GFP-RBM17. After 24 h of expression, cells were fixed and immunostaining was performed to visualize FLAG-ataxin-1. In cells co-expressing ataxin-1 and LANP, we found that LANP was present in the nucleus and cytoplasm, but the protein did not colocalize in nuclear bodies induced by either wildtype or polyQ-expanded ataxin-1 (Figure 2 A), which is in contrast to previous observations (Matilla et al., 1997).

Since PQBP-1 can form nuclear bodies that are comparable to ataxin-1 nuclear bodies (Enokido et al., 2002; Okazawa et al., 2001; Waragai et al., 2000; Waragai et al., 1999), we expected PQBP-1 to colocalize with ataxin-1 nuclear bodies. We observed that both PQBP-1 and ataxin-1 formed nuclear bodies (Fig. 2B first and second panel). We did not observe any colocalization of PQBP-1 and ataxin-1 in the same nuclear structures (Fig. 2B, last panel) although some nuclear bodies were found closely together. Similar to LANP, RBM17 was distributed throughout the nucleoplasm and cytoplasm but it did not colocalize into nuclear bodies (Fig. 2C). This is in agreement with the results of Lim et al. (Lim et al., 2008), and suggests that the interaction between ataxin-1 and RBM17 may take place in the nucleoplasm. The distribution and colocalization studies of all these interacting proteins were not altered when polyQ-expanded ataxin-1(Q85) was co-expressed (data not shown). In summary, interactions between LANP, RBM17 or PQBP-1 and ataxin-1 do not take place in ataxin-1 nuclear bodies. The distribution and colocalization of these proteins with ataxin-1 were not affected by polyQ expanded ataxin-1.

Mutant ataxin-1 does not alter the intracellular dynamics of LANP, PQBP-1 or RBM17. LANP, PQBP-1 and RBM17 did not colocalize with ataxin-1 in the nuclear bodies. The previously described effects of ataxin-1 polyQ expansions on altered association with these proteins may also occur outside the nuclear bodies. We expected in that case that the polyQ expansion of ataxin-1 would alter the intracellular dynamics of these proteins, for example as a result of increased affinity for ataxin-1. All three proteins were found in both the nucleus and the cytoplasm, despite the fact that LANP and PQBP-1 have a nuclear localization signal (Opal et al., 2003; Waragai et al., 1999). To study altered dynamics of these proteins due

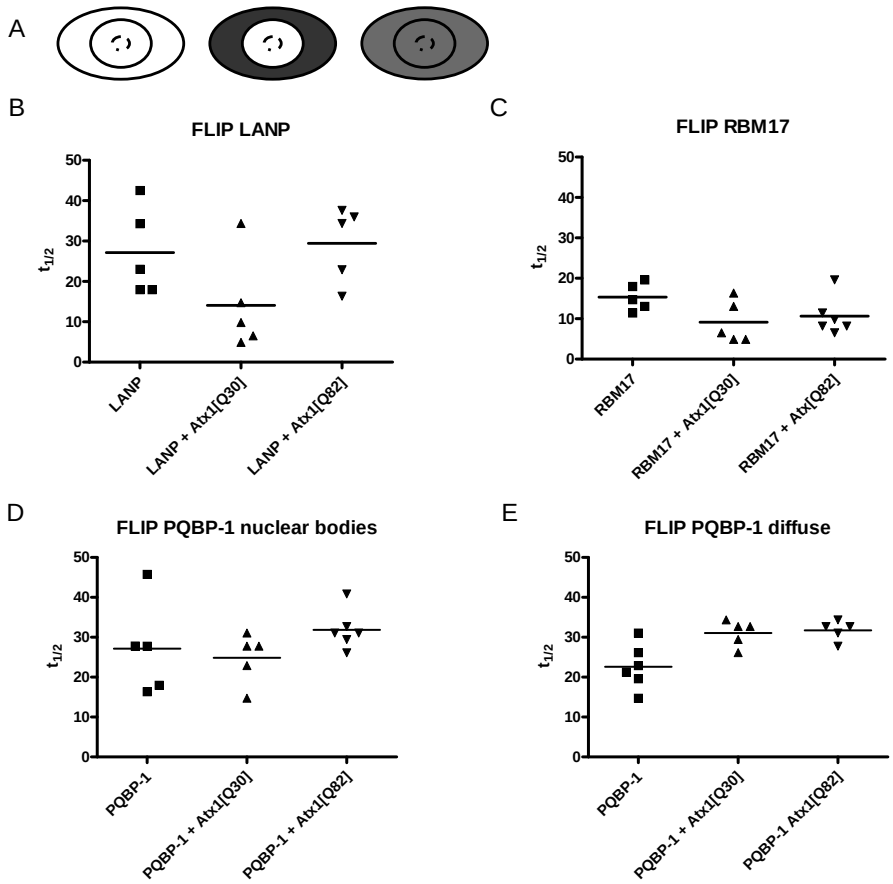

Figure 3. The nuclear-cytoplasmic shuttling dynamics of LANP and RBM17 are not affected by mutant ataxin-1. **(A)** Representation of a FLIP experiment, where the cytoplasm is repeatedly bleached and the speed of decrease of nuclear fluoresence is measured (determined by the $t_{1/2}$). White, fluorescence; dark, no fluorescence. FLIP data for LANP **(B)**, RBM17 **(C)**, cells having PQBP-1 mostly located in nuclear bodies **(D)**, and cells having PQBP-1 free in the nucleoplasm **(E)**. Every single dot is a single experiment. The y-axis represents the $t_{1/2}$ in seconds.

to the ataxin-1 polyQ expansion, we determined the rate of shuttling of these proteins between the nucleus and cytoplasm. An increased affinity of these proteins for polyQ-expanded ataxin-1 in the nucleus would lead to decreased nuclear-cytoplasmic shuttling. We performed a fluorescence loss in photobleaching (FLIP) assay by repeatedly photobleaching the cytoplasmic compartment, but not the nucleus (Fig. 3A). In case there is exchange between the compartments, fluorescence in the nucleus would drop upon bleaching of the cytoplasm, with the rate of nuclear fluorescence decreasing depending on the shuttling speed. We measured the $t_{1/2}$, which is the time point where half of the nuclear fluorescence was lost, using COS cells expressing either GFP-LANP, PQBP-1GFP or GFP-RBM17 together with wildtype or polyQ expanded FLAG-Atx1[Q30/Q82]. The shuttling capabilities of LANP were reduced by polyQ-expanded ataxin-1, since the $t_{1/2}$ was

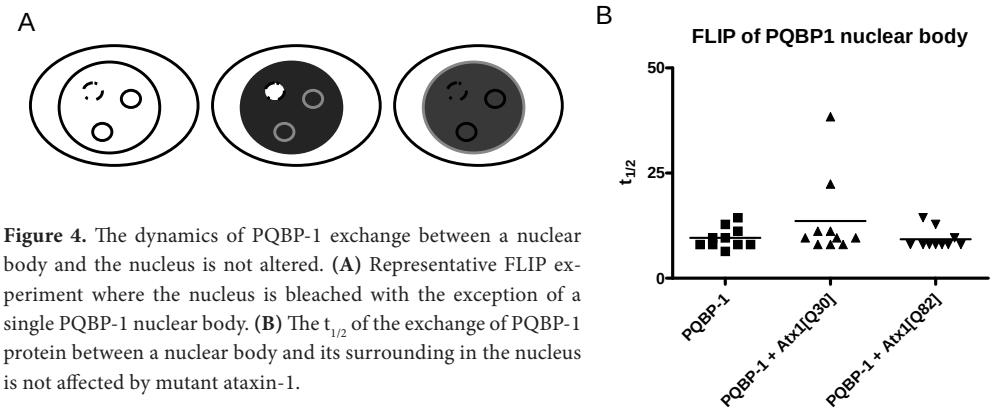

Figure 4. The dynamics of PQBP-1 exchange between a nuclear body and the nucleus is not altered. **(A)** Representative FLIP experiment where the nucleus is bleached with the exception of a single PQBP-1 nuclear body. **(B)** The $t_{1/2}$ of the exchange of PQBP-1 protein between a nuclear body and its surrounding in the nucleus is not affected by mutant ataxin-1.

increased when compared to wildtype ataxin-1 (Fig. 3B). Apparently, the increased affinity of LANP for polyQ-expanded ataxin-1 limited its shuttling rate between the cytoplasm and nucleus. In contrast, both RBM17 and PQBP-1 were not affected in their nuclear-cytoplasmic shuttling rates (Fig. 3C,D) indicating that the suspected interaction with mutant ataxin-1 did not affect the mobility of these proteins. Since PQBP-1 can form nuclear bodies, we performed FLIP assay experiments in cells with (Fig. 3D) and without (Fig. 3E) nuclear bodies. In both situations, fluorescence was measured in the nucleoplasmic pool. While there was a slight but non-significant increase in the $t_{1/2}$ when cells containing PQBP-1 bodies expressed mutant ataxin-1 (Fig3. D), cells expressing only free nucleoplasmic PQBP-1 did not show an effect of ataxin-1 polyQ expansion (Fig. 3E). To test whether the dynamics of a single PQBP-1 nuclear body was affected by the presence of wildtype or polyQ ataxin-1, we performed a similar FLIP experiment where the complete nucleus was bleached with the exception of a single fluorescent PQBP-1 nuclear body. In contrast to alterations in on/off rate in ataxin-1 nuclear bodies, the polyQ expansion of ataxin-1 did not affect the dynamics of a single PQBP-1 nuclear body (Fig. 4A,B).

Next, we performed FRAP experiments to determine whether the diffusion speed of the different proteins inside the nucleus was affected by ataxin-1 polyQ expansion, as interaction with polyQ-expanded ataxin-1 would lead to larger complexes and lower diffusion speed. A small region in the nucleus was bleached and the recovery of the bleached area was measured by determining the $t_{1/2}$ (which is the time point where the fluorescence was recovered for 50% of its original fluorescence intensity level). These FRAP experiments were performed under the same conditions as the FLIP experiments. Despite the earlier reports suggesting increased interactions with ataxin-1, the mobility of LANP, PQBP-1 and RBM17 in the nucleus was not affected by the polyQ expansion of ataxin-1 (data not shown). Therefore, we conclude that the polyQ-expansion of ataxin-1 does not affect nuclear dynamics of these interacting proteins.

Discussion

In the present study, we show that both wildtype and polyQ-expanded ataxin-1 form nuclear bodies not only *in vitro*, but also *in vivo*. This was shown by immunostaining of ataxin-1 in cerebellum of mice ex-

pressing wildtype or mutant ataxin-1 under a Purkinje-specific promoter. Surprisingly, overexpression of mutant ataxin-1 in mice even resulted in a diminished number of nuclear bodies in Purkinje cells. The apparent loss of these nuclear bodies are in line with our unpublished data using a transcription inhibitor, where cells expressing wildtype or mutant ataxin-1 showed rapid disappearance of nuclear bodies when transcription was blocked. If ataxin-1 nuclear bodies indeed represent transcriptional complexes or storage of transcription factors, loss of these structures in Purkinje cells of SCA1 mice indicate a state of dysfunction with a possible change in transcription. Whether this is causing Purkinje cell dysfunction or is the result of Purkinje cell dysfunction is unclear. The slow disappearance of nuclear bodies, however, may be directly related with down-regulation of the expression of certain genes that function in glutamate signaling (Lin et al., 2000).

The 3 ataxin-1-interacting proteins that we studied here were LANP, PQBP-1 and RBM17. They are all distinctly present in not only in the nucleus but also in the cytoplasm. LANP is a protein that is predominantly expressed in Purkinje cells (Matilla et al., 1997), the primary site of pathology in SCA1. It is a nuclear-cytoplasmic shuttling protein that has been implicated in the binding and shuttling of the RNA binding protein HuR (Gallouzi and Steitz, 2001). We showed that LANP is not recruited into ataxin-1 nuclear bodies, which is in contrast with earlier findings where ataxin-1 and LANP were found to be colocalized in nuclear bodies (Matilla et al., 1997). LANP and ataxin-1 appear to interact in the nucleoplasm as the nuclear-cytoplasmic shuttling capabilities of LANP were affected when ataxin-1 contained a polyQ-expanded tract. Future experiments should confirm whether LANP and ataxin-1 are perhaps interacting directly in small complexes outside the observed nuclear bodies.

No effect of polyQ expansion was observed when studying the interaction of RBM17 and ataxin-1. RBM17 was not present in ataxin-1 nuclear bodies as has been shown before (Lim et al., 2008). Since RBM17 is a RNA-binding protein involved in splicing, interaction with ataxin-1 may take place in the nucleoplasm. Similar to LANP, PQBP-1 is a protein that is highly expressed in brain regions susceptible to SCA1 mutations (Waragai et al., 1999). In a mouse model where PQBP-1 was overexpressed, a late onset of motorneuron disease and neuronal loss of regions that are also affected in SCA was observed (Okuda et al., 2003), suggesting that PQBP-1 is involved in the selective degeneration as a consequence of SCA1. We found that PQBP-1 forms nuclear bodies that are similar to ataxin-1 nuclear bodies but do not colocalize with ataxin-1 bodies.

We also studied whether mutant ataxin-1 affects the nuclear-cytoplasmic shuttling and nuclear dynamics of LANP, PQBP-1 and RBM17 and found that the dynamics were not affected, although there was a trend for both LANP and PQBP-1 that mutant ataxin-1 increased the dynamics of these proteins. The nuclear-cytoplasmic shuttling of RBM17 was not affected at all by the presence of mutant ataxin-1. So, in conclusion, mutant ataxin-1 affects the dynamics of the 3 proteins only marginally, if at all.

Previous studies reported that mutant ataxin-1 affects interactions with LANP, PQBP-1 and RMB17 (Lim et al., 2008; Matilla et al., 1997; Okazawa et al., 2002). For example, the amount of protein complexes in which RBM17 and ataxin-1 interact increased when compared to competing protein complexes containing Capicua and

ataxin-1 (Lim et al., 2008). Therefore, the dynamics of these proteins were expected to be affected, also because the polyQ mutation affects the dynamics of ataxin-1 itself (Krol et al., 2008). However, our current data show that both nuclear-cytoplasmic shuttling and nuclear dynamics of these proteins are not affected by mutant ataxin-1, raising doubt whether more RBM17 is retained in complexes together with ataxin-1. As the nuclear presence of mutant ataxin-1 is required to cause SCA1, it is likely that an interaction in this cellular compartment plays a role in toxicity, for example by altering transcription and splicing of specific genes. Still, we should also consider the cell body as a place where mutant ataxin-1 can induce toxicity, specifically since the Purkinje cells are the only neurons where ataxin-1 is present in the nucleus and cytoplasm (Koshy et al. , 1998) In the cytoplasm, ataxin-1 may alter transport of RNA and binding to mRNA or may interfere with translation of mRNA. In addition, ataxin-1 could alter the interaction or function of proteins highly or specifically expressed in Purkinje cells that is also present in nucleus and cytoplasm.

References

Burright EN, Clark HB, Servadio A, Matilla T, Feddersen RM, Yunis WS, Duvick LA, Zoghbi HY and Orr HT (1995) SCA1 transgenic mice: a model for neurodegeneration caused by an expanded CAG trinucleotide repeat. *Cell* 82: 937-48.

Chen HK, Fernandez-Funez P, Acevedo SF, Lam YC, Kaytor MD, Fernandez MH, Aitken A, Skoulakis EM, Orr HT, Botas J et al. (2003) Interaction of Akt-phosphorylated ataxin-1 with 14-3-3 mediates neurodegeneration in spinocerebellar ataxia type 1. *Cell* 113: 457-68.

Cummings CJ, Mancini MA, Antalffy B, DeFranco DB, Orr HT and Zoghbi HY (1998) Chaperone suppression of aggregation and altered subcellular proteasome localization imply protein misfolding in SCA1. *Nat Genet* 19: 148-54.

Cummings CJ, Reinstein E, Sun Y, Antalffy B, Jiang Y, Ciechanover A, Orr HT, Beaudet AL and Zoghbi HY (1999) Mutation of the E6-AP ubiquitin ligase reduces nuclear inclusion frequency while accelerating polyglutamine-induced pathology in SCA1 mice. *Neuron* 24: 879-92.

De Chiara C, Menon RP, Dal Piaz F, Calder L and Pastore A (2005) Polyglutamine is not all: the functional role of the AXH domain in the ataxin-1 protein. *J Mol Biol*. 354: 883-93.

Emamian ES, Kaytor MD, Duvick LA, Zu T, Tousey SK, Zoghbi HY, Clark HB and Orr HT (2003) Serine 776 of ataxin-1 is critical for polyglutamine-induced disease in SCA1 transgenic mice. *Neuron* 38: 375-87.

Enokido Y, Maruoka H, Hatanaka H, Kanazawa I and Okazawa H (2002) PQBP-1 increases vulnerability to low potassium stress and represses transcription in primary cerebellar neurons. *Biochem Biophys Res Commun* 294: 268-71.

Gallouzi IE and Steitz JA (2001) Delineation of mRNA export pathways by the use of cell-permeable peptides. *Science* 294: 1895-901.

Irwin S, Vandelft M, Pinchev D, Howell JL, Graczyk J, Orr HT and Truant R (2005) RNA association and nucleocytoplasmic shuttling by ataxin-1. *J Cell Sci* 118: 233-42.

Klement IA, Skinner PJ, Kaytor MD, Yi H, Hersch SM, Clark HB, Zoghbi HY and Orr HT (1998) Ataxin-1 nuclear localization and aggregation: role in polyglutamine-induced disease in SCA1 transgenic mice. *Cell* 95: 41-53.

Koshy BT, Matilla A, Zoghbi HY (1998) Clues about the pathogenesis of SCA1: from biochemical and molecular studies of ataxin-1. In: Genetic Instabilities and Hereditary Neurological disorders. Wells RD, Warren ST (eds). Academic Press, San Diego, CA, pp 241-8.

Krol HA, Krawczyk PM, Bosch KS, Aten JA, Hol EM and Reits EA (2008) Polyglutamine expansion accelerates the dynamics of ataxin-1 and does not result in aggregate formation. *PLoS ONE* 3: e1503.

Lim J, Hao T, Shaw C, Patel AJ, Szabo G, Rual JF, Fisk CJ,

Li N, Smolyar A, Hill DE, et al. (2006) A protein-protein interaction network for human inherited ataxias and disorders of Purkinje cell degeneration. *Cell* 125: 801-14.

Lim J, Crespo-Barreto J, Jafar-Nejad P, Bowman AB, Richman R, Hill DE, Orr HT and Zoghbi HY (2008) Opposing effects of polyglutamine expansion on native protein complexes contribute to SCA1. *Nature* 452: 713-8.

Lin X, Antalffy B, Kang D, Orr HT and Zoghbi HY (2000) Polyglutamine expansion down-regulates specific neuronal genes before pathologic changes in SCA1. *Nat Neurosci* 3: 157-63.

Matilla A, Koshy BT, Cummings CJ, Isobe T, Orr HT and Zoghbi HY (1997) The cerebellar leucine-rich acidic nuclear protein interacts with ataxin-1. *Nature* 389: 974-8.

Matilla-Duenas A, Goold R and Giunti P (2008) Clinical, genetic, molecular, and pathophysiological insights into spinocerebellar ataxia type 1. *Cerebellum* 7:106-14.

Mizutani A, Wang L, Rajan H, Vig PJ, Alaynick WA, Thaler JP and Tsai CC (2005) Boat, an AXH domain protein, suppresses the cytotoxicity of mutant ataxin-1. *Embo J* 24: 3339-51.

Mutz D, Weise C, Mechai N, Hofmann W, Horstkorte R, Bruning G and Danker K (2006) Integrin alpha-3beta1 interacts with I1PP2A/lanp and phosphatase PP1. *J Neurosci Res* 84: 1759-70.

Neubauer G, King A, Rappsilber J, Calvio C, Watson M, Ajuh P, Sleeman J, Lamond A and Mann M (1998) Mass spectrometry and EST-database searching allows characterization of the multi-protein spliceosome complex. *Nat Genet* 20: 46-50.

Okazawa H, Rich T, Chang A, Lin X, Waragai M, Kajikawa M, Enokido Y, Komuro A, Kato S, Shibata M, et al. (2002) Interaction between mutant ataxin-1 and PQBP-1 affects transcription and cell death. *Neuron* 34: 701-13.

Okazawa H, Sudol M and Rich T (2001) PQBP-1 (Np/PQ): a polyglutamine tract-binding and nuclear inclusion-forming protein. *Brain Res Bull* 56: 273-80.

Okuda T, Hattori H, Takeuchi S, Shimizu J, Ueda H, Palvimo JJ, Kanazawa I, Kawano H, Nakagawa M and Okazawa H (2003) PQBP-1 transgenic mice show a late-onset motor neuron disease-like phenotype. *Hum Mol Genet* 12: 711-25.

Opal P, Garcia JJ, Propst F, Matilla A, Orr HT and Zoghbi HY (2003) Mapmodulin/leucine-rich acidic nuclear protein binds the light chain of microtubule-associated protein 1B and modulates neuritogenesis. *J Biol Chem* 278: 34691-9.

Orr HT (2001) Beyond the Qs in the polyglutamine diseases. *Genes Dev* 15: 925-32.

Raspe M, Gillis J, Krol H, Krom S, Bosch K, Van Veen H and Reits E (2009) A novell cell-based tool that mimics proteasomal release of polyglutamine peptides. *J Cell Sci*: in press.

Riess O, Schols L, Bottger H, Nolte D, Vieira-Saecker AM, Schimming C, Kreuz F, Macek M Jr, Krebsova A, Macek MS, et al. (1997) SCA6 is caused by moderate CAG expansion in the alpha1A-voltage-dependent calcium channel gene. *Hum Mol Genet* 6: 1289-93.

Robitaille Y, Schut L and Kish SJ (1995) Structural and immunocytochemical features of olivopontocerebellar atrophy caused by the spinocerebellar ataxia type 1 (SCA-1) mutation define a unique phenotype. *Acta Neuropathol* 90: 572-81.

Stenoien DL, Mielke M and Mancini MA (2002) Intranuclear ataxin1 inclusions contain both fast- and slow-exchanging components. *Nat Cell Biol* 4: 806-10.

Tsai CC, Kao HY, Mitzutani A, Banayo E, Rajan H, McKeown M and Evans RM (2004) Ataxin 1, a SCA1 neurodegenerative disorder protein, is functionally linked to the silencing mediator of retinoid and thyroid hormone receptors. *Proc Natl Acad Sci USA* 101: 4047-52.

Waragai M, Junn E, Kajikawa M, Takeuchi S, Kanazawa I, Shibata M, Mouradian MM and Okazawa H (2000) PQBP-1/Npw38, a nuclear protein binding to the polyglutamine tract, interacts with U5-15kD/dim1p via the carboxyl-terminal domain. *Biochem Biophys Res Commun* 273: 592-5.

Waragai M, Lammers CH, Takeuchi S, Imafuku I, Udagawa Y, Kanazawa I, Kawabata M, Mouradian MM and Okazawa H (1999) PQBP-1, a novel polyglutamine tract-binding protein, inhibits transcription activation by Brn-2 and affects cell survival. *Hum Mol Genet* 8: 977-87.

Zhuchenko O, Bailey J, Bonnen P, Ashizawa , Stockton DW, Amos C, Dobyns WB, Subramony SH, Zoghbi HY and Lee CC (1997). Autosomal dominant cerebellar ataxia (SCA6) associated with small polyglutamine expansions in the alpha 1A-voltage-dependent calcium channel. *Nat Genet* 15: 62-9.

Chapter 4

Interaction of ataxin-1 and protein kinase Cγ mediates their phosphorylation and cellular localization status

Submitted for publication

Interaction of ataxin-1 and protein kinase Cγ mediates their phosphorylation and cellular localization status

Dineke S. Verbeek[1#*], Hilde A. Krol[2#], Edith van de Vijver[2], Klazien S. Bosch[2], Alicia Sanz[2], Elly M. Hol[3], Eric A. Reits[2*]

[1] Department of Genetics, University Medical Center Groningen, University of Groningen, The Netherlands; [2] Department of Cell Biology and Histology, Academic Medical Center, University of Amsterdam, The Netherlands; [3] Netherlands Institute for Neuroscience, an Institute of the Royal Netherlands Academy of Arts and Sciences, Amsterdam, The Netherlands

[#] Shared first author, * Corresponding authors

Address of correspondence: Eric Reits, PhD, Research Group Protein Degradation and Aggregation, M3-107, Department of Cell Biology and Histology, Academic Medical Center, University of Amsterdam, Meibergdreef 15, 1105 AZ Amsterdam, The Netherlands; tel: +31 20 5666259; fax: +31 20 6974156; email: d.s.verbeek@medgen.umcg.nl and e.a.reits@amc.uva.nl

Abstract

Spinocerebellar ataxias (SCAs) comprise a group of 30 neurodegenerative disorders caused by different types of mutations in various genes. Despite the genetic heterogeneity, the disease phenotypes show large overlap, as all subtypes are characterized by prominent loss of Purkinje cells. It is speculated that multiple SCA genes participate in common pathogenic pathways leading to neurodegeneration. Here, we studied whether the SCA1-related ataxin-1 and SCA14-related PKCγ proteins are functionally linked. Immunoprecipation experiments showed that ataxin-1 and PKCγ form complexes *in vitro* and *in vivo*. Furthermore, co-expression of ataxin-1 and PKCγ increased ataxin-1 phosphorylation levels, induced the formation of ataxin-1 nuclear bodies and increased their dynamics. Polyglutamine (polyQ)-expanded ataxin-1 also affected the localization and autophosphorylation levels of wildtype PKCγ *in vitro* and *in vivo*. We conclude that ataxin-1 and PKCγ indeed are functionally linked and our data point at a common biological pathway that underlies SCA1 and SCA14.

Keywords: Ataxin-1, PKCγ, spinocerebellar ataxia, Purkinje cell, phosphorylation, nuclear bodies

Introduction

Spinocerebellar ataxias (SCAs) comprise a group of 30 neurodegenerative disorders that share a majority of their clinical symptoms and neuropathological characteristics. The major feature is atrophy of the cerebellum with a prominent loss of Purkinje cells. In addition, other brain regions are affected such as the brainstem and spinal cord. This neurodegeneration leads to clinical symptoms including ataxia, dysarthria, and

oculomotor problems (Schols et al., 2004). The diseases manifest around midlife but the severity of the disease may vary between patients with identical SCA types or even between family members. SCA is a genetically heterogeneous disorder. Up to date, 15 different SCA genes have been identified, and an additionally 15 SCA loci have been mapped (Duenas et al., 2006). Intriguingly, the different SCAs can be caused by various mutational mechanisms such as coding polyQ (CAG) repeat expansions, non-coding (CTG, CAG) repeat expansions and missense or deletion mutations in the coding region of a SCA gene (Duenas et al., 2006). The fact that different SCA genes with diverse types of mutations show similar disease phenotypes and neurodegenerative features suggests that common underlying biological mechanisms or pathways are involved in the neuropathogenesis of these diseases.

SCA1 is caused by an expansion of the polyQ rich region in the protein ataxin-1. In the mutant ataxin-1 protein, the polyQ repeat numbers exceed the disease-inducing threshold of 36-40 glutamine residues. The resulting toxic gain of function leads to dysfunction and degeneration of Purkinje cells in the cerebellum, specific brain stem neurons, and loss of motoneurons in the spinal cord (Matilla-Duenas et al., 2008; Robitaille et al., 1995). Little is known about the precise function of ataxin-1 which complicates the understanding of the biology of the disease. Ataxin-1 can shuttle between the nucleus and cytoplasm of cells and interacts with RNA and proteins that are implicated in regulation of transcription and RNA binding and stability including capicua, RORα, RBM17 and pumilio-1 (Irwin et al., 2005; Krol et al., 2008; Lim et al., 2008; Lim et al., 2006; Serra et al., 2006; Yue et al., 2001). These data suggest that ataxin-1 may be involved in particular stages of transcription and/or translation, such as transcription regulation, mRNA nuclear export, mRNA stability and splicing. Ataxin-1 is predominantly localized in the nucleus of most neurons, but it is present in both nucleus and cytoplasm of Purkinje cells (Klement et al., 1999; Koshy et al., 1998). The sensitivity of Purkinje cells for mutated ataxin-1 may be caused by this difference in localization. On the other hand, nuclear localization of ataxin-1 seems to be critical for the pathogenesis of SCA1 as transgenic mice expressing ataxin-1 with a mutated nuclear localization signal (NLS) do not develop the disease (Klement et al., 1998). Overexpression of wildtype or mutant ataxin-1 protein leads to the formation of nuclear bodies *in vitro* (Krol et al., 2008; Stenoien et al., 2002), which is in accordance with transgenic mice studies that show similar nuclear structures upon overexpressing of wildtype or mutant human ataxin-1 (Koshy et al., 1998). These nuclear bodies may represent functional protein complexes containing ataxin-1, as these structures are dynamic and are not insoluble polyQ aggregates (Krol et al., 2008). The formation of nuclear bodies is also regulated by the phosphorylation status of ataxin-1, as ataxin-1 lacking serine 776 phosphorylation does not form nuclear bodies and exhibit a reduction of mutant ataxin-1 pathogenesis (Emamian et al., 2003). Moreover, this mutation disrupts the interaction with 14-3-3 *in vitro* and *in vivo* and impairs the formation of ataxin-1-capicua complexes (Chen et al., 2003a; Lam et al., 2006). These findings suggest that not only polyQ expansion, but also altered nuclear localization and phosphorylation levels can affect ataxin-1 function.

The role of altered phosphorylation in SCAs is underscored by SCA12 and SCA14 variants of the disease (Holmes et al., 1999; Yabe et al., 2003). SCA12 is caused by a muta-

tion in the brain-specific regulatory subunit of the protein phosphatase PP2A. SCA14 is caused by missense mutations in the protein kinase C gamma (PKCγ), which is the brain-specific isoform of the large serine/threonine kinase PKC family and is highly expressed in Purkinje cells (Chen et al., 2003a; Daniel et al., 1998; Schrenk et al., 2002). Throughout the coding region of PKCγ, 23 mutations have been identified, but particularly the C1B subdomain is a mutational hotspot since 75% of all SCA14 mutations are located in this particular subdomain (Chen et al., 2005). These mutations affect C1B accessibility and PKCγ kinase activity, leading to an aberrant MAPK signaling in SCA14 (Verbeek et al., 2008). PKCγ is known to be an important regulator of long term depression by controlling synapse plasticity at the parallel fiber of the Purkinje cell synapse (Daniel et al., 1998). However, the molecular mechanisms by which PKCγ controls these processes are still unknown. Furthermore, active PKCγ has an inhibitory effect on the growth and size of the dendritic tree of Purkinje cells (Abeliovich et al., 1993; Chen et al., 1995; Metzger and Kapfhammer, 2000; Newton, 2001; Schrenk et al., 2002). PKCγ is mostly present in neurites of Purkinje cells, including the dendritic shafts and dendrites. In other neurons such as pyramidal cells, the protein is predominantly located in the cytoplasm of the cell body (Sakai et al., 2004; Tanaka and Nishizuka, 1994).

Similarly to the altered distribution of ataxin-1 in Purkinje cells, the different location of PKCγ may contribute to the prominent Purkinje cell loss observed in SCA. There are indications that SCA1 and SCA14 have common underlying mechanisms that cause Purkinje cell degeneration, as ataxin-1 and PKCγ may be functionally linked. In a SCA1 mouse micro-array study, numerous genes involved in glutamate signaling were transcriptionally downregulated in Purkinje cells (Serra et al., 2004). This downregulation may be related to PKCγ as activated glutamate signaling activates PKC and also affects the intracellular levels of Ca2+, a second messenger of PKC (Conn and Pin, 1997; Serra et al., 2004). In addition, loss of PKCγ at the dendritic cell membrane and a decrease in total protein levels was observed in the SCA1 mouse model, whereas the mRNA levels were not changed. Moreover, PKCγ appeared to be mislocalized in cytoplasmic vacuoles in Purkinje cells (Skinner et al., 2001). In addition, the finding that the cerebellum of a SCA14 patient also showed reduced ataxin-1 immunostaining (Chen et al., 2003a) strengthens the hypothesis that ataxin-1 and PKCγ affect each other and are functionally linked.

To test whether SCA1 and SCA14 are functionally related, we investigated whether ataxin-1 and PKCγ are interaction partners and localize in complexes. Here, we show that PKCγ and ataxin-1 interact both *in vitro* and *in vivo* in mouse brain. Furthermore, we show that PKCγ can induce the phosphorylation of ataxin-1 and increases the formation and dynamics of ataxin-1 nuclear bodies. On the other hand, PKCγ phosphorylation is increased, and PKCγ is translocated to the plasma membrane of Purkinje cells in a SCA1 mutant mouse model.

Materials and Methods

DNA constructs. The generation of the human wildtype PKCγ-GFP and SCA14-mutant PKCγ-GFP and RFP constructs (G118D and V138E) have been described previously (Verbeek et al., 2008; Verbeek et al., 2005). The expression constructs of GST-tagged PKCγ were generated by amplifying the PKCγ cDNA using primers: forward 5'-GCCGGATCCACCATGGCTGGTCT-GGGCCCC-3' and reverse 3'- CGGGCGGCCGC-CATGACGGGCACAGGCACTG-5' generating

a BamHI site at the 5'-end and a NotI site at the 3'-end. This facilitated cloning into the pEBB-GST plasmid. The GFP-Atx1[2Q], GFP-Atx1[85Q], FLAG-Atx1[30Q] and FLAG-Atx1[82Q] constructs were kindly provided by Dr. Huda Zoghbi (Houston, TX) and Dr Ronald Evans (San Diego, CA), respectively. The Ser694Ala mutation was introduced into the ataxin-1 cDNA with the Quickchange II Site-Directed Mutagenesis kit (Stratagene, La Jolla, CA) using the following primers: forward 5'-GAACCTGAAGAACGGCGCTGTTAAAAAGGGCCAG-3' and reverse 5'-CTGGCCCTTTTTAACAGCGCCGTTCTTCAGGTTC-3'. All constructs were verified by sequencing.

Cell culture and transfection. COS-7 and mouse neuroblastoma N2A cells were cultured in Dulbecco's Modified Eagle Medium supplemented with 10% fetal bovine serum and 5% penicillin (100 U/ml), streptomycin (100 mg/ml) and glutamine (100 mg/ml). Cells were maintained at 37°C in an atmosphere of 5% CO_2. For live cell microscopy, 2 x105 cells were plated on glass coverslips (24 mm; Fischer Scientific, Braunschweig, Germany). The cells were subsequently transfected with the different constructs after 24 h using Lipofectamine 2000 transfection reagent according to the manufacturer's instructions (Invitrogen, Carlsbad, CA). HEK 293T cells were cultured in Iscove's Modified Dulbecco's Medium supplemented with high glucose, 10% fetal bovine serum, 5% penicillin (100 U/ml), streptomycin (100 mg/ml) and glutamine (100 mg/ml) in an atmosphere of 5% CO_2. One day before transfection, 2.2 x 10^6 cells were seeded into 10 cm dishes and transiently transfected with 4 µg DNA using polyethyleneimine (PEI; Polysciences, Warrington, PA). After transfection, cells were cultured at 37°C for 48 h before analysis.

Confocal laser scanning microscopy (CLSM) and fluorescence recovery after photobleaching (FRAP) analysis. Transiently transfected N2A cells were categorized based on co-expression of GFP-Atx1[2Q/85Q] and PKCγ-138-RFP by selecting GFP- and RFP-positive cells. Based on our previous data, cells were selected that contained ataxin-1 nuclear bodies that were approximately 1.5 µm in size (Krol et al., 2008). FRAP analysis was performed using an SP2 CLSM adapted for living cell analysis using a 63x oil immersion objective (Leica, Mannheim, Germany). A selected ataxin-1 nuclear body was repeatedly bleached in 10 frames at maximum laser power, resulting in a reduction of fluorescence to less than 10% of the initial value. Fluorescence recovery was measured as previously described (Krol et al., 2008).

GST-fusion protein pull-down assay and immunoprecipitation. To study interactions between ataxin-1 and PKCγ, HEK 293T cells were transiently transfected with full length PKCγ-138-GST and GFP-Atx1[2Q] and GFP-Atx1[85Q]. The transfected cells were lysed in buffer A (50 mM Na2HPO4, 1 mM sodium pyrophosphate, 20 mM NaF, 2 mM EDTA, 2 mM EGTA and 1% Triton) supplemented with complete mini protease inhibitor cocktail (Roche, Palo Alto, CA) and phosphatase inhibitor cocktail (Sigma, St. Louis, MO), at 48 h after transfection. The protein quantity was determined using the Bradford protein analysis. The detergent-soluble fraction was incubated with glutathione–Sepharose at 4°C for 2 h. The glass beads were washed twice in buffer A, and subsequently three times in buffer B (buffer A supplemented with 300 mM NaCl). The GST-bead bound proteins were analysed by SDS-PAGE and immunoblotting. Antibodies were used following the manufacturer's description (anti-GST; Tebu-Bio, Heerhugowaard, NL and anti-GFP; Clontech, Mountain View, CA). The proteins were visualized using enhanced chemiluminescence on radiograph films.

Cerebellum of control mice and the brains of A05 and B05 mice, kindly provided by Dr. Harry Orr (University of Minnesota, Minneapolis, US (Burright et al., 1995) were homogenized in Tris pH 8.0 supplemented with complete mini protease inhibitor cocktail and phosphatase inhibitor cocktail using glass beads and subsequently subjected to three freezing and thawing cycles. The protein quantity was determined using the Bradford protein analysis. Equal amounts of the soluble fractions were pre-cleared with washed protein A/G beads at 4°C for 4 h. Next, the pre-cleared soluble

fractions were incubated with 5 µg of the primairy antibody (anti-Atx1; kindly provided by Dr. H. Orr or anti-PKCγ; Santa Cruz Biotechnology, Santa Cruz, CA) at 4°C overnight. The following day, 50 µl washed protein A/G beads were added to the fractions and incubated at 4°C for 3 h. The beads were pelleted, and washed twice in buffer A, and subsequently three times in buffer B. The bound proteins were analysed as described above.

PCKγ and phorbol ester induced phosphorylation of ataxin-1. To induce phosphorylation of ataxin-1, HEK 293T cells were transiently transfected with FLAG-Atx1[30Q] and FLAG-Atx1[85Q] and treated with 400 nM phorbol myristate acetate (PMA) for 2 h. In addition, HEK293T cells were co-transfected with FLAG-Atx1[30Q/85Q] and PKCγ-138-GST and subsequently stimulated with 400 nM PMA. After 2 h, the cells were lysed in buffer A and the detergent soluble fraction was incubated with agarose-A/G beads (Santa Cruz), which were pre-bound with anti-FLAG antibody (Sigma) for 1 h at 4°C, overnight at 4°C. The beads were washed twice with buffer A and three times with buffer B. Bound ataxin-1 was analysed on 10% SDS-page gels by immunoblotting using a phospho-(Ser)-PKC-substrate antibody following the manufacturer's instruction (Cell Signalling, Danvers, MA). The proteins were visualized using ECL on films.

Immunoblotting. The HEK293T cells were harvested at 48 h after transfection and lysed immediately in 1x SDS sample buffer. After electrophoresis, the proteins were transferred onto a nitrocellulose membrane filter (Schleicher & Schuell, Dassel, Germany) and blocked in 5% milk to prepare for western blotting. The western blots were analyzed with anti-Atx1 (kindly provided by Dr. H. Orr), anti-PKC (Santa Cruz), anti-pT514, anti-pT655, anti-pT674 (all Cell Signalling), anti-phosho-p44/42-MAP kinase (Thr202/Tyr204), anti-p44/42 MAP kinase (both from Cell Signalling), and anti-actin (MP Biochemicals) antibodies.

Ataxin-1 aggregate scoring assay. To determine whether PKCγ-induced phosphorylation altered the number and distribution of ataxin-1 nuclear bodies, COS-7 and N2A cells were transiently transfected with either GFP-Atx1[2Q] or GFP-Atx1[85Q] and GFP-Atx1[2Q]/[85Q]-S694A and co-transfected with PKCγ-138-RFP. Next, the percentage of cells with nuclear ataxin-1 bodies versus cells with diffuse nuclear staining were scored using a IRB inverted fluorescent microscope (Leica). The scoring assays were performed in triplicate by an independent scorer.

Immunohistochemical staining of mouse SCA1 cerebella. Brains of SCA1 transgenic mice A02 and B05, expressing Atx1[Q30] and Atx1[Q82], respectively, under a Purkinje cell-specific promoter were kindly provided by Dr. Harry Orr (University of Minnesota, Minneapolis, US) (Burright et al., 1995). The brains of the sacrificed mice were frozen in liquid nitrogen, stored at -80°C and cut using a cryostat (section thickness 10 µm). Sections were post-fixed in 4% buffered paraformaldehyde for 10 min and blocked in 10% normal goat serum with 0.4% Triton-X100 in 0.05 M phosphate buffer (pH 7.4) for 1 h at room temp. For immunostaining, we used the dilutions 1:2500 and 1:8000 for the PKCγ-antibody (Santa Cruz) and 11750V-antibody (provided by Huda Zoghbi), respectively. Immunostaining of phosphosphorylated PKCγ was performed using the antibodies pT655 and pT674 (both Invitrogen) in a dilution of 1:500. Incubations with primary antibodies were performed overnight at 4°C in PBS containing 0.1% Triton and 1% FCS (PH 7.4) followed by an incubation with secondary goat anti-rabbit Cy3 (Jackson) in a dilution of 1:100 in PBS containing 1% FCS for 60 min at room temp. The sections were washed in PBS and cover slipped using vectashield (Vector Laboratories, Burlingame, CA).

Results

PKCγ interacts with ataxin-1. To test whether ataxin-1 and PKCγ interact, GST-pull down experiments were performed in HEK293T cells expressing both GST-tagged PKCγ and FLAG-tagged ataxin-1 (FLAG-Atx1[30Q]/[85Q]). As a negative control, FLAG-Atx1[30Q] was co-expressed with a

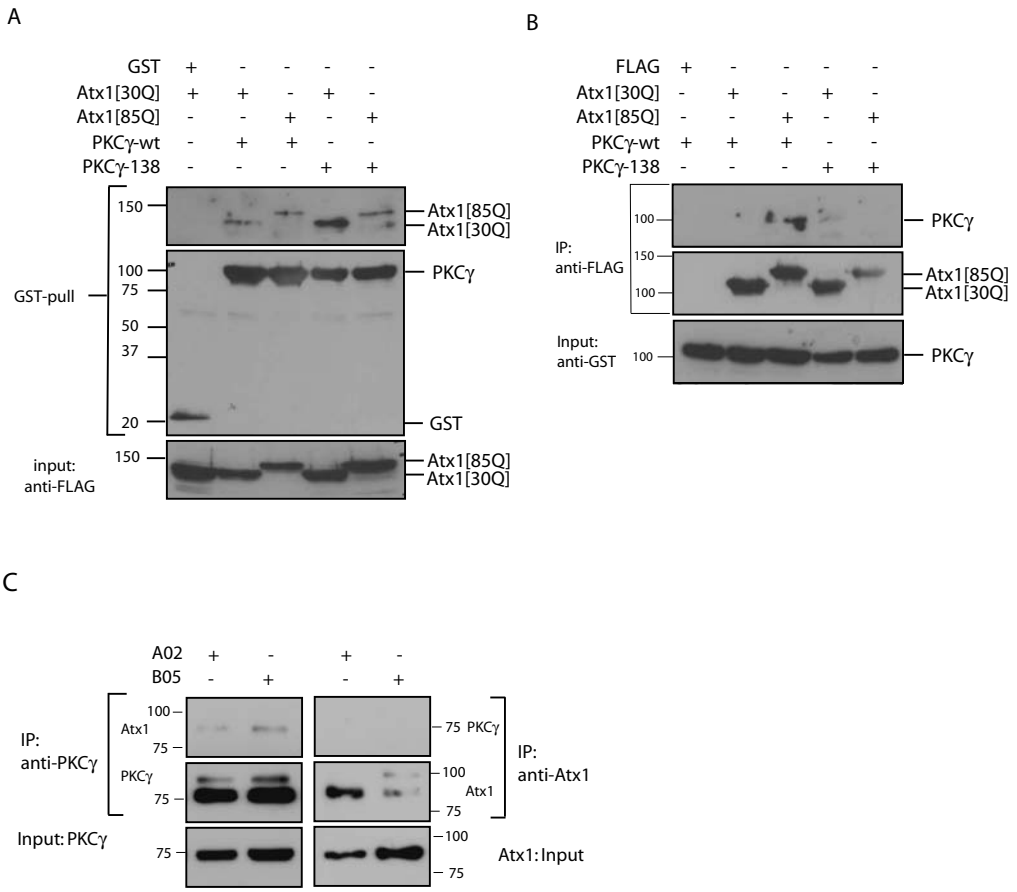

Figure 1. PKCγ interacts with ataxin-1. **(A)** Lysates of HEK293T cells co-transfected with FLAG-ataxin-1[30Q]/[85Q] and PKCγ-wt/mt-GST or empty-GST were immunoprecipitated by GST-pull down. The lysates (input) and immunoprecipitates were analyzed by immunoblotting with anti-FLAG antibodies. **(B)** Immunoprecipitation using the anti-FLAG antibody. Again the lysates and immunoprecipitates were analyzed by either anti-FLAG or anti-GST antibodies. **(C)** Lysates from A02 and B05 mouse brain (5 weeks) were immunoprecipitated with anti-PKCγ and anti-ataxin-1 antibodies. The lysates (input) and immunprecipitates were analyzed by immunoblotting using the anti-PKCγ and anti-ataxin-1 antibodies. The figures are representatives of at least 3 independent experiments.

non-fused GST. When PKCγ-wt was immunoprecipitated from lysates of cells transfected with PKCγ and ataxin-1, both Atx1[30Q] and Atx1[82Q] were co-immunoprecipitated (Fig. 1A). Both Atx1[30Q] and Atx1[82Q] were also detected in the immunoprecipitates of SCA14-mutant PKCγ (V138E). The interaction between SCA14-mutant PKCγ and wildtype ataxin-1 appeared to be stronger. When the intereactions were examined by pulling down ataxin-1, only Atx1[85Q] was co-immunoprecipitated with PKCγ (compare lane 2 and 3, Fig. 1B), as Atx1[30Q] failed to pull down any of the PKCγ. To test whether ataxin-1 and PKCγ interact *in vivo*, we investigated the interaction in the brain of transgenic ataxin-1 mice overexpressing either human Atx1[30Q] or Atx1[82Q]. Here,

both ataxin-1[30Q] and [82Q] were present in the immunoprecipitates of PKCγ (Fig. 1C left panel, lane 1 and 2). Similar to the *in vitro* data, PKCγ failed to be pulled down with ataxin-1 in 5 week old mice (Fig. 1C; right panel).

Taken together, these findings suggest that PKCγ and ataxin-1 interact, but that this interaction can only be visualised via pull-down of PKCγ. This may be explained by exclusive interaction in the cytoplasm, as most ataxin-1 is located in the nucleus.

PKCγ can phosphorylate ataxin-1. Because ataxin-1 and PKCγ interact, we examined whether PKCγ can phosphorylate ataxin-1 *in vitro*. To test the effect of PKCγ on phosphorylation of ataxin-1, we used an antibody that can detect all phosphorylated serines in PKC substrates. HEK293T cells were co-transfected with FLAG-Atx1[30Q] or [82Q] together with PKCγ-GST. In addition, cells expressing FLAG-Atx1[30Q] or FLAG-Atx1[82Q] were treated with 400 mM PMA for 30 min to activate endogenous PKCα and β. PMA induced increased phosphorylation of both wildtype and polyQ-expanded ataxin-1, as shown by the anti-phospho-(Ser)-PKC substrate antibody upon immunoprecipitation of ataxin-1 (Fig. 2; upper panel, lanes 3 and 4). Co-expression of PKCγ induced a similar phosphorylation level of Atx1[30Q/82Q] in the absence of PMA (Fig 2; compare lane 3, 4 with lane 5 and 6), suggesting that PKCγ can phosphorylate ataxin-1. Additional PMA stimulation did not significantly further increase the amount of ataxin-1 phosphorylation (Fig. 2; lane 7 and 8). These results suggest that ataxin-1 not only interacts with PKCγ but is also a substrate of PKCγ at a yet unknown amino acid position.

PKCγ enhances ataxin-1 nuclear body formation. Since the phosphorylation status of ataxin-1 can affect nuclear body formation and toxicity (Chen et al., 2003b; Emamian et al., 2003), we examined whether PKCγ protein levels affect the formation of ataxin-1 nuclear bodies or alter the kinetics of these structures. We overexpressed either GFP-Atx1[2Q] and GFP-Atx1[85Q] alone or together with PKCγ-RFP in COS-7 cells. Cells expressing GFP-Atx1 showed that endogenous PKCγ mostly resided in the cytoplasm, whereas ataxin-1 was predominantly present in the nucleus. Cells co-expressing both GFP-Atx1 and PKCγ-RFP showed no recruitment of PKCγ into nuclear ataxin-1 bodies (data not shown), suggesting that the interaction between PKCγ and ataxin-1 occurs elsewhere, for example after shuttling of ataxin-1 into the cytoplasm. Whereas a minority of COS-7 cells (25% and 32%) expressing GFP-Atx1[2Q] or GFP-Atx1[85Q] develop nuclear bodies (Fig. 3A; white bars), co-expression of PKCγ showed an increase in

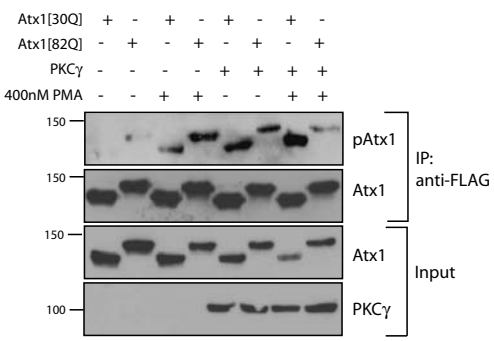

Figure 2. PKCγ phosphorylates ataxin-1. Lysates of HEK293T cells co-transfected with FLAG-ataxin-1[30Q]/[85Q] and PKCγ-wt-GST and stimulated with or without PMA (400 nM) were immunoprecipitated using the anti-FLAG antibody. The lysates (input) and immunoprecipitates were analyzed by immunoblotting with either anti-FLAG, anti-GST anti-p(Ser)-PKC-substate antibodies. The blot is a representative of 3 independent experiments.

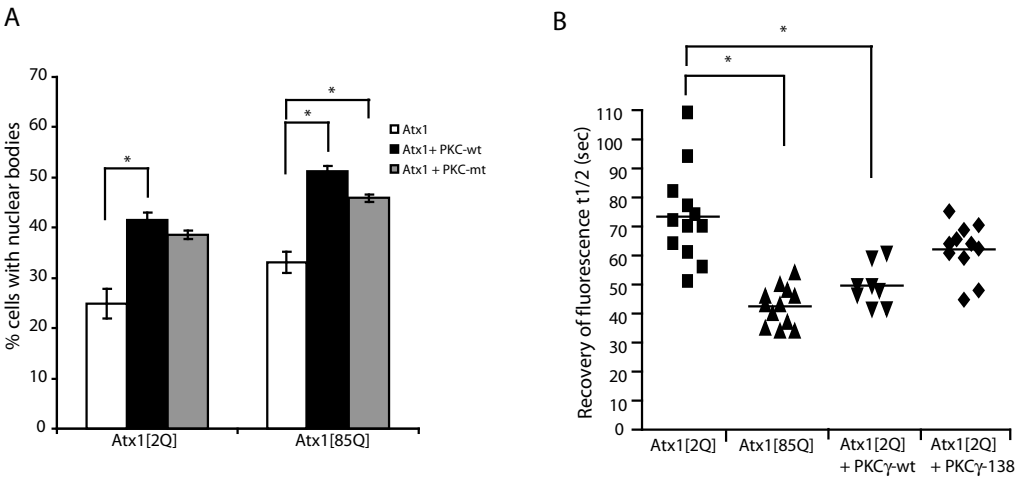

Figure 3. PKCγ enhances ataxin-1 nuclear body formation and dynamics. **(A)** COS-7 cells were transfected with either ataxin-1[2Q]/[85] or co-transfected with PKC-RFP (wt or SCA14-mutant). Ataxin-1 nuclear body formation was scored manually and analyzed with an unpaired t-test (*, p-value<0.05). **(B)** FRAP live cell experiments were performed on COS-7 cells transfected with ataxin-1[2Q] or co-transfected with PKC-RFP (wt or SCA14-mutant). Half time ($t_{½}$ recovery data have been tested non-parametrically (*, p-value <0.05). The scoring experiments were preformed in triplicate and were additionally analyzed by an independent scorer.

the number of nuclear bodies (42% and 53%, respectively; Fig. 3A). Co-expression of the SCA14-mutant PKCγ (V138E) showed less ataxin-1 nuclear bodies when compared to PKCγ-wt (38% and 46%; Fig. 3A), However, this decrease was not significant. These results imply that PKCγ stimulates the formation of nuclear bodies of both Atx1[2Q] and Atx1[85Q], but these effects are limited when PKCγ is mutated. As we showed earlier that SCA14 mutations lead to reduced PKCγ activity (Verbeek et al., 2008), this suggests that SCA14-mutant PKCγ induces less ataxin-1 phosphorylation and subsequently less nuclear body formation.

We used a motif scanner (http://scansite.mit.edu/motifscan_seq.phtml) to detect possible PKC binding motifs present in the ataxin-1 protein sequence to identify the PKC phosphorylation motif in ataxin-1. A putative PKCα, β, γ site was detected at S694 using medium stringency (Supplementary Fig. 1A). In order to determine the role of this putative PKC-specific-phosphoylation site S694 on the formation of ataxin-1 nuclear bodies, we mutated the serine 694 to alanine mimicking a non-phosphorylated status. This mutation led to a small, but not significant reduction of the formation of nuclear bodies in cells expressing GFP-Atx1-S694A (Supplementary Fig. 1B). To examine whether this reduction of nuclear bodies was caused by the inability of PKCγ to phosphorylate S694, we co-expressed Atx1[2Q/85Q]-S694A with PKCγ. Unexpectedly, co-expression of PKCγ induced ataxin-1 nuclear bodies after Atx1-S694A transfection similar as for Atx1[2Q] transfection. However, co-expression of PKCγ with Atx1[85Q]-S694A also caused increased numbers of nuclear bodies when compared to Atx1[85Q] alone, but remained significantly different (p<0.05) when

compared to Atx1[85Q] co-expressed with PKCγ. These results suggest that phosphorylation of S694 plays a role in the formation of ataxin-1 nuclear bodies, but this site is not the primary PKCγ phosporylation motif. Alternatively, the observed effect is phosphorylation-independent and may already be induced via the PKCγ-Atx1 interaction.

PKCγ increases nuclear dynamics of ataxin-1. Since cytoplasmic PKCγ can increase nuclear body formation of ataxin-1, we next examined whether PKCγ affected the dynamics of these structures that normally show a constant exchange of ataxin-1 between bodies and the nuclear environment. The on/off rate of ataxin-1 in nuclear bodies is affected by the length of the polyQ expansion in ataxin-1, with a higher on/off rate for ataxin-1 with an expanded polyQ tract (Krol et al., 2008). The on/off rate of ataxin-1 can be determined using FRAP, which was performed by measuring the fluorescent recovery of a single photobleached ataxin-1 nuclear body. The resulting $t_{1/2}$ (which is the time point where the fluorescence has recovered to 50% of its original fluorescence intensity level) was determined. FRAP was performed in N2A cells expressing only ataxin-1 (GFP-Atx1[2Q/85Q] + free mRFP) or GFP-Atx1[2Q] together with RFP-tagged PKCγ-wt or SCA14-mutant PKC (V138E). Interestingly, co-expression of PKCγ-wt significantly reduced the $t_{1/2}$ of Atx1[2Q] by 20 seconds (Fig. 3B). This is similar to the on/off rate of polyQ-expanded ataxin-1, with the $t_{1/2}$ of Atx1[85Q] (Fig. 3B), which is in accordance with our earlier data (Krol et al., 2008). Expression of SCA14-mutant PKCγ did not significantly decrease the $t_{1/2}$ of Atx1[2Q]. These data indicate that increased levels of PKCγ can accelerate the on/off rate of ataxin-1 nuclear bodies, which is similar to the effects of ataxin-1 polyQ-expansion (Krol et al., 2008).

Ataxin-1 alters PKCγ localization and autophosphorylation in a SCA1 mouse model. Since PKCγ and ataxin-1 can interact, and PKCγ can alter ataxin-1 kinetics, we investigated whether ataxin-1 also affected the intracellular location of PKCγ *in vivo*. We used a SCA1 mouse model that overexpresses either human Atx1[Q30] or Atx1[Q82] driven by a Purkinje cell specific promoter (Burright et al., 1995). The endogenous PKCγ protein levels and localization in cerebellar slices of Atx1[Q30] and Atx1[Q82] mice were determined in mice that were 5 or 12 weeks old. Atx1[Q30] mice displayed a diffuse intracellular PKCγ staining in Purkinje cells (Fig. 4A, top panels) similar to wildtype mice Purkinje cells, whereas PKCγ was predominantly present at the plasma membrane in Atx1[Q82] mice (Fig. 4A, lower panels) irrespective the age of the mice. This was accompanied by a slight loss of PKCγ protein expression, as was noticed previously by others (Skinner et al., 2001). Little staining of the dendrites was observed in Atx1[Q30] which may be due to overexpression of Atx1[30Q], that has been described to induce slight clinical symptoms (Fernandez-Funez et al., 2000).

To investigate whether the change in PKCγ protein localization correlated with altered PKC phosphorylation, we analyzed brain lysates of the Atx1[30Q] and Atx1[82Q] mice by immunoblotting using PKCγ-phospho-specific antibodies (pT655 and pT764, respectively). We observed increased phosphorylation levels of PKCγ in Atx1[82Q] mice that were 5 weeks old when compared to Atx1[30Q] mice with both antibodies. This suggests that mutant ataxin-1 affects endogenous PKCγ activation as well as its cellular localization. A similar increase in PKCγ phosphorylation was also observed in 12 week-old mutant Atx1 mice compared

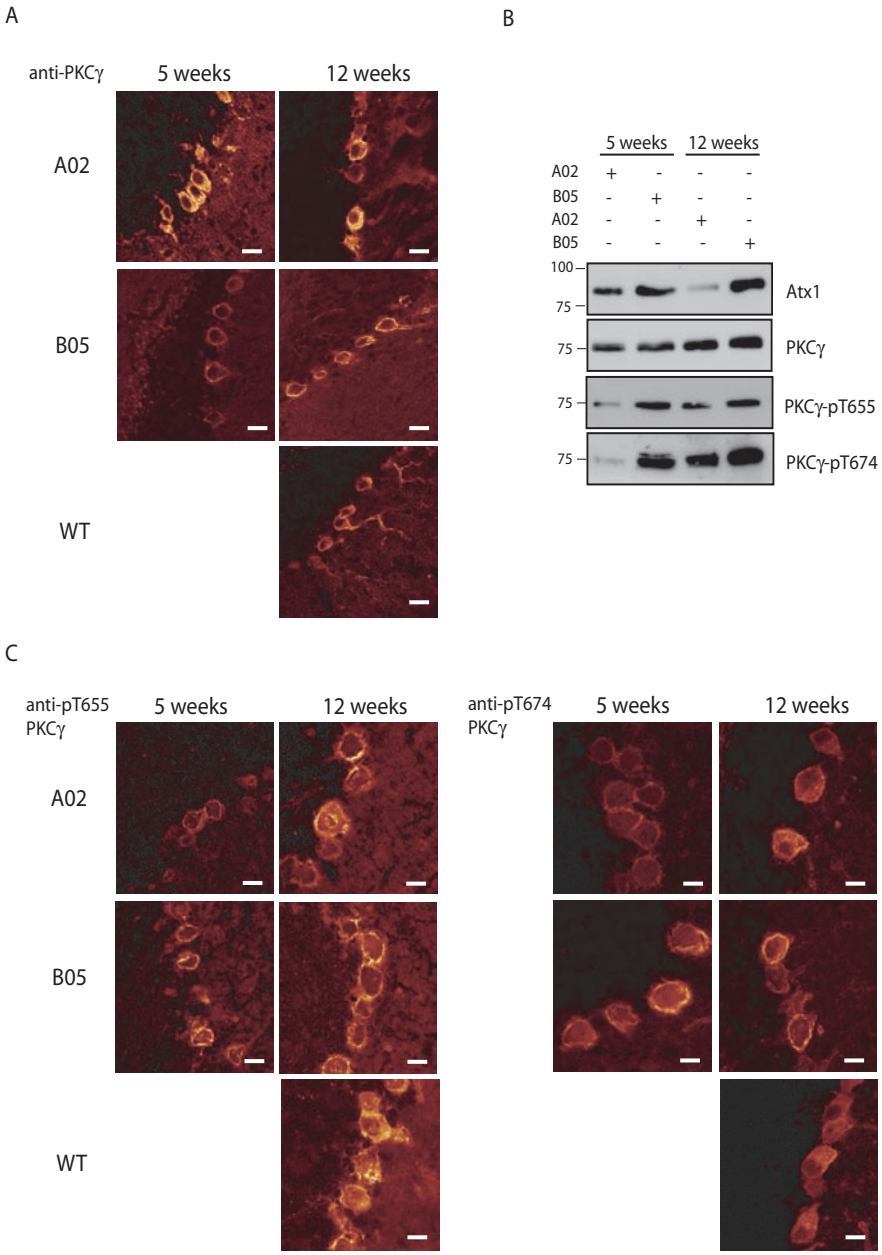

Figure 4. Mutant ataxin-1 affects localization and autophosphorylation of PKCγ in Purkinje cells. **(A)** Confocal images of cerebella of 5 and 12 weeks old A02 and B05 mice and of a 12 week old wild-type mouse. Sections were stained with anti-PKCγ antibody and visualized at 63x magnification. **(B)** Lysates of brains of A02 and B05 mice that were 5 and 12 weeks old were analyzed using immunoblotting with anti-PKCγ, anti-ataxin-1, anti-PKCγ-pT514, anti- PKCγ-pT655, and anti-PKCγ-pT674 antibodies. **(C)** Cerebellar slices of 5 and 12 weeks old A02 and B05 mice and of 12 weeks old wild-type mouse were investigated immunohistochemically using anti-PKCγ-pT655, and anti-PKCγ-pT674 antibodies.

to a Atx1[30Q] mouse. However, no mutant ataxin-1 allele in the [82Q] mice was observed, but increased levels of ataxin-1 were observed when compared to Atx1[30Q] mice (Fig. 4B ; top panel, lanes 1 and 3 versus lanes 2 and 4). As the mutant Atx1 is driven under a Purkinje cell-specific promoter only this type of cell expresses mutant Atx1. Therefore, protein levels are too low to be detected when analyzing complete mouse brain. However, both findings are in concurrence with previous reports (Klement et al., 1998). In addition, when Atx1[30Q/85Q] and PKCγ-wt/V138E were cotransfected in HEK293T cells, an increase in PKCγ pT655 and pT674 was also observed when compared to cells only overexpressing PKCγ using immunoblotting (Supplementary Fig. 2). Furthermore, phosphorylation levels of PKCγ-wt and mutant upon overexpression of Atx1 were not observed.

To confirm the increased PKCγ autophosphorylation levels in Purkinje cells of Atx1[82Q] mice, we performed immunohistochemistry to detect phosphorylated PKCγ. A significant amount of phosphorylated PKCγ (T655 and T674) was present at the plasma membrane of Purkinje cells of Atx1[30Q] and Atx1[82Q] mice that were 5 and 12 weeks old (Figure 4C). However, increased phosphorylation levels (T655 and T674) were found in Atx1[82Q] Purkinje cells when compared to Atx1[30Q] and wildtype mice (Fig. 4C; compare top panels versus middle panels).

Taken together, these results underscore our hypothesis that ataxin-1 and PKCγ are functionally related by regulating each others functionality by controlling nuclear ataxin-1 complex formation and local PKCγ activity in Purkinje cells.

Discussion

In SCAs, mainly the cerebellum is affected with a massive degeneration of Purkinje cells. The biological pathways leading to neurodegeneration are not understood yet and depend on both the function of the wildtype SCA protein as well as the context of the mutation. As most of the SCA genes do not show any homology in their mutational mechanism, protein function, and structure, this may be complex. However, recent studies led to the identification of some shared pathways leading to ataxia, consisting of dysfunction in gene expression, transcription, synaptic transmission or other intracellular signaling pathways such as calcium or glutamate signaling (Carlson et al., 2009; Lim et al., 2006; Seeley et al., 2009). Whether these biological pathways function independently or are interconnected remains to be determined. The fact that some of the ataxia proteins may interact directly or indirectly via protein-protein interactions (Lim et al., 2006), strengthens the hypothesis that shared pathways are indeed associated with ataxia.

Our study provides biochemical and cell biological evidence for a shared underlying mechanism involving two SCA-causing proteins, ataxin-1 (SCA1) and PKCγ (SCA14). By co-immunoprecipitation we showed that ataxin-1 and PKCγ are in a complex *in vitro* and *in vivo* (Fig. 1). It is yet not clear whether this is a direct or indirect interaction or that PKCγ and ataxin-1 both are present in a larger protein complex. Since their interaction could only be visualized via pull-down of PKCγ, it suggests that the interaction between the two proteins may occur only in the cytoplasm of Purkinje cells. Since ataxin-1 is solely restricted to the nucleus in other neuronal cell types it may be that their interaction occurs exclusively in Purkinje cells (1998; Klement et al., 1999; Koshy et al.,

1998; Orr, 2001). If this hypothesis is true, it may explain the increased sensitivity of Purkinje cells for mutations in SCA proteins when compared to other neuronal cells which also express the disease-related proteins. Intriguingly, SCA14-mutated PKCγ seemed to be stronger in complex with ataxin-1 when compared to wildtype PKCγ, which suggests that mutated PKCγ leads to alterations in ataxin-1 wildtype function that eventually also contributes to pathology.

In addition, overexpression of PKCγ increased phosphorylation levels of ataxin-1 and the formation and mobility of ataxin-1 nuclear bodies (see Figs. 2 and 3). Since activation of endogenous PKCα and β using a phorbol ester had a similar effect on ataxin-1 phosphorylation, this functional link is not exclusive for PKCγ. However, endogenous PKCα/β needed to be activated to induce ataxin-1 phosphorylation whereas PKCγ overexpression alone without PMA activation was sufficient to phosphorylate ataxin-1. This may be due to higher specificity of PKCγ for ataxin-1 than that of PKCα and β.

Overexpression of both wildtype and SCA14-mutant PKCγ significantly increased the number of ataxin-1-[2Q] and [85Q] nuclear bodies *in vitro*, suggesting that 1) the PKCγ-ataxin-1 interaction or 2) the phosphorylation of ataxin-1 by PKCγ is involved in the generation of additional functional ataxin-1 complexes. However, slightly less ataxin-1 nuclear bodies were observed in the SCA14-mutant PKCγ-expressing cells compared to wildtype PKCγ expressing cells. Given the fact that 1) SCA14-mutant PKCγ binds stronger to ataxin-1 than wildtype PKCγ, and 2) SCA14-mutant PKCγ is less active than wildtype but that 3) both PKCγ proteins induce the formation of nuclear bodies, suggest that alterations in ataxin-1 phosphorylation levels modify the formation of functional ataxin-1 complexes. This is in accordance with a previous study by Emanian et al. (Emamian et al., 2003) that showed phosporylation by Akt at ataxin-1-S776 to be crucial for nuclear body formation. Here, mutation of this amino acid to alanine (A776) impaired ataxin-1 phosphorylation at this site and resulted in a decrease of nuclear bodies (Chen et al., 2003b). In addition, phosphorylation plays an important role in the translocation of ataxin-1 from cytoplasm to the nucleus, as 80% of all phosphorylated ataxin-1 at serine 776 is present in the nucleus of cerebellar neurons (Dr. H. Orr, personal communication). Atx-S694 was predicted to have a putative PKCγ phosphorylation site. Therefore, we investigated whether mutation of this site to alanine had effect on ataxin-1 nuclear body formation. As Atx1[2Q]-A694 showed slightly reduced numbers of nuclear bodies, we suggest that also this site may play a role in ataxin-1 body formation. However, S694 is not the main PKCγ phosphorylation site in ataxin-1 as co-expression of PKCγ with Atx1[2Q]-A694 also resulted in significant increased numbers of nuclear bodies (Supplementary Fig. 1B). Unfortunately, we were unable to identify which phosphorylation site of ataxin-1 was targeted by PKCγ.

Overexpression of PKCγ also increased the mobility of ataxin-1 nuclear bodies in COS-7 cells (Fig. 3). We hypothesize that ataxin-1 oligomerization is modified because of additional PKCγ phosphorylation, leading to an altered conformation of the ataxin-1 protein. This matches with our previous finding that altered ataxin-1 protein conformations due to the expanded polyQ tract also led to increased ataxin-1 mobility in nuclear bodies (Krol et al., 2008).

Interestingly, cytoplasmic PKCγ is translocated to the plasma membrane in Purkinje cells of mutant-ataxin-1 mice (Fig. 4).

This change in cellular PKCγ location suggests that mutant ataxin-1 induces changes in PKCγ activity and subsequently its function. To investigate whether translocation of PKCγ to the plasma membrane is associated with increased PKCγ activity, we determined PKCγ autophosphorylation levels (Fig. 4 and Supplementary Fig. 2). We observed a significant increase in PKCγ autophosphorylation at T655 and T674 in brain lysate of mutant SCA1 mice, and in cells overexpressing both ataxin-1 and PKCγ proteins, using immunoblotting. This increase in autophosphorylation was confirmed by immunohistochemistry in Purkinje cells of mutant SCA1 mice. Moreover, we also noticed the loss of total PKCγ protein as has been described before by Skinner et al. (2001). Therefore, our results suggest that loss of intracellular PKCγ protein is compensated by increased PKCγ autophosphorylation and subsequently leads to increased kinase activity as was shown *in vitro* and *in vivo*.

In summary, we conclude that the two SCA proteins ataxin-1 and PKCγ are present in the same protein complex and may function in a common biological pathway that is specifically vulnerable to alterations in Purkinje cells. As mutant ataxin-1 has been shown to cause downregulation of proteins involved in glutamate signaling in neurons (Lin et al., 2000), we suggest that PKCγ is affected as it is implicated in regulating glutamate signaling (Zheng and Keifer, 2008). The change in PKCγ localization and autophosphorlation may thus be caused by 1) disturbed glutamate signaling or 2) loss of total PKC protein. As a consequence, additional important downstream signaling pathways such as calcium signaling and MAPK signaling are affected resulting in dysfunction of Purkinje cells and subsequent neurodegeneration.

Acknowledgements

We would like to thank Dr. Harry Orr and Dr. Huda Zoghbi for providing the ataxin-1 constructs, mouse material, and the ataxin-1 antibody.

Supplementary Figures

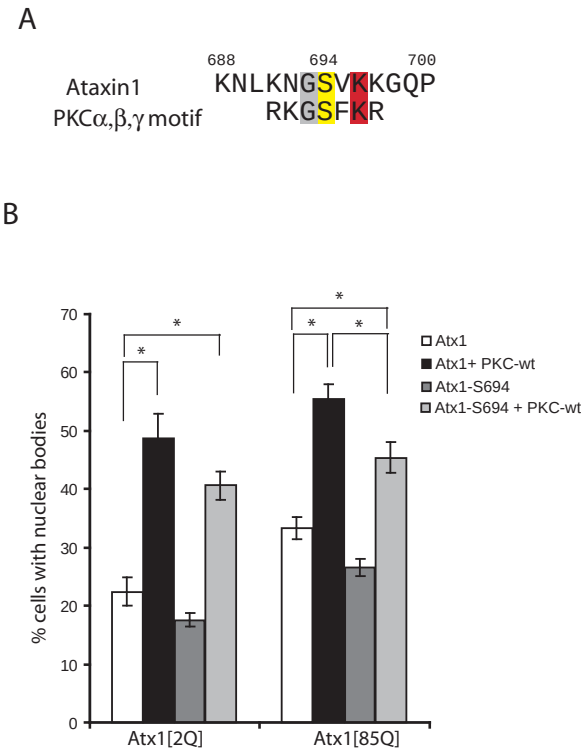

Supplementary Figure 1. PKC motif at ataxin-1-S674 is not the unique action site for PKCγ. (**A**) Ataxin-1 contains a predicted PKCα, β, γ phosphorylation motif at S674. (**B**) COS7 cells were transfected with either ataxin-1[2Q]/[85] (S697 and A697) or co-transfected with PKC-wt-RFP. Ataxin-1 nuclear body formation was scored manually and analyzed with an unpaired t-test (*, p-value<0.05).

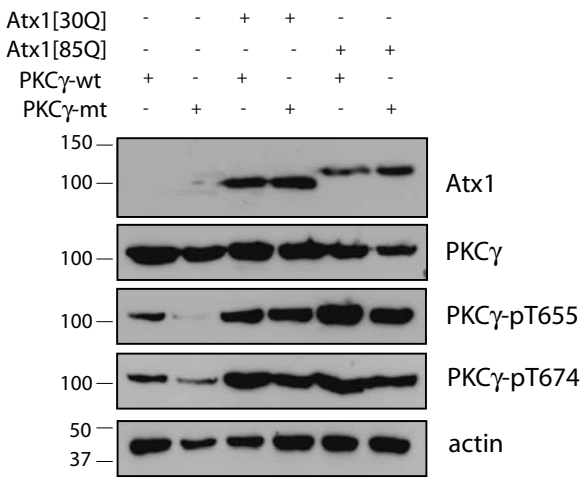

Supplementary Figure 2. Ataxin-1 enhances PKCγ autophosphorylation levels. Lysates of HEK293T cells transfected with either FLAG-ataxin-1[30Q]/[85Q] or cotransfected with PKCγ-GFP (wt or SCA14-mutant) were analyzed with immunoblotting using anti-GFP, anti-ataxin-1, anti-PKCγ-pT514, anti- PKCγ-pT655, and anti-PKCγ-pT674 antibodies.

References

Abeliovich A, Paylor R, Chen C, Kim JJ, Wehner JM and Tonegawa S (1993) PKC gamma mutant mice exhibit mild deficits in spatial and contextual learning. *Cell* 75: 1263-71.

Burright EN, Clark HB, Servadio A, Matilla T, Feddersen RM, Yunis WS, Duvick LA, Zoghbi HY and Orr HT (1995) SCA1 transgenic mice: a model for neurodegeneration caused by an expanded CAG trinucleotide repeat. *Cell* 82: 937-48.

Carlson KM, Andresen JM and Orr HT (2009) Emerging pathogenic pathways in the spinocerebellar ataxias. *Curr Opin Genet Dev*. 19:247-53.

Chen C, Kano M, Abeliovich A, Chen L, Bao S, Kim JJ, Hashimoto K, Thompson RF and Tonegawa S (1995) Impaired motor coordination correlates with persistent multiple climbing fiber innervation in PKC gamma mutant mice. *Cell* 83: 1233-42.

Chen DH, Brkanac Z, Verlinde CL, Tan XJ, Bylenok L, Nochlin D, Matsushita M, Lipe H, Wolff J, Fernandez M et al. (2003a) Missense mutations in the regulatory domain of PKC gamma: a new mechanism for dominant nonepisodic cerebellar ataxia. *Am J Hum Genet* 72: 839-49.

Chen DH, Cimino PJ, Ranum LP, Zoghbi HY, Yabe I, Schut L, Margolis RL, Lipe HP, Feleke A, Matsushita M. et al. (2005) The clinical and genetic spectrum of spinocerebellar ataxia 14. *Neurology* 64: 1258-60.

Chen HK, Fernandez-Funez P, Acevedo SF, Lam YC, Kaytor MD, Fernandez MH, Aitken A, Skoulakis EM, Orr HT, Botas J et al. (2003b) Interaction of Akt-phosphorylated ataxin-1 with 14-3-3 mediates neurodegeneration in spinocerebellar ataxia type 1. *Cell* 113: 457-68.

Conn PJ and Pin JP (1997) Pharmacology and functions of metabotropic glutamate receptors. *Annu Rev Pharmacol Toxicol* 37: 205-37.

Daniel H, Levenes C and Crepel F (1998) Cellular mechanisms of cerebellar LTD. *Trends Neurosci* 21: 401-7.

Duenas AM, Goold R and Giunti P (2006) Molecular pathogenesis of spinocerebellar ataxias. *Brain* 129: 1357-70.

Emamian ES, Kaytor MD, Duvick LA, Zu T, Tousey SK, Zoghbi HY, Clark HB and Orr HT (2003) Serine 776 of ataxin-1 is critical for polyglutamine-induced disease in SCA1 transgenic mice. *Neuron* 38: 375-87.

Fernandez-Funez P, Nino-Rosales ML, de Gouyon B, She WC, Luchak JM, Martinez P, Turiegano E, Benito J, Capovilla M, Skinner PJ et al. (2000) Identification of genes that modify ataxin-1-induced neurodegeneration. *Nature* 408: 101-6.

Holmes SE, O'Hearn EE, McInnis MG, Gorelick-Feldman DA, Kleiderlein JJ, Callahan C, Kwak NG, Ingersoll-Ashworth RG, Sherr M, Sumner AJ et al. (1999) Expansion of a novel CAG trinucleotide repeat in the 5' region of PPP2R2B is associated with SCA12. *Nat Genet* 23: 391-2.

Irwin S, Vandelft M, Pinchev D, Howell JL, Graczyk J, Orr HT and Truant R (2005) RNA association and nucleocytoplasmic shuttling by ataxin-1. *J Cell Sci* 118: 233-42.

Klement IA, Skinner PJ, Kaytor MD, Yi H, Hersch SM, Clark HB, Zoghbi HY and Orr HT (1998) Ataxin-1 nuclear localization and aggregation: role in polyglutamine-induced disease in SCA1 transgenic mice. *Cell* 95: 41-53.

Klement IA, Zoghbi HY and Orr HT (1999) Pathogenesis of polyglutamine-induced disease: A model for SCA1. *Mol Genet Metab* 66: 172-8.

Koshy BT, Matilla A, Zoghbi HY (1998) Clues about the pathogenesis of SCA1: from biochemical and molecular studies of ataxin-1. In: Genetic Instabilities and Hereditary Neurological disorders. Wells RD, Warren ST (eds). Academic Press, San Diego, CA, pp 241-8.

Krol HA, Krawczyk PM, Bosch KS, Aten JA, Hol EM and Reits EA (2008) Polyglutamine expansion accelerates the dynamics of ataxin-1 and does not result in aggregate formation. *PLoS ONE* 3, e1503.

Lam YC, Bowman AB, Jafar-Nejad P, Lim J, Richman R, Fryer JD, Hyun ED, Duvick LA, Orr HT, Botas J et al. (2006) ATAXIN-1 interacts with the repressor Capicua in its native complex to cause SCA1 neuropathology. *Cell* 127: 1335-47.

Lim J, Crespo-Barreto J, Jafar-Nejad P, Bowman AB, Richman R, Hill DE, Orr HT and Zoghbi HY (2008) Opposing effects of polyglutamine expansion on native protein complexes contribute to SCA1. *Nature* 452: 713-8.

Lim J, Hao T, Shaw C, Patel AJ, Szabo G, Rual JF, Fisk CJ, Li N, Smolyar A, Hill DE et al. (2006) A protein-protein interaction network for human inherited ataxias and disorders of Purkinje cell degeneration. *Cell* 125: 801-14.

Lin X, Antalffy B, Kang D, Orr HT and Zoghbi HY (2000) Polyglutamine expansion down-regulates specific neuronal genes before pathologic changes in SCA1. *Nat Neurosci* 3: 157-63.

Matilla-Duenas A, Goold R and Giunti P (2008) Clinical, genetic, molecular, and pathophysiological insights into spinocerebellar ataxia type 1. *Cerebellum* 7: 106-14.

Metzger F and Kapfhammer JP (2000) Protein kinase C activity modulates dendritic differentiation of rat Purkinje cells in cerebellar slice cultures. *Eur J Neurosci* 12: 1993-2005.

Newton AC (2001) Protein kinase C: structural and spatial regulation by phosphorylation, cofactors, and macromolecular interactions. *Chem Rev* 101: 2353-64.

Orr HT (2001) Beyond the Qs in the polyglutamine diseases. *Genes Dev* 15: 925-32.

Robitaille Y, Schut L and Kish SJ (1995) Structural and immunocytochemical features of olivopontocerebellar atrophy caused by the spinocerebellar ataxia type 1 (SCA-1) mutation define a unique phenotype. *Acta Neuropathol* 90: 572-81.

Sakai N, Tsubokawa H, Matsuzaki M, Kajimoto T, Takahashi E, Ren Y, Ohmori S, Shirai Y, Matsubayashi H, Chen J et al. (2004) Propagation of gammaPKC translocation along the dendrites of Purkinje cell in gammaPKC-GFP transgenic mice. *Genes Cells* 9: 945-57.

Schols L, Bauer P, Schmidt T, Schulte T and Riess O (2004) Autosomal dominant cerebellar ataxias: clinical features, genetics, and pathogenesis. *Lancet Neurol* 3: 291-304.

Schrenk K, Kapfhammer JP and Metzger F (2002) Altered dendritic development of cerebellar Purkinje cells in slice cultures from protein kinase Cgamma-deficient mice. *Neuroscience* 110: 675-89.

Seeley WW, Crawford RK, Zhou J, Miller BL and Greicius MD (2009) Neurodegenerative diseases target large-scale human brain networks. *Neuron* 62: 42-52.

Serra HG, Byam CE, Lande JD, Tousey SK, Zoghbi HY and Orr HT (2004) Gene profiling links SCA1 pathophysiology to glutamate signaling in Purkinje cells of transgenic mice. *Hum Mol Genet* 13: 2535-43.

Serra HG, Duvick L, Zu T, Carlson K, Stevens S, Jorgensen N, Lysholm A, Burright E, Zoghbi HY, Clark HB et al. (2006) RORalpha-mediated Purkinje cell development determines disease severity in adult SCA1 mice. *Cell* 127: 697-708.

Skinner PJ, Vierra-Green CA, Clark HB, Zoghbi HY and Orr HT (2001) Altered trafficking of membrane proteins in purkinje cells of SCA1 transgenic mice. *Am J Pathol* 159: 905-13.

Stenoien DL, Mielke M and Mancini MA (2002) Intranuclear ataxin1 inclusions contain both fast- and slow-exchanging components. *Nat Cell Biol* 4: 806-10.

Tanaka C and Nishizuka Y (1994) The protein kinase C family for neuronal signaling. *Annu Rev Neurosci* 17: 551-67.

Verbeek DS, Goedhart J, Bruinsma L, Sinke RJ and Reits EA (2008) PKC gamma mutations in spinocerebellar ataxia type 14 affect C1 domain accessibility and kinase activity leading to aberrant MAPK signaling. *J Cell Sci* 121: 2339-49.

Verbeek DS, Knight MA, Harmison GG, Fischbeck KH and Howell BW (2005) Protein kinase C gamma mutations in spinocerebellar ataxia 14 increase kinase activity and alter membrane targeting. *Brain* 128: 436-42.

Yabe I, Sasaki H, Chen DH, Raskind WH, Bird TD, Yamashita I, Tsuji S, Kikuchi S and Tashiro K (2003) Spinocerebellar ataxia type 14 caused by a mutation in protein kinase C gamma. *Arch Neurol* 60 1749-51.

Yue S, Serra HG, Zoghbi HY and Orr HT (2001) The spinocerebellar ataxia type 1 protein, ataxin-1, has RNA-binding activity that is inversely affected by the length of its polyglutamine tract. *Hum Mol Genet* 10: 25-30.

Zheng Z and Keifer J (2008) Protein kinase C-dependent and independent signaling pathways regulate synaptic GluR1 and GluR4 AMPAR subunits during *in vitro* classical conditioning. *Neuroscience* 156: 872-84.

Chapter 5

Spinocerebellar ataxia-1: insights in the function of ataxin-1 and the significance for other polyglutamine expansion disorders

Manuscript in preparation

Spinocerebellar ataxia-1: insights in the function of ataxin-1 and the significance for other polyglutamine expansion disorders

Hilde A Krol[1], Elly M Hol[2] and Eric A Reits[1]

[1] Department of Cell Biology and Histology, Academic Medical Center, University of Amsterdam, The Netherlands; [2] Netherlands Institute for Neuroscience, an institute of the Royal Netherlands Academy of Arts and Sciences, Amsterdam, The Netherlands

PolyQ disorders and spinal cerebellar ataxia's

Polyglutamine (polyQ) expansion disorders is a group of dominantly inherited neurodegenerative disorders that includes Huntington's disease , dentatorubropallidoluysian atrophy , spinobulbar muscle atrophy and the spinocerebellar ataxias (SCAs) types 1, 2, 3, 6, 7 and 17. These polyQ disorders are caused by an expansion of the CAG-trinucleotide repeat that encodes for the amino acid glutamine. In the non-pathogenic form, these disease-related proteins contain a short polyQ-rich region, whereas the protein is converted into a disease-inducing form when the glutamine expansion exceeds the threshold of 36-40 amino acids (Orr and Zoghbi, 2007). SCA6 is an exception since a repeat of 20-33 amino acids is enough to trigger disease (Riess et al., 1997; Zhuchenko et al., 1997). The length of the polyQ stretch is inversely related to the age of onset. Although the disease-related proteins are widely expressed, specific cell types appear to be particular vulnerable. Each polyQ disorder is characterized by neurodegeneration in specific restricted regions of the brain. PolyQ disorders are generally characterized by the formation of intracellular aggregates in the patient's brain, which can be mimicked *in vitro*. These aggregates were previously considered to be toxic but recent studies suggest that they have a protective role by sequestering smaller oligomeric aggregates. These small aggregates are composed of polyQ protein fragments and are now considered to represent the toxic species (Arrasate and Finkbeiner, 2005). In addition, the polyQ expansion alters the normal function of the protein. For example, polyQ expansion in the huntingtin protein (htt) affects its normal role in vesicle trafficking (Arrasate and Finkbeiner, 2005; Trushina et al., 2004).

SCA types 1, 2, 3, 6, 7 and 17 are autosomal domintant SCAs. At present, 29 SCAs have been identified that all cause cerebellar atrophy leading to ataxia, tremor and dysarthria. There are three different types of mutational mechanisms that can cause SCA: polyQ expansions, non-coding repeat expansions and missense mutations. In all SCAs, the Purkinje cells in the cerebellum are affected. Since different mutations in seemingly unrelated proteins can cause a similar disease phenotype and neuropathological changes, one or multiple common pathways

likely underlie the pathogenesis of the SCAs.

SCA1 is by far the most extensively studied and described SCA disorder. However, the pathogenic mechanisms causing disease are still unclear. SCA1 is caused by a polyQ expansion mutation in the protein ataxin-1, and is characterized by a neurodegenerative process in the cerebellum which initially mainly affects the Purkinje cells. In time, however, degeneration of other brain regions such as specific brain stem neurons and loss of motoneurons in the spinal cord becomes apparent (Matilla-Duenas et al., 2008; Robitaille et al., 1995). This leads to clinical symptoms that become manifest around middle age and include slurred speech, problems with swallowing, cognitive impairments and spasticity.

The function of ataxin-1

Functions of ataxin-1 are still elusive and this complicates the understanding of the SCA1 disease process. Nonetheless, various studies have revealed important information about the functional domains of ataxin-1 as well as ataxin-1-interacting proteins. The majority of these interacting proteins play a role in transcriptional regulation or RNA synthesis, processing and degradation.

Functional domains of ataxin-1

Ataxin-1 contains three regions that regulate the function of ataxin-1 (Figure 1): the AXH-domain, the nuclear localization signal (NLS), and the phosphorylation site at Ser776. The AXH domain is a domain that is highly homologous to a portion of the HMG box transcription factor binding protein1 (HBP1) (Chen et al., 2004; de Chiara et al., 2005). In ataxin-1, the AXH domain is able to bind to RNA and a number of proteins including transcription regulators such as capicua, the silencing mediator of retinoic acid (SMRT) and thyroid hormone receptors (Tsai, 2004; Mizutani et al., 2005; Tsuda et al., 2005; (Lam et al., 2006; Mizutani et al., 2005; Serra et al., 2006; Tsai et al., 2004; Tsuda et al., 2005). In addition, the AXH domain acts as a dimerization domain and has a cluster of charged surface residues (Chen et al., 2004). This cluster is very well conserved among species and has been suggested to constitute a second binding surface for a yet unidentified partner (Carlson et al., 2008; Chen et al., 2004). The second region is the NLS which targets ataxin-1 to the nucleus. Lastly, the phosphorylation status of ataxin-1 at Ser776 has been described to be involved in nuclear body formation and interactions with several proteins such as RBM17 and 14-3-3 (Chen et al., 2003b; Emamian et al., 2003; Lim et al., 2008).

Purified ataxin-1 can bind to RNA (Yue et al., 2001). Ataxin-1 may therefore function as an RNA-binding and RNA-transporting protein, which is also suggested by its ability to shuttle between the nucleus and the cytoplasm (Irwin et al., 2005; Krol et al., 2008). A screen for modifiers of ataxin-1 function in Drosophila resulted in a nuclear pore protein and five proteins containing RNA-binding domains, one of which was the protein pumilio (Fernandez-Funez et al., 2000). In a yeast, two hybrid screens for protein interactors involved in SCAs and Purkinje cell degeneration identified, three proteins (RBM9, A2BP1 and RBPMS) which are involved in RNA binding and splicing. These proteins may link ataxia-causing proteins as most of the proteins causing SCA are not functionally related, but likely they interplay in common pathways. RNA binding and splicing could be one of these pathways. All these data suggest that ataxin-1 may indeed be involved in particular stages of RNA tran-

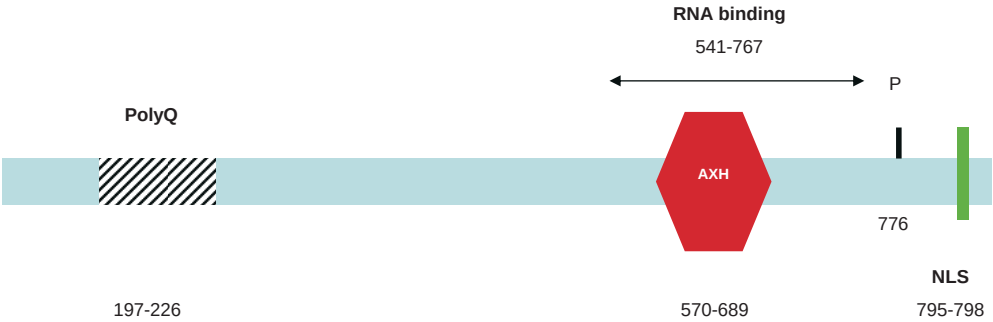

Figure 1. Schematic representation of human ataxin-1. Nuclear localization signal (NLS) targets ataxin-1 to the nucleus. AXH domain exhibits significant sequence similarity to the transcription factor HBP1and is implicated in RNA binding and self-association. Phosphorylation of serine 776 is implicated in the interaction with other proteins and nuclear body formation.

scription or processing, such as transcription regulation, mRNA nuclear export, translation, mRNA stability and splicing.

Cellular localization and nuclear body formation by ataxin-1

Whereas ataxin-1 is a predominantly nuclear protein in most neurons, Purkinje cells show both nuclear and cytoplasmic staining (Koshy et al., 1998; Servadio et al., 1995; Skinner et al., 1997). This difference may contribute to the specific sensitivity of Purkinje cells for polyQ-expanded ataxin-1, as it may be the cytoplasmic function of ataxin-1 that is specifically affected by the polyQ expansion. Overexpression of wildtype or mutant ataxin-1 protein leads to the formation of nuclear structures *in vitro* (Krol et al., 2008; Stenoien et al., 2002) Fig. 2A,B). This is in accordance with transgenic mice studies that show similar nuclear bodies upon overexpression of wildtype or mutant ataxin-1 (Koshy et al., 1998, Fig. 2C,D). Initially, these structures were regarded as insoluble polyQ aggregates. However, more recent studies showed that these nuclear bodies do not represent sequestered aggregates but ataxin-1 accumulations with a high on/off rate of ataxin-1 and may therefore represent functional protein complexes.

The role of ataxin-1 in RNA transport

The ability of ataxin-1 to bind RNA, as well as the shuttling of ataxin-1 between nucleus and cytoplasm suggests that ataxin-1 may be involved in a particular stage of RNA transport (Cooper et al., 2009). Gene transcription takes place in the nucleus where several proteins and protein complexes interplay to transcribe DNA into pre-mRNA. This pre-mRNA often transiently accumulates at the sites of transcription to undergo a number of modifications that determines the protein encoded as well as the stability and translatability of the mRNA, such as capping of the 5' end (Cooper et al., 2009; Neugebauer and Roth, 1997). Once the mRNA is transcribed, it is transported to the cytoplasm for translation into proteins. It is not known what mechanism is involved in this transport and whether this is an active or passive process (Cooper et al., 2009; Politz and Pederson, 2000). The mRNA is shuttled in so-called ribonucleotide protein (RNP) complexes. These complexes contain RNA

and *trans*-acting factors (TAFs) that support RNA transport and/or localization by binding to *cis*-acting elements of the mRNA (Kiebler and Bassell, 2006; Kindler et al., 2005). Once outside the nucleus, the RNP complexes travel along cytoskeletal filaments (actin filaments or microtubules) with the help of motor proteins until they reach their destination (Bassell and Kelic, 2004; Muslimov et al., 2002).

During transport, mRNAs in these RNPs are translationally arrested by the action of regulatory RNAs and RNA-binding proteins. Finally, translation can be initiated by several signaling pathways that target the translation initiation factor eIF4E, such as the mitogen-activated protein kinase (MAPK) signaling pathway. This mechanism enables local and controlled gene expression, which is particularly relevant in neurons such as Purkinje cells where distances between cell body and the endings of axon and dendrites can be significant and the localization of mRNA at the synapses has been proposed as a mechanism for synaptic plasticity and thus Purkinje cell function (Klann and Dever, 2004). This mRNA at the synapses has been transported from the nucleus in the cell body to the endings of the axon and dendrites. An example is mRNA of PKCγ, which has been reported to be present either in proximal dendrites or at low concentrations within the dendritic arbor (Moriya and Tanaka, 1994). PKCγ is highly expressed in Purkinje cells, is involved in synaptic plasticity and when mutated it causes SCA14. It is also a protein that interacts with ataxin-1 and promotes ataxin-1 dynamics, phosphorylation, and nuclear body formation (Verbeek et. al 2009, submitted). The targeting and local translation of mRNA has also been shown to have a role in axon guidance and neurodegeneration, which are important processes during brain development and plasticity (Willis et al., 2005). Several TAFs have indeed been shown to be nuclear-cytosplasmic shuttling proteins that first appear to associate with transcripts in the nucleus and subsequently direct mRNA transport to the cytoplasm (Farina and Singer, 2002).

Besides the presence of RNA in RNP-bodies during transport, cytoplasmic RNA can also be present in so-called P-bodies that appear to be related to neuronal RNP granules (Chen et al., 2003a). In P-bodies, mRNA accumulates and is stalled together with proteins involved in small RNA-mediated gene silencing, translational repression, mRNA surveillance and mRNA degradation (Eulalio et al., 2007; Parker and Sheth, 2007). The final destiny of mRNA in cells is determined in these P-bodies. RNP-and P-bodies share certain components and a common function is that of storing non-translated RNA. A difference between RNP-bodies and P-bodies is that P-bodies are not associated with translation-initiation factors (Eulalio et al., 2007). Other granules which contain RNA are stress granules, which are formed upon stress and keep mRNA in translation arrest. Recently, it has been reported that mRNAs can shuttle between stress granules and P-bodies (Spector, 2006). One of the P-body-marker proteins, GW182, contains a polyQ-rich domain that is essential for its P-body recruitment (Eulalio et al., 2007). It is confirmed in a recent study in yeast that proteins with Q/N rich prion-like domains contribute to the recruitment of RNPs to P-bodies (Savas et al., 2008). The RNA-binding protein pumilio and the stress granule protein TIAR both contain a glutamine rich region (Karlin and Burge, 1996; Vessey et al., 2006; Zhang et al., 2005), which is in agreement with the observation that Q stretches are needed for recruitment to P-bodies and stress granules. Thus, polyQ-

rich regions are present in RNA-binding proteins and can function as a domain that is essential in protein-protein interactions and protein complex formation in RNA granules, P-bodies and stress granules.

Thus, ataxin-1 may have functions in both the nucleus and the cytoplasm in Purkinje cells. The possible functions in each cellular compartment are summarized in Figure 3. In the nucleus, ataxin-1 forms nuclear bodies that are dynamic and disappear upon transcriptional inhibition. We suggest that ataxin-1 plays a role here in transcription, splicing and/or nuclear-cytoplasmic shuttling. No studies have been performed thus far to unravel ataxin-1 function in the cytoplasm. Here, ataxin-1 may play a role in the transport of mRNA to specific locations such as the post synapse in dendrites where it may function in repressing or activating the translation of mRNA that is present in the periphery of Purkinje cells.

What causes disease in SCA1 patients?

Purkinje cells provide the sole output from the cerebellum and each Purkinje cell receives two types of excitatory inputs namely from climbing fibers and parallel fibers. Climbing fibers are axons from cells in the inferior olive and parallel fibers are axons from granular cells in the cerebellar cortex. Both form synaptic contacts all over the dendrites of Purkinje cells. Each Purkinje cell receives input from only one climbing fiber and from hundred thousands of parallel fiber axons (Ogasawara et al., 2008). Purkinje cells rely on two types of glutamate receptors: AMPA receptors and the metabotropic glutamate receptor, mGluR1, which is abundantly expressed in Purkinje cells. When climbing fibers and parallel fibers release pre-synapse glutamate, glutamate binds to the AMPA and mGluR1 receptors at the Purkinje cell post-synapse membrane thereby producing a complex post-synaptic response involving several proteins and consisting of a calcium-release signal from intracellular stores (Hartmann and Konnerth, 2008; Serra et al., 2004). In the SCA1 mutant mouse, some neuronal genes that are involved in glutamate signaling and calcium homeostasis are downregulated in Purkinje cells, already before the onset of motor impairment and neuropathology (Lin et al., 2000; Serra et al., 2004). These genes (Homer-3, G-substrate, EAAT4, IP3I and CARP) are normally highly expressed in Purkinje cells (Gold et al., 2003) where the proteins are localized in the dendritic tree of Purkinje cells. As a result of the downregulation in SCA1, intracellular calcium levels and calcium signaling may be altered, which is likely to be detrimental for the Purkinje neurons in particular. These cells are very sensitive to fluxes in intracellular calcium levels (Duenas et al., 2006) and disruption of calcium homeostasis in SCA1 may contribute or may even initiate the pathogenic process. The *lurcher* mouse demonstrates that indeed altered glutamate signaling can cause Purkinje cell degeneration. In this mouse, a gain of function mutation in the delta2 glutamate receptor (GluRdelta2) alters glutamate signaling that results in Purkinje cell degeneration (Yue et al., 2002). By taking the downregulation of the expression of these genes as a major pathological hallmark of SCA1, we will follow step-by-step how polyQ expansion can affect ataxin-1 function at different stages of SCA1 and how these alterations may contribute to the pathology of the disease.

I. Ataxin-1 sequestration into polyQ aggregates

A general neuropathological hallmark of polyQ disorders is the presence of intra-

Table 1. Polyglutamine disorders

Disease	*Gene*	*Normal repeat length*	*Expanded repeat length*	*Primary affected brain area*	*References*
HD	Huntingtin	6-34	36-121	Striatum and cortex	Cummings and Zoghbi, 2000; Vonsattel et al., 1985
SCA1	Ataxin-1	6-44	39-82	Cerebellum, brain stem and spinal cord	Matilla-Duenas et al., 2007; Robitaille et al., 1995
SCA2	Ataxin-2	15-24	32-200	Cerebellum and brain stem	Durr et al., 1995; Orozco et al., 1989
SCA3	Ataxin-3	13-36	16-84	Cerebellum, basal ganglia, brain stem, and spinal cord	Durr, 1996;Takiyama, 1994; Woods, 1972
SCA6	$CACNA1_A$	4-19	10-33	Cerebellum	Ikeuchi et al., 1997; Zhuchenko et al., 1997
SCA7	Ataxin-7	4-35	37-306	Cerebellum and inferior olive	David et al., 1998; Martin et al., 1994
SCA17	TBP	25-42	47-63	Cerebellum, brain stem and cerebrum	Koeppen et al., 1981; Rolfs et al., 2003
SBMA	Androgen receptor	9-36	38-62	Anterior horn, bulbar region and dorsal root ganglion	Sobue et al., 1989
DRPLA	Atrophin	7-34	49-88	Cerebellum, globus pallidus, striatum, and the dentate, subthalamic and red nuclei	Burke et al., 1994; Takahashi et al., 1988

cellular aggregates in the affected neurons of patients, and this has been assumed to be the common toxic gain-of-function leading to neuronal dysfunction and eventually cell death. Although aggregates are widespread in polyQ disorders, this phenomenon cannot explain the vulnerability of specific types of neurons in each polyQ disorder (Table 1). Nuclear bodies formed by ataxin-1 can easily be misinterpreted for aggregates but we and others have shown that ataxin-1 aggregates are highly dynamic structures (Krol et al., 2008; Stenoien et al., 2002). In addition, mutant ataxin-1 has a higher on/off rate and a faster diffusion speed between nuclear bodies. This may result in the higher percentage of larger nuclear bodies (Krol et al., 2008). Nuclear body formation can be affected by the phosphorylation status of ataxin-1 at Ser776 because substitution of Ser776 by alanine to mimic a non-phosphorylation status disrupts the formation of nuclear bodies (Emamian et al., 2003). Furthermore, when ataxin-1 and the kinase PKCγ are both overexpressed in cell culture there is an increase in ataxin-1 phosphorylation and nuclear body formation (Verbeek et al. 2009, submitted). This implicates that phosphorylation modifies ataxin-1 in such a way that the ability to form nuclear bodies is increased. Various studies have questioned whether the large 'inclusions' of mutant ataxin-1 in SCA1 are pathogenic, including studies in which transgenic mice with polyQ-expanded ataxin-1 were crossed with a mice lacking the E3 ubiquitin ligase UBE3A. Since the ubiquitin proteasome system is involved in removal of mutant proteins and aggregates, it was expected that this would result in increased numbers of polyQ aggregates. However, the offspring of these mice had no nuclear inclusions at all, and even suffered from a more

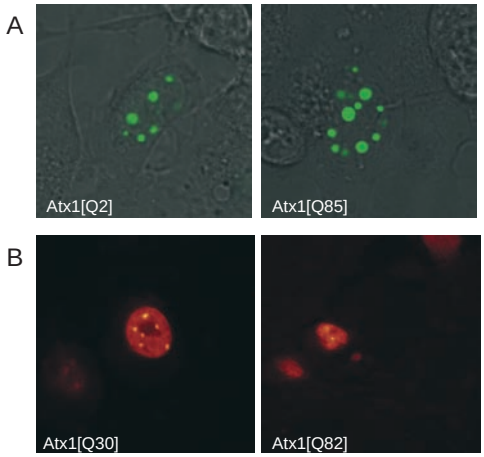

Figure 2. Both GFP-tagged (**A**) and endogenous (**B**) ataxin-1 forms nuclear bodies in Cos cells in culture and in Purkinje cells in mouse cerebellum (Krol et al., 2008). Live Cos cells expressing GFP-Atx[Q2] and GFP-Atx[Q85] (**A**) and Purkinje cells in cerebellum of a SCA1 mouse expressing Atx1[Q30] or Atx 1[Q82] (**B**) under a Purkinje cell-specific promoter.

severe Purkinje cell pathology (Cummings et al., 1999). Surprisingly, a mouse model expressing ataxin-1 with a deletion of the self-association AXH region developed a similar pathology as SCA1-mutant mice but without nuclear ataxin-1 bodies (Klement et al., 1998). These findings suggest that the nuclear bodies represent functional complexes involving ataxin-1 protein and inhibition of their formation does not prevent SCA1 pathology.

II. Altered transcriptional complex formation

The presence of mutant ataxin-1 in the nucleus is crucial for the induction of SCA1 pathogenesis. Disruption of the NLS in ataxin-1 inhibits SCA1 pathogenesis despite of the polyQ expansion mutation (Klement et al., 1998). Ataxin-1 may become incorporated into a nuclear body when transcription is initiated and stay in this complex until the process of splicing starts.

The fact that ataxin-1 is involved in transcription is also implied by the disappearance of ataxin-1 nuclear bodies when a transcription inhibitor is added to cells that express GFP-ataxin-1[Q2/A85] (unpublished data; (Irwin et al., 2005). Ataxin-1 has been described to be present in at least two different protein complexes. The first complex is involved in transcription and in this complex ataxin-1 interacts with capicua, Rorα and tip 60 (Lam et al., 2006; Zoghbi and Orr, 2009). In the second protein complex, ataxin-1 interacts with RBM17 and phosphorylation of ataxin-1 at Ser776 strengthens this interaction (Lim et al., 2008; Zoghbi and Orr, 2009). RBM17 is an RNA-binding protein that is involved in splicing. Recently, Lim et al. (2008) reported that the polyQ expansion in ataxin-1 increases the number of ataxin-1/RBM17 complexes, whereas the amount of mutant ataxin-1 is decreased in complex with capicua. Thus, polyQ expanded ataxin-1 may cause a loss of ataxin-1/capicua complexes and an increase in ataxin-1/RBM17 complexes. As a result, mutant ataxin-1 may mediate toxicity by affecting the function of protein partners that are specific for vulnerable types of neurons such as the Purkinje cells, especially since Purkinje cells are one of the few cells that co-express ataxin-1, capicua and Rorα. Here, Rorα is an orphan nuclear receptor that mediates the expression of a group of genes known to have a role in Purkinje cell development and function (Gold et al., 2003).

Twelve genes that have a Purkinje cell-specific function are downregulated in the SCA1 mouse model and also a decrease of the Rorα protein itself has been reported. In addition, partial loss of Rorα enhanced the pathogenicity of mutant ataxin-1 (Serra

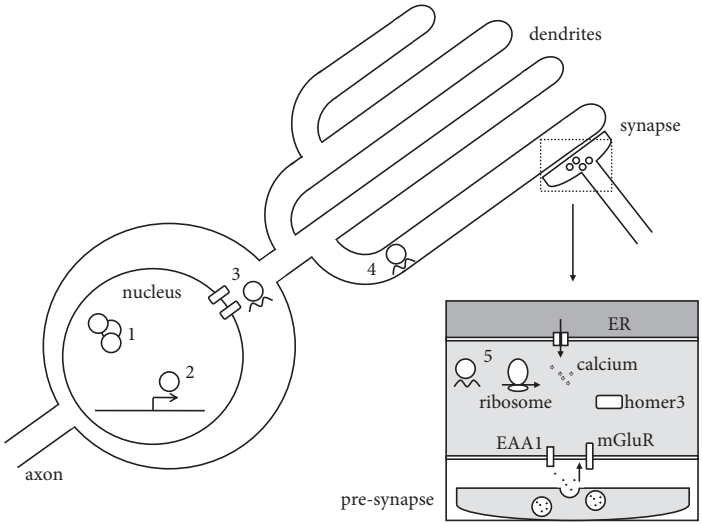

Figure 3. Schematic representation of a Purkinje cell including possible ataxin-1 functions. 1. Ataxin-1 forms dynamic nuclear bodies that disappear when transcription is blocked. 2. Ataxin-1 is involved in the process of gene transcription and splicing. 3. Ataxin-1 shuttles mRNA from the nucleus to the cytoplasm. 4. Ataxin-1 transports mRNA to specific locations in the Purkinje cell such as the postsynaptic areas in dendrites. 5. Ataxin-1 is involved in translational activation or repression of local mRNA.

et al., 2004). This could be a direct result of reduced transcription triggered by the reduced interaction between capicua,Rorα and mutant ataxin-1.

RBM17 has a relatively high expression level in Purkinje cells compared to other neurons (Zoghbi and Orr, 2009). Mutant ataxin-1 can possibly interact with splicing through the direct interaction with RBM17 resulting in either impaired splicing or incorrect splicing. Incorrectly spliced mRNAs is degraded by cellular mechanisms, such as nonsense-mediated RNA decay (Chang et al., 2007; Culbertson, 1999). As a result, these specific mRNAs and their subsequent proteins are downregulated.

An alternative pathway by which ataxin-1 could affect splicing is through its interaction with polyQ-binding protein-1 (PQBP-1). PolyQ expansion in ataxin-1 increases its affinity for PQBP-1, resulting in reduction of transcription through the interaction with RNA polymerase II (Okazawa et al., 2002). PQBP-1 is abundant in the central nervous system, and is particularly highly expressed in the cerebellum (Okazawa et al., 2002). PQBP-1 contains a domain rich in polar amino acids which is a known binding site for polyQ repeats in proteins like htt, the androgen receptor and ataxin-1, and this binding affinity is increased when the polyQ tract is expanded (Okazawa et al., 2002; Waragai et al., 1999). Overexpression of PQBP-1 in transgenic mice results in neuronal dysfunction with loss of Purkinje cells and granular cells in the cerebellum as well as loss of spinal motor neurons (Okuda et al., 2003). Overexpression of PQBP-1 in cultured cells results in the formation of nuclear bodies, similar to bodies formed by ataxin-1. PQBP-1 has been functionally linked to pre-mRNA splicing, as it has been identified as a component of spli-

ceosomal complexes and has been described to interact with the pre-mRNA splicing factor U5-15kDA (Waragai et al., 2000; Zhang et al., 2000) and the activator of pre-mRNA splicing SIPP1 (Nicolaescu et al., 2008). PQBP-1 interacts also with RNA polymerase II. Therefore, it may be a link between transcription and splicing (Okazawa et al., 2002). When PQBP-1 and SIPP1 are co-expressed in cell culture, nuclear bodies are formed (Nicolaescu et al., 2008) that resemble ataxin-1 nuclear bodies that we have observed (Krol et al., 2008). These PQBP-1/SIPP1 nuclear bodies are highly dynamic (Nicolaescu et al., 2008) like ataxin-1 bodies. Moreover, SIPP1 is a nuclear-cytoplasmic shuttling protein and binds to RNA (Craggs et al., 2001; Llorian et al., 2005).

Colocalisation of PQBP-1 and ataxin-1 has not been demonstrated yet in nuclear bodies but the interaction of ataxin-1 and PQBP-1 in the nucleus points at a role in transcription and/or splicing. Possibly, ataxin-1 alters the normal interaction between proteins that are present in these transcription and/or splicing complexes causing the downregulation of gene transcripts. However, we did not find any significant differences between the dynamics of LANP, RBM17 and PQBP-1 which all interact with ataxin-1 in the presence of wildtype and mutant ataxin-1 (Krol et al., unpublished data).

III. Impaired nuclear-cytoplasmic shuttling

Since ataxin-1 can shuttle between the nucleus and the cytoplasm, it has been suggested that ataxin-1 transports mRNA to the periphery of cells (Irwin et al., 2005; Krol et al., 2008). Earlier reports suggested that polyQ expansion of ataxin-1 impaired nuclear shuttling (Irwin et al., 2005), but our data show that polyQ-expanded ataxin-1 is still capable of shuttling between nucleus and cytoplasm with similar kinetics (Krol et al., 2008). Therefore, it is unlikely that impaired nuclear-cytoplasmic shuttling of polyQ-expanded ataxin-1 is underlying SCA1 disease.

One of the proteins that interacts with ataxin-1 in the nucleus, leucine-rich acidic nuclear protein (LANP), is a nuclear-cytoplasmic shuttling protein and this protein is predominantly present in Purkinje cells (Matilla et al., 1997). The polyQ expansion in ataxin-1 enhances the interaction between ataxin-1 and LANP. LANP is involved in processes such as regulation of gene expression, RNA transport, apoptosis, intracellular signaling and cytoskeletal dynamics (Matilla and Radrizzani, 2005). When co-transfected with ataxin-1, LANP is recruited into ataxin-1 nuclear bodies (Matilla et al., 1997). LANP is homologous to the U2A small nuclear ribonucleoprotein particle, snRNP U2A, that is involved in alternative splicing of RNA. In addition, LANP has been shown to bind and shuttle the RNA-binding protein HUR, which is involved in RNA stability and transport (Opal et al., 2003). The dynamics of LANP are not or only marginally affected by polyQ-expanded ataxin-1.

IV. Altered posttranscriptional regulation: RNA bodies and local translation

Ataxin-1 can be a component of RNP complexes or P-bodies where it contributes to the transport and/or local translation of specific mRNAs. When ataxin-1 binds directly to RNA, it can be a TAF that binds to specific cis-elements in mRNAs. Here, the polyQ expansion mutation may disrupt this interaction. Indeed, it has been described that the binding to RNA is diminished when the length of the polyQ tract increases (Yue et al., 2001). This specific element could be present in mRNAs of proteins downregulated in glutamate signaling. However, no known RNA-binding element in ataxin-1 has been

discovered yet. Other possibilities are that mutant ataxin-1 disrupts transport towards the periphery of a neuron so that mRNAs do not arrive at the destination or that mutant ataxin-1 affects local translation of specific mRNAs, for example mRNAs involved in glutamate signaling. It may keep mRNA in translational arrest or interfere with signaling pathways like that of MAPK that is required for local translation. This all can result in downregulation of the expression of glutamate signaling proteins leading to disturbed signaling and calcium homeostasis. Thus, mutant ataxin-1 may perturb mRNA processing and trafficking or local translation in critical neurons leading to the unique pathology of SCA1.

Altered posttranscriptional control of gene expression through the interaction of disease-related proteins with P-bodies is also observed in other polyQ disorders. The SCA-2-causing protein, ataxin-2, colocalizes and affects the assembly of P-bodies and stress granules through an interaction with the P-body component DDX6 (Nonhoff et al., 2007). Furthermore, genetic screens in Drosophila have revealed that mutations in the neuronally-expressed RNA-binding proteins staufen, muscle-blind, split ends and CG3249 modulate neurodegeneration in SCA8 (Mutsuddi et al., 2004). SCA8 is caused by a non-coding repeat in the SCA8 gene and is a controversial disease, since not all patients that have the mutation develop the disease. The SCA8 transcript functions as a gene regulator. Therefore, it has been proposed that an RNA gain-of-function mechanism underlies neurodegeneration. The CUG expansion in the SCA8 gene may alter the association of SCA8 protein with specific RNA-binding proteins. In addition, in the opposite direction, 3' to 5', the SCA8 gene contains a CAG expansion encoding a polyQ expansion protein (Ikeda et al., 2008). Thus, SCA8 could be both a non-coding expansion repeat and a polyQ expansion disease. Possibly, more than one pathogenic mechanism is involved. SCA8 mice and human patients have intranuclear inclusions in Purkinje cells and brainstem neurons that are positive for expanded polyQ (Soong and Paulson, 2007). Furthermore, Savas et al. (2008) showed that the Huntington's disease causing protein htt plays a role in gene silencing by means of colocalization with P-bodies and the interaction with Argonaute-2 (Ago2). Overexpression of mutant htt reduced the number of P-bodies and reporter gene silencing activity (Savas et al., 2008). Both the polyQ and the nearby proline-rich regions of htt are involved in the interaction with Ago2 (Savas et al., 2008). Thus, two polyQ disease causing proteins (htt and ataxin-2) and one gene involved in SCA8 are linked to posttranscriptional control of gene expression through the interference with processes of RNA binding or metabolism. Altered posttranscriptional regulation may be a common factor in some if not all polyQ expansion disorders.

Summary

Ataxin-1 has a number of functions but it is unknown at what level mutant ataxin-1 induces toxicity. Ataxin-1 may initially be involved in transcription in the nucleus, then remains in a complex in the nucleus during splicing (together with RBM17), acts as an RNA-binding protein or TAF for mRNA nuclear-cytoplasmic shuttling, and finally is instrumental in targeting mRNAs to distants parts of cells (dendrites, axons) for local protein production. Perhaps if ataxin-1 is involved in the recruitment of several proteins and RNAs into nuclear bodies such as Cic, RBM17, RNA, a change in its interaction

with one component may affect its interactions with the other component resulting in a gain of function alteration. Mutant ataxin-1 can induce toxicity in the nucleus by altering transcription and splicing of specific genes. It can also induce toxicity in the cell body as it may alter the transport of RNA in the cytoplasm or interfere with local translation of the mRNA

So far, the cytoplasmic functions of ataxin-1 have hardly been investigated, which may be due to the most visible hallmark of ataxin-1, the nuclear bodies. While the nuclear function is indeed affected by polyQ expansion, understanding the role of ataxin-1 in the periphery of Purkinje cells may bring us closer to the understanding why these neurons are so vulnerable to mutant ataxin-1 expression, and hopefully lead to a better understanding of the dysfunction and atrophy of these cells.

References

Arrasate M and Finkbeiner S (2005) Automated microscope system for determining factors that predict neuronal fate. *Proc Natl Acad Sci USA* 102: 3840-5.

Bassell GJ and Kelic S (2004) Binding proteins for mRNA localization and local translation, and their dysfunction in genetic neurological disease. *Curr Opin Neurobiol* 14: 574-81.

Burke JR, Wingfield MS, Lewis KE, Roses AD, Lee JE, Hulette C, Pericak-Vance MA and Vance JM (1994) The Haw River syndrome: dentatorubropallidoluysian atrophy (DRPLA) in an African-American family. *Nat Genet* 7: 521-4.

Carlson KM, Melcher L, Lai S, Zoghbi HY, Brent Clark H and Orr HT (2008) Characterization of the Zebrafish atxn1/axh Gene Family. *J Neurogenet* PMID: 19085187

Chen DH, Brkanac Z, Verlinde CL, Tan XT, Bylenok L, Nochlin D, Matsushita M, Lipe H, Wolff J, Fernandez M et al. (2003a) Missense mutations in the regulatory domain of PKC gamma: a new mechanism for dominant nonepisodic cerebellar ataxia. *Am J Hum Genet* 72: 839-49.

Chen HK, Fernandez-Funez P, Acevedo SF, Lam YC, Kaytor MD, Fernandez MH, Aitken A, Skoulakis EM, Orr HT, Botas J et al. (2003b) Interaction of Akt-phosphorylated ataxin-1 with 14-3-3 mediates neurodegeneration in spinocerebellar ataxia type 1. *Cell* 113: 457-68.

Chen YW, Allen MD, Veprintsev DB, Lowe J and Bycroft M (2004) The structure of the AXH domain of spinocerebellar ataxin-1. *J Biol Chem* 279: 3758-65.

Cooper TA, Wan L and Dreyfuss G (2009) RNA and disease. *Cell* 136: 777-93.

Craggs G, Finan PM, Lawson D, Wingfield J, Perera T, Gadher S, Totty NF and Kellie S (2001) A nuclear SH3 domain-binding protein that colocalizes with mRNA splicing factors and intermediate filament-containing perinuclear networks. *J Biol Chem* 276: 30552-60.

Cummings CJ, Reinstein E, Sun Y, Antalffy B, Jiang Y, Ciechanover A, Orr HT, Beaudet AL and Zoghbi HY (1999) Mutation of the E6-AP ubiquitin ligase reduces nuclear inclusion frequency while accelerating polyglutamine-induced pathology in SCA1 mice. *Neuron* 24: 879-92.

Cummings CJ and Zoghbi HY (2000) Trinucleotide repeats: mechanisms and pathophysiology. *Annu Rev Genomics Hum Genet* 1: 281-328.

David G, Durr A, Stevanin G, Cancel G, Abbas N, Benomar A, Belal S, Lebre AS, Abada-Bendib M, Grid D et al. (1998) Molecular and clinical correlations in autosomal dominant cerebellar ataxia with progressive macular dystrophy (SCA7). *Hum Mol Genet* 7: 165-70.

De Chiara C, Menon RP, Dal Piaz F, Calder L and Pastore A (2005) Polyglutamine is not all: the functional role of the AXH domain in the ataxin-1 protein. *J Mol Biol* 354: 883-93.

Duenas AM, Goold R and Giunti P (2006) Molecular pathogenesis of spinocerebellar ataxias. *Brain* 129:

1357-70.

Durr A, Smadja D, Cancel G, Lezin A, Stevanin G, Mikol J, Bellance R, Buisson GG, Chneiweiss H, Dellanave J et al. (1995) Autosomal dominant cerebellar ataxia type I in Martinique (French West Indies). Clinical and neuropathological analysis of 53 patients from three unrelated SCA2 families. *Brain* 118: 1573-81.

Emamian ES, Kaytor MD, Duvick LA, Zu T, Tousey SK, Zoghbi HY, Clark HB and Orr HT (2003) Serine 776 of ataxin-1 is critical for polyglutamine-induced disease in SCA1 transgenic mice. *Neuron* 38: 375-87.

Eulalio A, Behm-Ansmant I and Izaurralde E (2007) P bodies: at the crossroads of post-transcriptional pathways. *Nat Rev Mol Cell Biol* 8: 9-22.

Farina KL and Singer RH (2002) The nuclear connection in RNA transport and localization. *Trends Cell Biol* 12: 466-72.

Fernandez-Funez P, Nino-Rosales ML, de Gouyon B, She WC, Luchak JM, Martinez P, Turiegano E, Benito J, Capovilla M, Skinner PJ et al. (2000) Identification of genes that modify ataxin-1-induced neurodegeneration. *Nature* 408: 101-6.

Gold DA, Baek SH, Schork NJ, Rose DW, Larsen DD, Sachs BD, Rosenfeld MG and Hamilton BA (2003) RORalpha coordinates reciprocal signaling in cerebellar development through sonic hedgehog and calcium-dependent pathways. *Neuron* 40: 1119-31.

Hartmann J and Konnerth A (2008) Mechanisms of metabotropic glutamate receptor-mediated synaptic signaling in cerebellar Purkinje cells. *Acta Physiol*. PMID: 18983450

Ikeda Y, Daughters RS and Ranum LP (2008) Bidirectional expression of the SCA8 expansion mutation: one mutation, two genes. *Cerebellum* 7: 150-8.

Ikeuchi T, Takano H, Koide R, Horikawa Y, Honma Y, Onishi Y, Igarashi S, Tanaka H, Nakao N, Sahashi K et al. (1997) Spinocerebellar ataxia type 6: CAG repeat expansion in alpha1A voltage-dependent calcium channel gene and clinical variations in Japanese population. *Ann Neurol* 42: 879-84.

Irwin S, Vandelft M, Pinchev D, Howell JL, Graczyk J, Orr HT and Truant R (2005) RNA association and nucleocytoplasmic shuttling by ataxin-1. *J Cell Sci* 118: 233-42.

Karlin S and Burge C (1996) Trinucleotide repeats and long homopeptides in genes and proteins associated with nervous system disease and development. *Proc Natl Acad Sci USA* 93: 1560-5.

Kiebler MA and Bassell GJ (2006) Neuronal RNA granules: movers and makers. *Neuron* 51: 685-90.

Kindler S, Wang H, Richter D and Tiedge H (2005) RNA transport and local control of translation. *Annu Rev Cell Dev Biol* 21: 223-45.

Klann E and Dever TE (2004) Biochemical mechanisms for translational regulation in synaptic plasticity. *Nat Rev Neurosci* 5: 931-42.

Klement IA, Skinner PJ, Kaytor MD, Yi H, Hersch SM, Clark HB, Zoghbi HY and Orr HT (1998) Ataxin-1 nuclear localization and aggregation: role in polyglutamine-induced disease in SCA1 transgenic mice. *Cell* 95: 41-53.

Koeppen AH, Goedde HW, Hiller C, Hirth L and Benkmann HG (1981) Hereditary ataxia and the sixth chromosome. *Arch Neurol* 38: 158-64.

Koshy BT, Matilla A, Zoghbi HY (1998) Clues about the pathogenesis of SCA1: from biochemical and molecular studies of ataxin-1. In: Genetic Instabilities and Hereditary Neurological disorders. Wells RD, Warren ST (eds). Academic Press, San Diego, CA, pp 241-8.

Krol HA, Krawczyk PM, Bosch KS, Aten JA, Hol EM and Reits EA (2008) Polyglutamine expansion accelerates the dynamics of ataxin-1 and does not result in aggregate formation. *PLoS ONE* 3, e1503.

Lam YC, Bowman AB, Jafar-Nejad P, Lim J, Richman R, Fryer JD, Hyun ED, Duvick LA, Orr HT, Botas J et al. (2006) ATAXIN-1 interacts with the repressor Capicua in its native complex to cause SCA1 neuropathology. *Cell* 127: 1335-47.

Lim J, Crespo-Barreto J, Jafar-Nejad P, Bowman AB, Richman R, Hill DE, Orr HT and Zoghbi HY (2008) Opposing effects of polyglutamine expansion on native protein complexes contribute to SCA1. *Nature* 452: 713-8.

Lin X, Antalffy B, Kang D, Orr HT and Zoghbi HY (2000) Polyglutamine expansion down-regulates specific neuronal genes before pathologic changes in SCA1. *Nat Neurosci* 3: 157-63.

Llorian M, Beullens M, Lesage B, Nicolaescu E, Beke L, Landuyt W, Ortiz JM and Bollen M (2005) Nucleocytoplasmic shuttling of the splicing factor SIPP1. *J Biol Chem* 280: 38862-9.

Martin JJ, Van Regemorter N, Krols L, Brucher JM, de Barsy T, Szliwowski H, Evrard P, Ceuterick C, Tassignon MJ, Smet-Dieleman H et al. (1994) On an autosomal dominant form of retinal-cerebellar de-

generation: an autopsy study of five patients in one family. *Acta Neuropathol* 88: 277-86.

Matilla, A., B.T. Koshy, C.J. Cummings, T. Isobe, H.T. Orr, and H.Y. Zoghbi. (1997) The cerebellar leucine-rich acidic nuclear protein interacts with ataxin-1. *Nature* 389: 974-8.

Matilla A and Radrizzani M (2005) The Anp32 family of proteins containing leucine-rich repeats. *Cerebellum* 4: 7-18.

Matilla-Duenas A, Goold R and Giunti P (2008) Clinical, genetic, molecular, and pathophysiological insights into spinocerebellar ataxia type 1. *Cerebellum* 7: 106-14.

Mizutani A, Wang L, Rajan H, Vig PJ, Alaynick WA, Thaler JP and Tsai CC (2005) Boat, an AXH domain protein, suppresses the cytotoxicity of mutant ataxin-1. *Embo J* 24: 3339-51.

Moriya M and Tanaka S (1994) Prominent expression of protein kinase C (gamma) mRNA in the dendrite-rich neuropil of mice cerebellum at the critical period for synaptogenesis. *Neuroreport* 5: 929-32.

Muslimov IA, Titmus M, Koenig E and Tiedge H (2002) Transport of Neuronal BC1 RNA in Mauthner Axons. *J Neurosci* 22: 4293-301.

Mutsuddi M, Marshall CM, Benzow KA, Koob MD and Rebay I (2004) The spinocerebellar ataxia 8 noncoding RNA causes neurodegeneration and associates with staufen in Drosophila. *Curr Biol* 14: 302-8.

Neugebauer KM and Roth MB (1997) Transcription units as RNA processing units. *Genes Dev* 11: 3279-85.

Nicolaescu E, Beullens M, Lesage B, Keppens S, Himpens B and Bollen M (2008) Nature of the nuclear inclusions formed by PQBP1, a protein linked to neurodegenerative polyglutamine diseases. *Eur J Cell Biol* 87: 817-29.

Nonhoff U, Ralser M, Welzel F, Piccini I, Balzereit D, Yaspo ML, Lehrach H and Krobitsch S (2007) Ataxin-2 interacts with the DEAD/H-box RNA helicase DDX6 and interferes with P-bodies and stress granules. *Mol Biol Cell* 18: 1385-96.

Ogasawara H, Doi T and Kawato M (2008) Systems biology perspectives on cerebellar long-term depression. *Neurosignals* 16: 300-17.

Okazawa H, Rich T, Chang A, Lin X, Waragai M, Kajikawa M, Enokido Y, Komuro A, Kato S, Shibata M et al. (2002) Interaction between mutant ataxin-1 and PQBP-1 affects transcription and cell death. *Neuron* 34: 701-13.

Okuda T, Hattori H, Takeuchi S, Shimizu J, Ueda H, Palvimo JJ, Kanazawa I, Kawano H, Nakagawa M and Okazawa H (2003) PQBP-1 transgenic mice show a late-onset motor neuron disease-like phenotype. *Hum Mol Genet* 12: 711-25.

Opal P, Garcia JJ, Propst F, Matilla A, Orr HT and Zoghbi HY (2003) Mapmodulin/leucine-rich acidic nuclear protein binds the light chain of microtubule-associated protein 1B and modulates neuritogenesis. *J Biol Chem* 278: 34691-9.

Orozco G, Estrada R, Perry TL, Arana J, Fernandez R, Gonzalez-Quevedo A, Galarraga J and Hansen S (1989) Dominantly inherited olivopontocerebellar atrophy from eastern Cuba. Clinical, neuropathological, and biochemical findings. *J Neurol Sci* 93: 37-50.

Orr HT and Zoghbi HY (2007) Trinucleotide repeat disorders. *Annu Rev Neurosci* 30: 575-621.

Parker R and. Sheth U (2007) P bodies and the control of mRNA translation and degradation. *Mol Cell* 25: 635-46.

Politz JC and Pederson T (2000) Review: movement of mRNA from transcription site to nuclear pores. *J Struct Biol* 129: 252-7.

Riess O, Schols L, Bottger H, Nolte D, Vieira-Saecker AM, Schimming C, Kreuz F, Macek M Jr, Krebsova A, Macek MS et al. (1997) SCA6 is caused by moderate CAG expansion in the alpha1A-voltage-dependent calcium channel gene. *Hum Mol Genet* 6: 1289-93.

Robitaille Y, Schut L and Kish SJ (1995) Structural and immunocytochemical features of olivopontocerebellar atrophy caused by the spinocerebellar ataxia type 1 (SCA-1) mutation define a unique phenotype. *Acta Neuropathol* 90: 572-81.

Rolfs A, Koeppen AH, Bauer I, Bauer P, Buhlmann S, Topka H, Schols L and Riess O (2003) Clinical features and neuropathology of autosomal dominant spinocerebellar ataxia (SCA17). *Ann Neurol* 54: 367-75.

Savas JN, Makusky A, Ottosen S, Baillat D, Then F, Krainc D, Shiekhattar R, Markey SP and Tanese N (2008) Huntington's disease protein contributes to RNA-mediated gene silencing through association with Argonaute and P bodies. *Proc Natl Acad Sci USA* 105: 10820-5.

Serra HG, Byam CE, Lande JD, Tousey SK, Zoghbi

HY and Orr HT (2004) Gene profiling links SCA1 pathophysiology to glutamate signaling in Purkinje cells of transgenic mice. *Hum Mol Genet* 13: 2535-43.

Serra HG, Duvick L, Zu T, Carlson K, Stevens S, Jorgensen N, Lysholm A, Burright E, Zoghbi HY, Clark HB et al. (2006) RORalpha-mediated Purkinje cell development determines disease severity in adult SCA1 mice. *Cell* 127: 697-708.

Servadio A, Koshy B, Armstrong D, Antalffy B, Orr HT and Zoghbi HY (1995) Expression analysis of the ataxin-1 protein in tissues from normal and spinocerebellar ataxia type 1 individuals. *Nat Genet* 10: 94-8.

Skinner PJ, Koshy BT, Cummings CJ, Klement IA, Helin K, Servadio A, Zoghbi HY and Orr HT (1997) Ataxin-1 with an expanded glutamine tract alters nuclear matrix-associated structures. *Nature* 389: 971-4.

Sobue G, Hashizume Y, Mukai E, Hirayama M, Mitsuma T and Takahashi A (1989) X-linked recessive bulbospinal neuronopathy. A clinicopathological study. *Brain* 112: 209-32.

Soong BW and Paulson HL (2007) Spinocerebellar ataxias: an update. *Curr Opin Neurol* 20: 438-46.

Spector DL (2006) SnapShot: Cellular bodies. *Cell* 127: 1071.

Stenoien DL, Mielke M and Mancini MA (2002) Intranuclear ataxin1 inclusions contain both fast- and slow-exchanging components. *Nat Cell Biol* 4: 806-10.

Takahashi H, Ohama E, Naito H, Takeda S, Nakashima S, Makifuchi T and Ikuta F (1988) Hereditary dentatorubral-pallidoluysian atrophy: clinical and pathologic variants in a family. *Neurology* 38: 1065-70.

Trushina E, Dyer RB, Badger JD, Ure D, Eide L, Tran DD, Vrieze BT, Legendre-Guillemin V, McPherson PS, Mandavilli BS et al. (2004). Mutant huntingtin impairs axonal trafficking in mammalian neurons *in vivo* and *in vitro*. *Mol Cell Biol* 24: 8195-209.

Tsuda H, Jafar-Nejad H, Patel AJ, Sun Y, Chen HK, Rose MF, Venken KJ, Botas J, Orr HT, Bellen HJ et al. (2005) The AXH domain of Ataxin-1 mediates neurodegeneration through its interaction with Gfi-1/Senseless proteins. *Cell* 122: 633-44.

Vessey JP, Vaccani A, Xie Y, Dahm R, Karra D, Kiebler MA and Macchi P (2006) Dendritic localization of the translational repressor Pumilio 2 and its contribution to dendritic stress granules. *J Neurosci* 26: 6496-508.

Vonsattel JP, Myers RH, Stevens TJ, Ferrante RJ, Bird ED and Richardson EP Jr (1985) Neuropathological classification of Huntington's disease. *J Neuropathol Exp Neurol* 44: 559-77.

Waragai M, Junn E, Kajikawa M, Takeuchi S, Kanazawa I, Shibata M, Mouradian MM and Okazawa H (2000) PQBP-1/Npw38, a nuclear protein binding to the polyglutamine tract, interacts with U5-15kD/dim1p via the carboxyl-terminal domain. *Biochem Biophys Res Commun* 273: 592-5.

Waragai M, Lammers CH, Takeuchi S, Imafuku I, Udagawa Y, Kanazawa I, Kawabata M, Mouradian MM and Okazawa H (1999) PQBP-1, a novel polyglutamine tract-binding protein, inhibits transcription activation by Brn-2 and affects cell survival. *Hum Mol Genet* 8: 977-87.

Willis D, Li KW, Zheng JQ, Chang JH, Smit A, Kelly T, Merianda TT, Sylvester J, Van Minnen J and Twiss JL (2005) Differential transport and local translation of cytoskeletal, injury-response, and neurodegeneration protein mRNAs in axons. *J Neurosci* 25: 778-91.

Yue S, Serra HG, Zoghbi HY and Orr HT (2001) The spinocerebellar ataxia type 1 protein, ataxin-1, has RNA-binding activity that is inversely affected by the length of its polyglutamine tract. *Hum Mol Genet* 10: 25-30.

Yue Z, Horton A, Bravin M, DeJager PL, Selimi F and Heintz N (2002) A novel protein complex linking the delta 2 glutamate receptor and autophagy: implications for neurodegeneration in lurcher mice. *Neuron* 35: 921-33.

Zhang T, Delestienne N, Huez G, Kruys V and Gueydan C (2005) Identification of the sequence determinants mediating the nucleo-cytoplasmic shuttling of TIAR and TIA-1 RNA-binding proteins. *J Cell Sci* 118: 5453-63.

Zhang Y, Lindblom T, Chang A, Sudol M, Sluder AE and Golemis EA (2000) Evidence that dim1 associates with proteins involved in pre-mRNA splicing, and delineation of residues essential for dim1 interactions with hnRNP F and Npw38/PQBP-1. *Gene* 257: 33-43.

Zhuchenko O, Bailey J, Bonnen P, Ashizawa T, Stockton DW, Amos C, Dobyns WB, Subramony SH, Zoghbi HY and Lee CC. (1997) Autosomal dominant cerebellar ataxia (SCA6) associated with small polyglutamine expansions in the alpha 1A-voltage-depen-

dent calcium channel. *Nat Genet* 15: 62-9.

Zoghbi HY and Orr HT (2009) Pathogenic mechanisms of a polyglutamine mediated neurodegenerative disease: SCA1. *J Biol Chem* 284:7425-9.

Chapter 6

Mimicking proteasomal release of polyglutamine peptides initiates aggregation and toxicity

Journal of Cell Science, in press

Mimicking proteasomal release of polyglutamine peptides initiates aggregation and toxicity

Marcel Raspe[1], Judith Gillis[1], Hilde Krol, Sabine Krom, Klazien Bosch, Henk van Veen and Eric A. Reits*

Department of Cell Biology and Histology, Academic Medical Center, Meibergdreef 15, 1105 AZ Amsterdam, The Netherlands

* Author for correspondence (email: e.a.reits@amc.uva.nl), [1] Shared first authors

Summary

Several neurodegenerative disorders, including Huntington's disease, are caused by expansion of the polyglutamine (polyQ) tract over 40 glutamines in the disease-related protein. Fragments of these proteins containing the expanded polyQ tract are thought to initiate aggregation and represent the toxic species. While it is not clear how these toxic fragments are generated, *in vitro* data suggest that proteasomes are unable to digest polyQ tracts. To examine whether the resulting polyQ peptides could initiate aggregation in living cells, we mimicked proteasomal release of monomeric polyQ peptides. These peptides lack the commonly used starting methionine residue or any additional tag. Only expanded polyQ peptides appeared peptidase-resistant, and their accumulation initiated the aggregation process. As observed in polyQ disorders, these aggregates led to the sequestration of proteasomes, ubiquitin and polyQ proteins in time, and the association of Hsp70. The generated expanded polyQ peptides were toxic to neuronal cells. Our approach mimics proteasomal release of pure polyQ peptides in living cells, and represents a valuable tool to screen for proteins and compounds that affect aggregation and toxicity.

Introduction

Numerous neurodegenerative diseases are manifested by the accumulation and aggregation of intracellular proteins. These diseases include polyglutamine (polyQ) expansion disorders like Huntington's disease, spinal bulbar muscular atrophy and various spinocerebellar ataxia's (SCAs). PolyQ disorders are dominantly inherited and caused by expansions of CAG repeats. Normally, the disease-related proteins involved contain sequences of 6-40 glutamine repeats, whereas expansion of these tracts to 40-300 repeats leads to disease. The age of onset of the disorder is inversely related with the repeat length of the polyQ tracts (reviewed by Orr and Zoghbi, 2007).

The presence of proteolytic protein fragments harbouring a polyQ tract in aggregates (DiFiglia et al., 1997; Goti et al., 2004; Li et al., 1998; Schmidt et al., 1998) has

led to the 'toxic fragment hypothesis', which states that proteolytic fragments of polyQ-expanded huntingtin (Cooper et al., 1998), androgen receptor (Merry et al., 1998) or certain ataxins (Haacke et al., 2006; Ikeda et al., 1996; Young et al., 2007) initiate protein aggregation and induce neuronal toxicity. Full length polyQ proteins aggregate, but at a much slower rate than their proteolytic fragments (Merry et al., 1998). These fragments can be generated by proteases like caspases, aspartic endopeptidases, calpains and the proteasome (Gafni et al., 2004; Goldberg et al., 1996; Graham et al., 2006; Lunkes et al., 2002; Wellington et al., 1998). Accumulation of these proteolytic fragments may therefore function as a nucleation centre that sequesters full-length polyQ proteins in time. The proteasome can degrade both wildtype and expanded forms of most polyQ proteins, as was demonstrated in cultured cells and animal models (Bence et al., 2001; Jana et al., 2005). Surprisingly, polyQ-expanded proteins are not degraded to completion by the proteasome both *in vitro* and *in vivo* (Holmberg et al., 2004; Venkatraman et al., 2004). Venkatraman and colleagues (2004) showed that isolated proteasomes cannot digest polyQ tracts present in proteins, which results in the release of polyQ peptides. While flanking amino acids may be removed by exo-peptidases, the polyQ tracts themselves accumulate when not efficiently cleared by downstream peptidases.

To examine the fate of these polyQ peptides downstream the proteasome, we mimicked proteasomal generation of polyQ peptides in living cells. If polyQ peptides are degradation-resistant upon release into the cytoplasm, they may subsequently accumulate and initiate aggregation. Most studies investigating polyQ disorders use polyQ constructs that contain a starting methionine and/or fusion tags like fluorescent proteins. These polyQ constructs, including polyQ, huntingtin exon-1 or their short-lived variants, do not represent polyQ peptides generated by the proteasome. To mimic pure polyQ peptide generation, we generated a fusion protein containing green fluorescent protein (GFP), ubiquitin and polyQ peptides (GFP-Ub-polyQ). This fusion protein efficiently releases non-tagged polyQ peptides upon cleavage by ubiquitin C-terminal hydrolases (Johnson et al., 1995). We show that upon release, only polyQ peptides of disease-related lengths accumulated inside cells, and initiated intracellular protein aggregation. Proteasomes were rapidly sequestered, followed by ubiquitinated proteins, and association of chaperones, as has been observed in various polyQ disorders (Haacke et al., 2006; Holmberg et al., 2004; Kim et al., 2002). Also, various proteins containing either wildtype or expanded polyQ stretches were sequestered (Haacke et al., 2006; Perez et al., 1998). In addition, accumulation of expanded polyQ peptides led to neuronal toxicity.

Results

PolyQ-expanded peptides accumulate and induce intracellular aggregates. To examine the fate of proteasomal-released polyQ peptides in living cells, we generated fusion proteins of fluorescently-tagged Ub with polyQ peptides of wildtype and disease-related lengths. Upon expression, the C-terminal polyQ peptide is efficiently released from GFP-Ub by immediate cleavage via ubiquitin C-terminal hydrolases (Johnson et al., 1995). As a result, the generated polyQ peptide does not contain a starting methionine residue, which may affect degradation properties due to similarities with the N-terminus of a full-length protein (Bachmair et

al., 1986). Also no tags (such as fluorophores or antibody epitopes) were directly attached to the polyQ peptide. As Ub was fluorescently tagged, the fluorescence intensity reflected the amount of generated polyQ peptides. PolyQ peptides of 16, 65 or 112 glutamine residues were fused to GFP-Ub resulting in GFP-Ub-Q16, GFP-Ub-Q65 and GFP-Ub-Q112, respectively (Fig. 1A).

Expression of the different GFP-Ub-polyQ proteins and subsequent release of polyQ peptides were analyzed at 48 hours after transfection. Western blot analysis demonstrated the presence of GFP-Ub (36kDa) in all lanes (Fig. 1B, left panel). In addition, a large Ub conjugate was present, as shown before for GFP-Ub (Dantuma et al., 2006). No additional bands were detected that could represent uncleaved GFP-Ub-polyQ proteins. Efficient cleavage was also observed when the western blot was analysed for Ub (Fig. 1B, right panel). These results indicate that all polyQ peptides were efficiently cleaved from the GFP-Ub protein. Subsequent immunoblotting against polyQ using the antibody 1C2 (Trottier et al., 1995) showed that polyQ peptides were present in the GFP-Ub-Q65 and GFP-Ub-Q112 lanes (Fig. 1C). The mobility on SDS-PAGE of expanded polyQ peptides was different from their calculated molecular weights, as has been observed before for polyQ-containing proteins (Holmberg et al., 2004; Servadio et al., 1995). Some additional high molecular weight bands were present, which may represent oligomeric polyQ structures as these bands were GFP and Ub negative (Fig. 1B). The absence of Q16 peptides in cells expressing GFP-Ub-Q16 indicates that small Q peptides were efficiently cleared from the cytoplasm. It is unlikely that small Q peptides were not recognized by the 1C2 antibody, since a Q16-GFP fusion protein was recognized by 1C2 with almost equal efficiency as expanded GFP-polyQ fusions (supplementary Fig. S1A). Accumulation of Q65 and Q112 peptides, but not of Q16 peptides, suggests that expanded polyQ peptides were not efficiently degraded in living cells. To our knowledge, these peptides represent the first group of peptides that are resistant to degradation.

Since proteolytic protein fragments containing polyQ tracts are more aggregation prone than the full-length protein, we examined whether the accumulation of Q65 and Q112 peptides initiated aggregate formation. We observed a similar intracellular distribution of GFP-Ub in cells transfected with either GFP-Ub or GFP-Ub-Q16. GFP-Ub was enriched in the nucleus but was also present in the cytoplasm and in vesicles (Fig. 1D), similarly to the distribution of endogenous Ub (Dantuma et al., 2006; Qian et al., 2002). In contrast, expression of GFP-Ub-Q65 and GFP-Ub-Q112 resulted in the appearance of distinct intracellular structures decorated with fluorescent Ub in a high percentage of the transfected cells, present in either the nucleus or cytoplasm. The numbers of cells containing these structures increased both in time and with polyQ length (Fig. 1E). To investigate whether the length dependency of aggregate formation also held true for polyQ lengths nearby the threshold, we expressed GFP-Ub fused to polyQ peptides of 33 or 48 glutamine residues. Whereas GFP-Ub-Q33 did not produce aggregates, cells expressing GFP-Ub-Q48 showed aggregates, although in a much lower percentage when compared to cells expressing Q65 or Q112 peptides (supplementary Fig. S1B; data not shown). GFP-Ub fluorescence was usually present in a ring around a dark core indicating that Ub was recruited (Fig. 1F). At the ultrastructural level, this structure showed a radiating dense core similar to aggregates

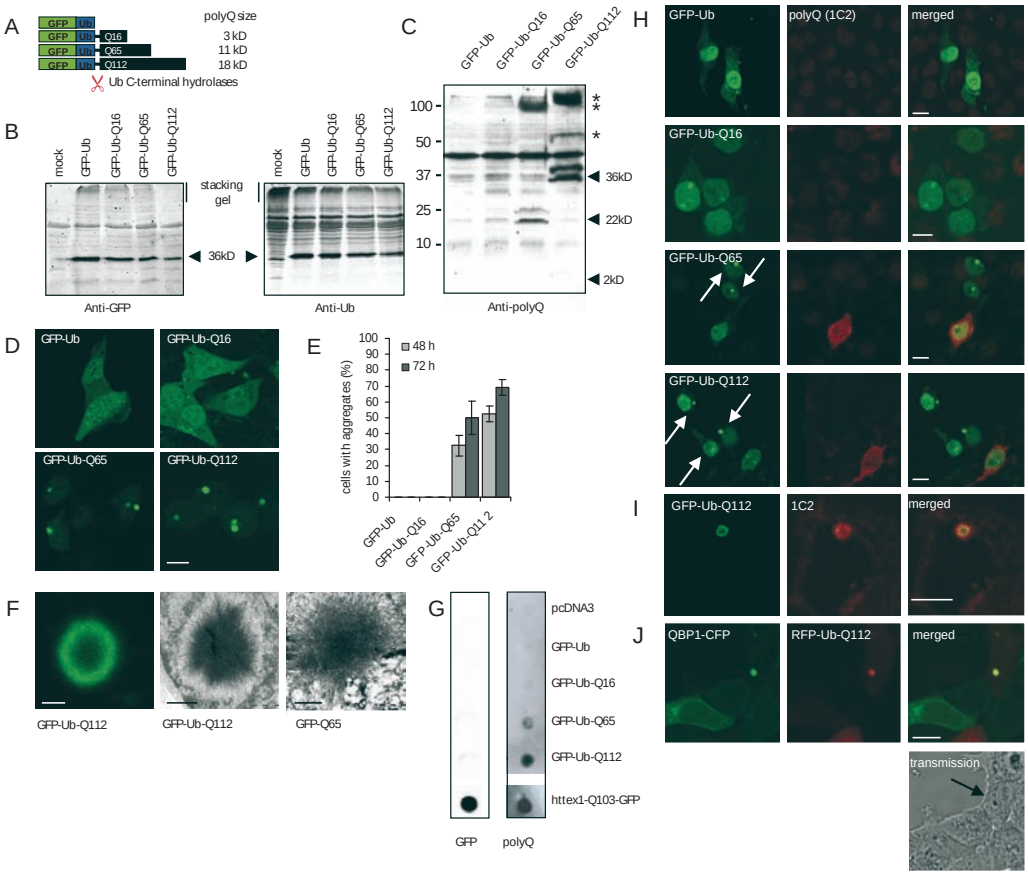

Figure 1. PolyQ-expanded peptides induce intracellular aggregates. **(A)** Schematic representation of GFP-Ub-polyQ (Q16, Q65 and Q112) fusion proteins and the generation of polyQ peptides upon synthesis and cleavage by Ub C-terminal hydrolases. **(B)** Cytosolic cell lysates of HEK293T expressing the different GFP-Ub-polyQ fusions were immunoblotted against GFP (left) or Ub (right) at 48 hours after transfection. GFP-Ub migrated at the same height for all three fusion proteins, indicating efficient cleavage of polyQ from GFP-Ub. Transfection efficiencies were lower for expanded polyQ peptide constructs. **(C)** Subsequent staining with an antibody against polyQ (1C2) revealed only the presence of polyQ peptides in cells expressing GFP-Ub-Q65 and GFP-Ub-Q112, and not of GFP-Ub-Q16. The asterix indicates potential oligomeric structures. **(D)** Confocal images of GFP-Ub and the various GFP-Ub-polyQ distribution in Mel JuSo cells. GFP-Ub-Q16 showed an Ub distribution similar to free GFP-Ub, whereas a high percentage of cells expressing GFP-Ub-Q65 and GFP-Ub-Q112 showed Ub redistribution into aggregates. Scalebar ~5µm. **(E)** Percentage of transfected HEK293T cells exhibiting fluorescent aggregate at 48 and 72 h after transfection of cells (data are mean ± SEM of 3 different experiments). The amount of aggregates in cells expressing expanded polyQ peptides increased both in time and with polyQ length. **(F)** GFP-Ub was present in a ring around the aggregate induced by GFP-Ub-Q112 (left panel) that had a fibrillar structure at the ultrastructural level (middle panel), similar to structures induced by non-cleavable GFP-Q65 (right panel). Scalebar ~1µm. **(G)** Filter retardation assay showed entrapment of aggregates in HEK293T cells expressing GFP-Ub-Q65, GFP-Ub-Q112 and httex1-Q103-GFP, after immunostaining using the 1C2 antibody. In contrast, GFP was only present when the non-cleavable fusion protein Htt-exon1-GFP was used. **(H)** Confocal images of cells expressing GFP-Ub or the various GFP-Ub-polyQ constructs after immunostaining using antibodies against polyQ (1C2). Mel Juso cells expressing GFP-Ub or GFP-Ub-Q16 showed no polyQ staining. Cells expressing GFP-Ub-Q65 and GFP-Ub-Q112 showed cytoplasmic polyQ staining when no aggregates were present. The presence of aggregates depleted the cells of free polyQ peptides, preventing polyQ staining. The arrows indicate ▷

▷ an aggregate. Scalebar ~5µm. **(I)** Protease K treatment dissolved the protein shells around the polyQ aggregate, resulting in labeling the outside of the aggregation core with the anti-polyQ antibody 1C2. Scalebar ~5µm. **(J).** The Q-binding peptide QBP1-CFP was redistributed into aggregates induced by RFP-Ub-Q112. The arrow indicates the presence of a visible aggregate by phase contrast. Scalebar ~5 µm.

formed by non-cleavable GFP-polyQ fusion proteins (Fig. 1F) and expanded huntingtin (Qin et al., 2004). In cells expressing Q65 and Q112 peptides, these dense structures were resistant to SDS and selectively trapped in a filter-retardation assay (Wanker et al., 1999). Immunostaining using 1C2 antibody showed that the trapped structures contained polyQ peptides (Fig. 1G), similar to huntingtin exon-1-Q103 (httex1-Q103-GFP) (Wanker et al., 1999). This suggests that expanded polyQ peptides induced intracellular SDS-resistant aggregates. Whereas Httex1-GFP was also positive for GFP, no GFP was present on the filter trap when using the GFP-Ub-polyQ constructs, indicating efficient cleavage of the GFP-Ub-polyQ fusion proteins (Fig. 1G). Analysis of the soluble and insoluble fractions of cell lysates showed no uncleaved GFP-Ub-Q112 fusion proteins in either fraction (supplementary Fig. S1C).

To confirm the presence of polyQ peptides in intracellular aggregates, we immunostained cells expressing Q16, Q65 or Q112 peptides with 1C2 antibody. As expected, no polyQ peptides were detected in cells expressing GFP-Ub or GFP-Ub-Q16 (Fig. 1H). However, cells transfected with GFP-Ub-Q65

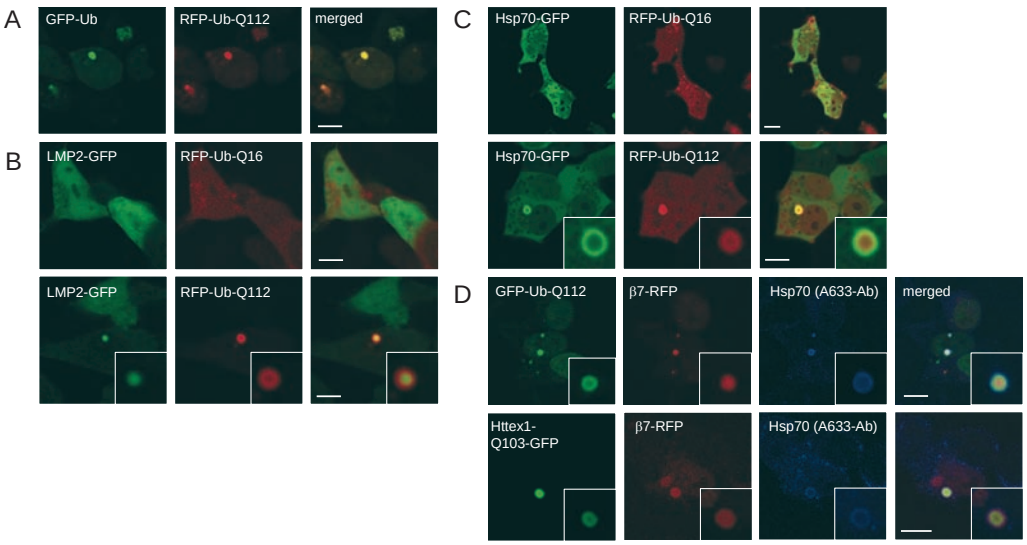

Figure 2. PolyQ peptide aggregates recruit UPS components and chaperones. Mel Juso cells were transfected with the indicated constructs and imaged at 48 hours after transfection. **(A).** Co-expression of GFP-Ub and RFP-Ub derived from RFP-Ub-Q112 resulted in identical redistribution into aggregates. **(B).** Proteasomes labeled with LMP2-GFP colocalized with the core of aggregates induced by RFP-Ub-Q112, with RFP-Ub surrounding the core. LMP2-GFP was freely distributed in nucleus and cytoplasm of cells expressing RFP-Ub-Q16. **(C).** The chaperone Hsp70-GFP was redistributed into aggregates induced by RFP-Ub-Q112, and formed an additional ring around the Ub-positive polyQ peptide aggregate. **(D).** Upon transfection with GFP-Ub-Q112 or httex1-Q103-GFP together with the proteasomal subunit β7-RFP, cells were immunostained for endogenous Hsp70. The proteasome was within the aggregate core, surrounded by Ub and an additional ring of chaperones. Scalebar ~5 µm.

or GFP-Ub-Q112 showed two patterns of polyQ staining, dependent on the presence of aggregates. When aggregates were not present, cells showed cytoplasmic polyQ staining, whereas GFP-Ub localization was predominantly nuclear. On the other hand, cells containing polyQ peptide aggregates were not recognized by 1C2 antibody (Fig. 1H; arrows indicate an aggregate). A similar difference in immunostaining was obtained using the anti-polyQ antibody MW1 (Ko et al., 2001) (supplementary Fig. S1D). The absence of polyQ staining in cells containing aggregates was likely due to the dense aggregate structure and its surrounding protein layers that may have shielded the polyQ core. Indeed, pretreatment with proteinase K degraded shielding proteins and resulted in positive immunostaining of polyQ peptide aggregates (Fig. 1I), as has been observed previously for huntingtin aggregates (Qin et al., 2004). To further confirm that the aggregates contained polyQ peptides, we used a cyan fluorescent protein (CFP)-tagged Q-binding peptide (QBP-1) which selectively binds to polyQ aggregates (Nagai et al., 2000). QBP-1 showed a cytoplasmic distribution pattern when expressed alone or together with RFP-Ub or RFP-Ub-Q16 (data not shown). However, cells harboring aggregates initiated by Q112 peptides showed binding of QBP-1 to aggregates (Fig. 1J). Taken together, these results indicate that expanded polyQ peptides are not efficiently degraded and subsequently initiate formation of aggregates that display all characteristics of disease-related polyQ aggregates.

PolyQ peptide aggregates recruit proteasomes, ubiquitin and chaperones. Aggregates formed by expanded polyQ proteins often sequester proteins involved in the ubiquitin proteasome system (UPS) but also chaperones (Holmberg et al., 2004; Kim et al., 2002). We examined whether aggregates induced by expanded polyQ peptides showed a similar sequestration of UPS components. GFP-Ub was present in a ring around the aggregates (Fig. 1F). Absence of Ub in the aggregate core can be explained by the lack of lysine residues in polyQ peptides, thereby excluding ubiquitination of the polyQ peptides. The presence of GFP-Ub around the core was not due to inefficient cleavage of GFP-Ub-polyQ, since no uncleaved GFP-Ub-polyQ fusions were detected by SDS-PAGE (Figs. 1B and S1C) and filtertrap (Fig. 1G). In addition, co-expression of GFP-Ub with RFP-Ub-Q112 showed a similar sequestration of both fluorescently-tagged Ub proteins into aggregates (Fig. 2A), indicating efficient cleavage. This suggests that the presence of GFP-Ub is due to ubiquitination of sequestered proteins.

We examined whether proteasomes colocalized with polyQ aggregates in our model, by co-expressing the different RFP-Ub-polyQ constructs with GFP-tagged immuno-proteasomal subunit LMP2. LMP2 is efficiently incorporated into active proteasomes (Reits et al., 1997). Notably, LMP2-GFP was present in the core of polyQ aggregates, suggesting that proteasomes were recruited to aggregates even before Ub sequestration (Fig. 2B). A similar recruitment was observed when using the constitutive proteasome subunit β7 (Fig. 2D). This finding most likely reflects a proteasomal attempt to degrade accumulating polyQ peptides. The sequestered proteasomes and Ub seemed irreversibly trapped, which was revealed with FRAP (Reits and Neefjes, 2001) to determine on/off rates of the sequestered molecules. Upon photobleaching of one half of an aggregate, no exchange between the sequestered proteasomes or Ub and the surroundings was observed (supplementary Fig. S2A). This indicates that the proteasome became im-

mobilized, as has been previously observed (Holmberg et al., 2004).

We also examined whether chaperones like Hsp70 were bound to polyQ aggregates, as has been observed in polyQ diseases (Kim et al., 2002; Matsumoto et al., 2006). Upon co-transfection of the different RFP-Ub-polyQ fusion proteins with GFP-tagged Hsp70, we observed an additional ring-like structure of Hsp70-GFP around Ub-positive aggregates (Fig. 2C). FRAP analysis revealed that Hsp70 was not irreversibly trapped in the aggregate (supplementary Fig. S2A), consistent with previous observations (Kim et al., 2002; Matsumoto et al., 2006). To compare the composition of aggregates initiated by Q112 peptides with aggregates formed by polyQ-expanded huntingtin exon-1, cells were transfected with either GFP-Ub-Q112 or httex1-Q103-GFP together with β7-RFP-tagged proteasomes, and cells were subsequently immunostained for endogenous Hsp70. Triple color analysis showed that the core of the aggregate was positive for proteasomes (red). This core was surrounded by Ub or httex1-Q103 (green). Finally, Hsp70 was present within the most outer layer of the aggregate (blue) (Fig. 2D). This suggests that various proteins associate at different stages or with different affinities during aggregate formation. The presence of GFP-Ub and httex1-Q103 in a similar layer may suggest the recruitment of ubiquitinated proteins and polyQ proteins in this stage of aggregate formation. Since aggregates initiated by expanded polyQ peptides also contained Ub, proteasomes and chaperones as has been described before, our model faithfully mimics aggregate formation in polyQ diseases.

Sequestering of glutamine-containing proteins into polyQ peptide aggregates. The presence of httex1-Q103 in ring-like structures around the aggregate and not within the core (Fig. 2D) suggests recruitment of large polyQ fragments into aggregates in a later stage. To examine this hypothesis, we co-expressed RFP-Ub-Q112 and httex1-Q103-GFP. Indeed, we found that httex1-Q103-GFP was sequestered into aggregates induced by polyQ peptides (Fig. 3A). In addition, the aggregation rate of httex1-Q103-GFP was also dramatically increased when Q112 peptides were present (supplementary Fig. S2B), which suggests that polyQ peptides initiate aggregates that accelerate huntingtin aggregation. Similar results were obtained with truncated polyQ-expanded ataxin-3 (Atx3-Q85-GFP) and the SBMA-related truncated androgen receptor with a Q84 repeat (AR-Q84-GFP) (data not shown).

Aggregates induced by disease-related polyQ proteins also sequester the wildtype protein expressed by the non-expanded allele (Busch et al., 2003; Haacke et al., 2006). We examined whether polyQ peptide aggregates also sequester non-expanded, wildtype polyQ proteins. The non-expanded httex1-Q25-GFP remained freely distributed in cells that co-expressed either RFP-Ub or RFP-Ub-Q16 (supplementary Fig. S2B). In contrast, httex1-Q25-GFP was recruited into polyQ peptide aggregates when co-transfected with RFP-Ub-Q112 (Figs. 3B and S2B). A similar entrapment of wildtype truncated ataxin-3 (Atx3-Q28-GFP) (supplementary Fig. S2C) and the truncated androgen receptor (AR-Q19-GFP) was observed (data not shown). This sequestration of wildtype polyQ proteins may therefore lead to loss of function. Sequestering of non-expanded polyQ proteins was not limited to disease-related proteins, as other polyQ proteins were recruited into aggregates initiated by polyQ peptides, including Q16-GFP (Fig. 3C), but also the Q-stretch containing transcription factor TBP1

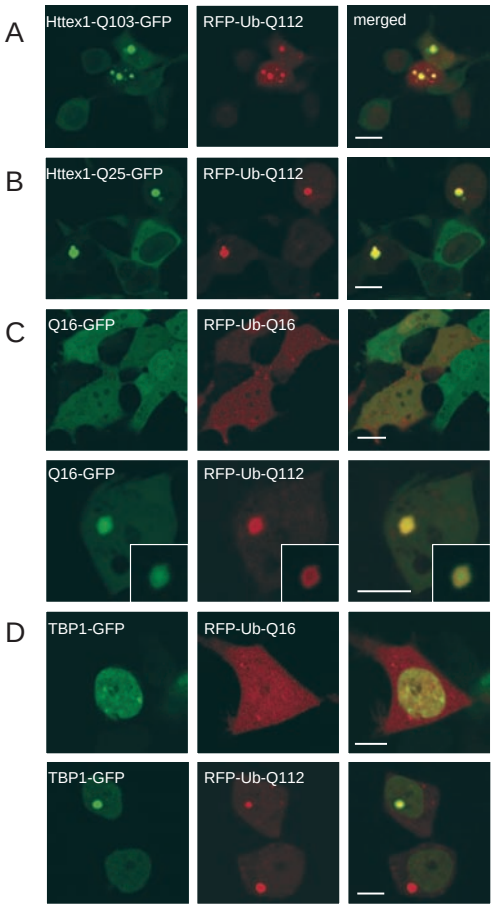

Figure 3. Sequestration of glutamine-containing proteins into polyQ peptide aggregates. Mel Juso cells were transfected with the indicated constructs and imaged at 48 hours after transfection. **(A).** Expression of RFP-Ub-Q112 led to the sequestering of httex1-Q103-GFP into polyQ aggregates. **(B).** Httex1-Q25-GFP became sequestered into polyQ peptide aggregates when cells were co-transfected with RFP-Ub-Q112. **(C).** The non-cleavable fusion protein Q16-GFP was diffusely distributed in cytoplasm and nucleus of cells expressing RFP-Ub-Q16, but co-localized with aggregates induced by RFP-Ub-Q112. (**D**). The Q-containing transcription factor TBP1 was recruited to aggregates induced by RFP-Ub-Q112 peptides, but only when the polyQ peptide aggregate was localized in the nucleus. Scalebar ~5 µm.

when nuclear aggregates were present (Fig. 3D).

PolyQ peptides induce aggregates and toxicity in neuronal cells. To examine whether polyQ peptides also initiate aggregate formation in neuronal cells, we transiently transfected N2A neuroblastoma cells with the various GFP-Ub-polyQ constructs. N2A cells transfected with either GFP-Ub-Q65 or GFP-Ub-Q112 developed aggregates similar to those present in non-neuronal cells (Fig. 4A), whereas GFP-Ub-Q16 expressing cells showed an Ub distribution comparable to GFP-Ub alone. Since Huntingtons disease mostly affects striatal cells, we also used immortalized STHdh+/+ striatal cells (Trettel et al., 2000) which similarly generated intracellular aggregates when transfected with GFP-Ub-Q65 or Q112 (Fig. 4A). Many cells rounded up after expression of expanded polyQ peptides, suggesting toxicity, although it did not correlate with the presence of GFP-Ub positive aggregates. To determine whether the expressed polyQ peptides were toxic, the viability of transfected N2A cells was tested using propidium iodide (PI). Expression of expanded polyQ peptides resulted in increased numbers of PI-positive cells (data not shown). However, hardly any double-positive cells were observed. This is presumably explained by the fact that uptake of PI into polyQ peptide expressing cells was often preceded by loss of GFP fluorescence (Fig. 4B) as observed before (Arrasate and Finkbeiner, 2005). Since loss of fluorescence seemed to be associated with cell death, we used another approach to quantify polyQ-peptide induced toxicity. To determine changes in the number of GFP-Ub positive cells in time, we used FACS analysis and compared cell populations expressing the different GFP-Ub-polyQ proteins at 24 and 48 hours after transfection. There was no

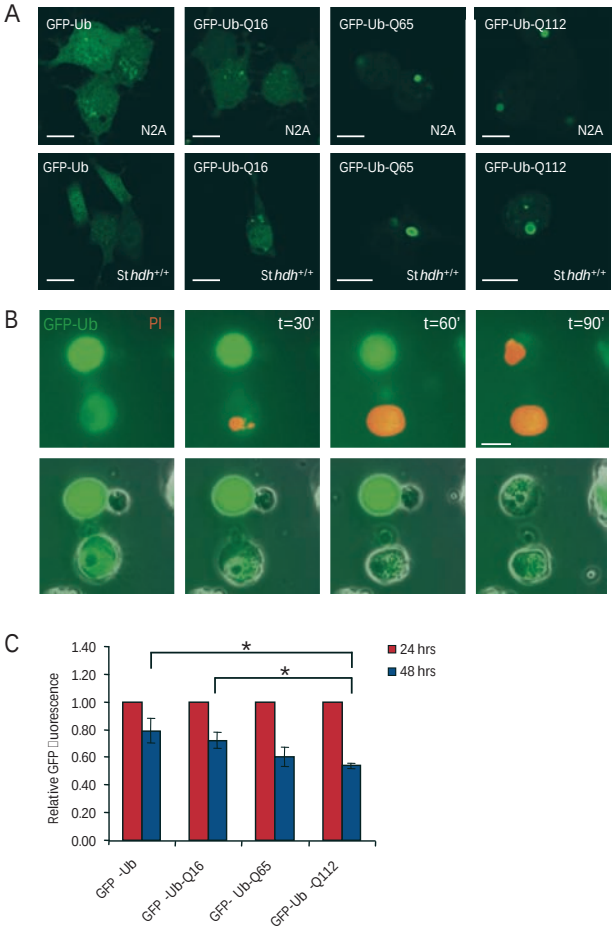

Figure 4. PolyQ peptides induce aggregates and toxicity in neuronal cells. **(A).** Confocal images of N2A neuroblastoma (upper panel) and immortalized STHdh+/+ striatal cells (lower panel) showed diffuse cytoplasmic, nuclear and vesicular distribution of ubiquitin in cells expressing GFP-Ub or GFP-Ub-Q16. GFP-Ub was sequestered into aggregates when cells were transfected with GFP-Ub-Q65 or GFP-Ub-Q112. **(B).** Loss of GFP-Ub coincided with cell death induced by GFP-Ub-Q112 expression as visualized by PI uptake. Timescale is 30 minutes between images taken by automated fluorescence microscopy. **(C).** Loss of GFP-positive cells was determined by FACS analysis 24 (red) or 48 (blue) hours after transfection (mean ± SEM of 3 different experiments, each in triplicate). GFP-Ub-Q112 showed a significant increase in neurotoxicity in N2A neuroblastoma cells when compared to GFP-Ub or GFP-Ub-Q16 ($p<0.05$, two-tailed unpaired t-test). Scalebar ~5 μm.

difference in GFP-Ub fluorescence between cells expressing either GFP-Ub or GFP-Q16 in time. However, a significant decrease in fluorescence was observed in cells expressing GFP-Ub-Q112 when compared to GFP-Ub or GFP-Ub-Q16 ($p<0.05$), indicating that expression of Q112 peptides induced cell death (Fig. 4C). GFP-Ub-Q65 had a mild, although not significant, effect on cell death. Taken together, these results showed that expanded

polyQ peptides form aggregates and become toxic to neuronal cells.

Discussion

Proteolytic fragments-containing expanded polyQ tracts are more aggregation-prone than original full-length proteins, as has been shown for huntingtin (Cooper et al., 1998), androgen receptor (Merry et al., 1998), ataxin-3 (Haacke et al., 2006) and ataxin-7 (Young et al., 2007). Recently, it was also postulated that an expanded polyQ fragment was expressed in SCA8 due to antisense transcription resulting in polyQ inclusions (Ikeda et al., 2007). These data suggest that polyQ fragments may be fundamental in initiating aggregation. However it has been shown that expanded polyQ proteins are efficiently targeted to the proteasome (Holmberg et al., 2004), which can degrade entire proteins with the exception of polyQ tracts (Venkatraman et al., 2004). Degradation by the proteasome may result in the release of polyQ peptides, whose flanking amino acids may be removed by exo-peptidases. It is unknown whether the resulting pure polyQ peptides are rapidly degraded by peptidases. If resistant, their subsequent accumulation may initiate aggregation and toxicity as observed in polyQ disorders. In order to examine this toxic fragment hypothesis, we mimicked intracellular proteasomal polyQ peptide generation as closely as possible by fusing pure polyQ peptides to GFP-tagged Ub. While Ub-polyQ fusions have been used before, these polyQ fragments also included either GFP tags (Kaytor et al., 2004; Verhoef et al., 2002) or additional amino acids including a starting methionine residue (Marsh et al., 2000). Expression of our constructs resulted in the efficient release of "naked" polyQ peptides due to immediate cleavage by Ub C-terminal hydrolases. This was shown both by SDS-PAGE that showed a band at equal height for GFP-Ub irrespective of the original construct (Fig. 1B), analysis of the filtertrap assay (Fig. 1G) and the insoluble fraction (supplementary Fig. S1C) and different intracellular locations of GFP-Ub and polyQ peptides (Fig. 1H). Since the released polyQ peptides did not contain a starting methionine or additional tags, they closely resembled peptide generation by the proteasome. All previous studies have relied on expression of polyQ fusions that did include such features, which can significantly alter the *in vivo* behavior of polyQ fragments. Starting methionines lend the peptides resemblance to the N-terminus of proteins, possibly affecting the rate of degradation (Bachmair et al., 1986). Fluorescent tags contain lysine residues, which can serve as targets for ubiquitination and subsequent degradation by the proteasome. The intracellular release of monomeric polyQ peptides is also closer to the *in vivo* situation than the addition of synthesized polyQ peptide aggregates to cells (Yang et al., 2002).

We showed that only polyQ peptides of disease-related lengths accumulated in cells and initiated aggregation. The characteristics of aggregates induced by expanded polyQ peptides were similar to aggregates initiated by expression of expanded polyQ-containing proteins (Holmberg et al., 2004; Kim et al., 2002; Perez et al., 1998; Qin et al., 2004). These characteristics include sequestration of proteasomes, ubiquitin and other polyQ containing proteins such as TBP, and the presence of Hsp70. While previous studies only speculated on the effect of proteasomal release of polyQ peptides in living cells, we show here that 'proteasomal-derived' expanded polyQ peptides by themselves are sufficient to accumulate and initiate aggregation. Accumulation of expanded

polyQ peptides is toxic to neuronal cells, but it remains to be established which particular step in aggregate formation is toxic. The toxicity seems to be induced by necrosis instead of apoptosis, as no apoptotic markers such as annexin-5 or activated caspases were detected (data not shown). The toxic species may be either small polyQ peptide oligomers or large polyQ aggregates. Further studies are required to determine whether the proteasome can indeed generate similar polyQ peptides from different polyQ proteins. If so, these released polyQ peptides may be the common feature of the different polyQ disorders.

Based on our findings, we propose a model in which expanded polyQ peptides are degradation-resistant, and their accumulation leads to intracellular polyQ aggregates (Fig. 5). Proteasomes are rapidly recruited into the polyQ core, possibly in a final attempt to degrade the expanded polyQ peptides. Subsequently, other proteins are sequestered and ubiquitinated, perhaps due to (partial) unfolding. These events also lead to the binding of chaperones like Hsp70 that may recognize denatured proteins. All these events result in concentric ring-like structures formed around the aggregate (Fig. 5). Essential proteins are depleted from the cell, contributing to cellular dysfunction. We conclude that polyQ peptides may be fundamental in initiating aggregation and sequestration of different types of proteins including polyQ proteins. Whereas FRAP experiments indicated that UPS components were immobilized, we could not detect proteasomes or Ub in the SDS-insoluble fraction of cell lysates (data not shown) or by filtertrap (Fig. 1G). This suggests that the recruited UPS components could still be solubilized.

We were able to detect expanded polyQ peptides containing Q65 or Q112 on Western blot and by immunostaining in fixed cells, but we were unable to detect any Q16 peptides. These short polyQ peptides are most likely rapidly degraded by downstream peptidases like PSA (Bhutani et al., 2007) that can digest short polyQ peptides and perhaps also extended peptides with less efficiency. Alternatively, a technical explanation for this result might be poor staining by the 1C2 antibody. It has been suggested that anti-polyQ antibodies do not detect the polyQ peptide itself, but interact with the secondary structure created by the expanded polyQ peptide (Li et al., 2007). Nonetheless, we showed that the 1C2 antibody was able to recognize a Q16 peptide fused to GFP with almost equal efficiency as GFP-Q65 and GFP-Q112 proteins. Similarly, the polyQ-antibody MW1 was able to detect a Q16-GFP fusion protein but no Q16 peptides derived from GFP-Ub-Q16 (data not shown). This shows our inability to detect Q16 peptides is not likely to be caused by the intrinsic inability of the 1C2 antibody to recognize this peptide species. Thus, the inability to detect any Q16 peptides in cells expressing GFP-Ub-Q16 is most likely due to rapid and efficient degradation of non-expanded polyQ peptides. During the preparation of this manuscript, it has been suggested that isolated proteasomes are able to cleave multiple times within a short polyQ-containing peptide (Pratt and Rechsteiner, 2008). They argued that Venkatraman and colleagues (Venkatraman et al., 2004) underestimated the amount of cleaved polyQ-fragments as a consequence of their mass-spectrometry methods. However, their conclusion was also based on other experiments such as Western blot analysis of polyQ protein products generated by proteasomes, and are in line with the conclusions by Holmberg and colleagues (2004). The observation by Pratt and Rechsteiner (2008) was done in

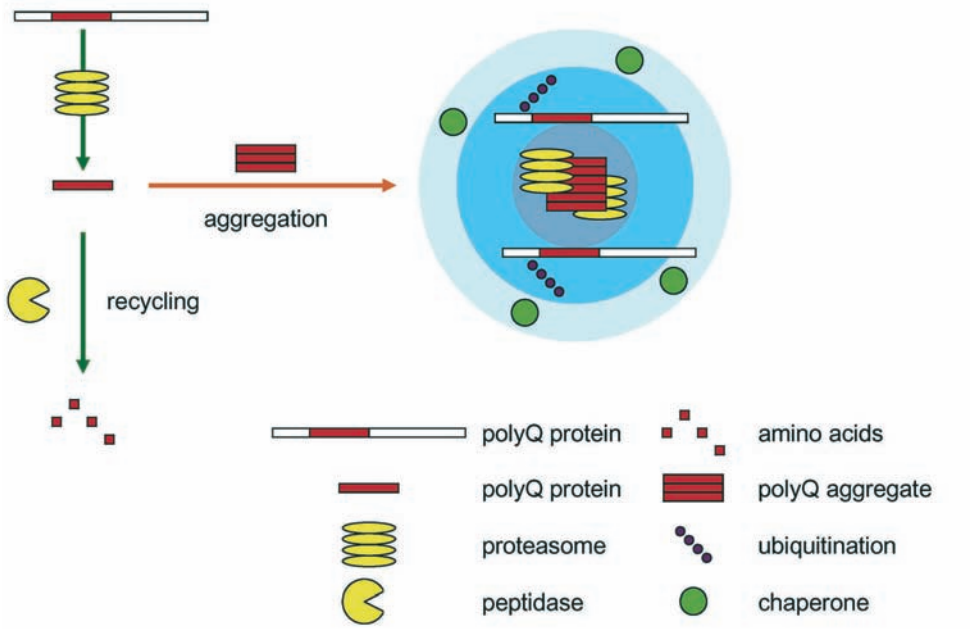

Figure 5. Model of polyQ peptide aggregate formation and sequestering of UPS components. Upon proteasomal degradation of polyQ proteins, pure polyQ peptides are released into the cytoplasm, where peptidases recycle them into amino acids. Expanded polyQ peptides show resistance to degradation, leading to accumulation and initiation of aggregate formation. Proteasomes are rapidly recruited in an attempt to degrade the fragments. In time, other proteins including various polyQ proteins are irreversibly sequestered, which become subsequently ubiquitinated. Finally, chaperones like Hsp70 are recruited, possibly as sequestered proteins become partly unfolded.

the presence of a mutated PA28γ subunit, which alters proteasomal access and specificity to peptides. In addition, although isolated proteasomes may be able to cleave short polyQ peptides, our observation that Q65 and Q112 peptides readily aggregate suggests that the proteasome cannot efficiently degrade expanded polyQ peptides and thus cannot prevent their accumulation.

PolyQ aggregation is commonly visualized using full-length or truncated polyQ-proteins that are GFP-tagged, which therefore represent proteins that require degradation by the proteasome. When such GFP-tagged proteins are degraded by the proteasome, it results in the release of non-fluorescent polyQ peptides that initiate aggregation and subsequently sequester GFP-tagged fragments or full-length polyQ proteins in time. Visualization of aggregation using GFP-tagged polyQ proteins thus represents a later stage in aggregate formation and does not reveal much about the initiation of aggregation. Long- or short-lived polyQ proteins have been used to link degradation to aggregation kinetics, where long-lived GFP-polyQ (Michalik and Van Broeckhoven, 2004; Verhoef et al., 2002) and GFP-tagged polyQ expanded httex1 (Kaytor et al., 2004) fusion proteins were compared to short lived variants. In these studies, proteasomal degradation of short-lived expanded polyQ proteins resulted in reduced formation of GFP positive aggregates compared to their long-

lived counterparts. Strikingly, toxicity was higher in cells expressing the short-lived expanded httex1 when compared to the long-lived version (Kaytor et al., 2004). Our model can explain this unexpected finding: short-lived polyQ proteins are more rapidly degraded than long-lived proteins, resulting in aggregation-prone and toxic polyQ peptides. However, such aggregates remain invisible as GFP fluorescence of the short-lived proteins is lost due to rapid breakdown, preventing its incorporation in the aggregates. Consequently, these results have likely led to an underestimation of the real number of aggregates formed by short-lived proteins in these studies. The increased toxicity was in fact presumably caused by higher levels of generated polyQ peptides. The reduced toxicity in GFP- positive cells by Verhoef and colleagues (2002) may similarly be explained by preferential loss of fluorescence by toxic fragments, since only toxicity of GFP-positive cells were analyzed.

Our method mimicking proteasomal release of polyQ peptides is a valuable tool to investigate a number of important questions concerning the role of polyQ peptides in Huntingtons disease and related neurodegenerative disorders. It enables us to identify proteases or peptidases that can target intracellular polyQ peptides *in vivo*, providing a strategy to prevent accumulation of toxic polyQ peptides. Similarly, the role of alternative degradation pathways, such as autophagy, in clearance of polyQ aggregates can be investigated. Our approach may also be useful to screen for compounds that reduce aggregation and decrease toxicity.

Materials and Methods

Plasmid constructs. Ub was generated by PCR from GFP-Ub (Dantuma et al., 2006) with forward primer 5'-CCCGAGCTCAGATGCAGATCTTCGTGAAG-3' and reverse primer 5'-CTCGGGCCCTCACCCACCTCTGAGACGG-3' and ligated into EGFP-C1 (Clonetech, USA). The resulting construct GFP-Ub was again generated by PCR with forward primer 5'-CGCGGATCCATGGTGAGCAAGGGCGAG-3' and a reverse primer 5'- CGGGAATTCCTGCAGCCCACCTCTGAGACGGAG-3', and ligated into Ub-x-GFP-Q16/65/112 (Verhoef et al., 2002) where the Ub-x-GFP insert was replaced by GFP-Ub, resulting in GFP-Ub-Q16/Q65/Q112. This procedure was required to remove the restriction site PstI present between GFP and Ub, since PstI was also required for Ub-polyQ ligation. The use of restriction sites required the presence of some flanking amino acids, resulting in an N-terminal Leu residue and a Glu-Thr-Ser-Pro-Arg sequence at the C-terminus. GFP was exchanged for mRFP to generate the different RFP-Ub-polyQ fusions. The alternative polyQ peptide lengths of Q33 and Q48 were generated by re-transformation of GFP-Ub-Q65, leading to altered polyQ lengths. Q16-GFP was generated by inserting a Q16 repeat (derived from Ub-M-GFP-Q16) in front of GFP. Htt exon-1 was kindly provided by Ron Kopito (University of California, Stanford, CA), Atx3 by Henry Paulson (University of Michigan, Ann Arbor, MI), AR by Paul Taylor (University of Pennsylvania School of Medicine, Philadelphia, PA) GFP-Ub, RFP-Ub, Ub-M-GFP-polyQ (used to express GFP-polyQ) and β7-RFP by Nico Dantuma (Karolinska Institutet, Stockholm, Sweden) HSP70-GFP by Harm Kampinga (University of Groningen, Groningen, The Netherlands), TBP1 by Rick Morimoto (Northwestern University, Evanston, IL) and QBP1-CFP by Yoshitaka Nagai (Osaka University, Osaka, Japan).

Transfections, cell culture and toxicity assay. Human embryonic kidney cells (HEK293T) and Mel JuSo fibroblasts were cultured in IMDM (GIBCO) supplemented with 10% FCS and penicillin/streptomycin/L-glutamine. The cells were transiently transfected with Fugene6 (Roche) and analyzed at indicated time-points after transfection. Mouse ST*Hdh*$^{+/+}$(Q7) cells (kindly provided by Marcy MacDonald) (Trettel et al., 2000) and N2A neuroblastoma cells were cultured in DMEM

supplemented with 10% FCS and penicillin/streptomycin/L-glutamine. Neuronal cells were transiently transfected with Lipofectamine 2000 (Invitrogen). Mouse ST*Hdh*$^{+/+}$(Q7) cells were incubated at 32°C. For toxicity measurements, N2A cells were analyzed by FACS LSRII for GFP fluorescence 24 or 48 hours after transfection, and the percentage of GFP-positive cells was quantified.

Western blot. Cytosolic extracts were generated by lysing cells with 0.1% Triton X-100 for 30 minutes one ice, and the supernatant was used after spinning down the lysate. 20 µg of cytosolic protein lysates were separated by 18% SDS-PAGE and transferred to Protan nitrocellulose membranes. Membranes were blocked in 5% dry milk in TBS containing 0.3% tween and probed with 1:1000 anti-GFP (Molecular Probes, UK), 1:100 anti-Ub (Sigma, USA) or the anti-Polyglutamine 1C2 (MAB1574, Millipore, USA). Polyclonal Horseradish Peroxidase (HRP) conjugated secondary antibodies, anti-rabbit (Sigma, USA) or anti-mouse (DAKO, Denmark) were used 1:10.000 to detect the primary antibodies via Lumi-light-PLUS westernblotting substrate (Roche, USA). Preparation of SDS-soluble and SDS–insoluble protein fractions was described before (Carra et al., 2008). Briefly, cells were trypsinized, homogenized, and heated for 10 min at 99°C in sample buffer (70 mM Tris pH 6.8, 1.5% SDS, 20% glycerol) supplemented with 50 mM DTT 72 hours after transfection. Cell lysates were centrifuged for at least 30 minutes at 14.000 rpm at room temperature. Supernatants were used as SDS-soluble fraction to which 0.05% bromophenol blue was added. Pellets represented SDS-insoluble fractions and were dissolved in 100% formic acid, incubated 30 minutes at 37°C, lyophilized overnight in a speed vac (Eppendorf), and resuspended in a 1/4th of the volume of sample buffer containing 0.05% bromophenol blue. Samples were separated on either 18% SDS-PAGE (anti-polyQ), or 12.5% SDS-PAGE (anti-GFP) and further treated as Western blots.

Fluorescence, confocal and electron microscopy. HEK293T cells were transfected with the indicated constructs and the percentages of aggregates were scored using an inverted fluorescence microscope (Leica DMR). For imaging, Mel Juso cells were transiently transfected with the indicated constructs and images were obtained using a confocal microscope (Leica SP2) using a 63x objective. Note that some pictures show 'over-exposed' fluorescent aggregates in order to visualize non-sequestered, cytoplasmic staining. For immunostaining, Mel Juso cells were fixed with 4% paraformaldehyde and permeabilized using 0.1% triton in PBS containing 1% FCS and stained with the primary antibodies 1C2 or MW1 (Ko et al., 2001) (1:1000), followed by goat anti-mouse Cy3 labeling (Jackson ImmunoResearch Laboratories). The MW1 antibody developed by Ko, Ou and Patterson was obtained from the Developmental Studies Hybridoma Bank under the auspices of the NICHD and maintained by the University of Iowa. For endogenous Hsp70 labeling, Mel Juso cells were stained against Hsp70/Hsc70 (Calbiochem, 1:200) followed by anti-mouse AlexaFluor 633 (Invitrogen). For electron microscopy, Mel Juso cells were embedded *in situ*. Preceding fixation, cells were washed briefly in 20 mM PBS (pH 7.4). Fixation was done in a mixture of 4% paraformaldehyde, 1% glutaraldehyde in 0.1 M Phosphate Buffer (pH 7.4) for 60 minutes. After fixation cells were washed in distilled water, osmicated for 60 minutes in 1% OsO4 in water, washed again in distilled water, dehydrated through a series of ethanol baths and embedded in LX-112. After polymerization the plastic was removed and small parts of the epon block containing the cells were prepared for ultra-thin sectioning. Ultra-thin sections were cut, collected on formvar coated grids and stained with uranyl acetate and lead citrate. Sections were examined with a Philips EM-420 electron microscope.

Filter retardation assay. Filter retardation assay was performed as described before (Wanker et al., 1999). Briefly, 72 hours after transfection, HEK293T cells were lysed for 30 minutes on ice in Nondinet P-40 (NP-40) buffer (100 mM TrisHCl, pH 7.5, 300 mM NaCl, 2% NP-40, 10 mM EDTA, pH 8.0, supplemented with complete mini protease inhibitor cocktail (Roche) and phosphatase inhibitor cocktail (Sigma). After centrifugation 15 minutes at 14.000 rpm at 4°C, cell pellets were re-

suspended in benzonase buffer (1 mM MgCl2, 50 mM Tris-HCl; pH 8.0) and incubated for 1 hour at 37°C with 250U benzonase (Merck). Reactions were stopped by adding 2x termination buffer (40 mM EDTA, 4% SDS, 100 mM DTT). Aliquots of 30 µg protein extract were diluted into 2% SDS buffer (2% SDS, 150 mM NaCl, 10 mM Tris pH 8.0) and filtered through a 2 µm cellulose acetate membrane (Schleicher and Schuell) pre-equilibrated in 2% SDS buffer. Filters were washed twice with 0.1% SDS buffer (0.1% SDS, 150 mM NaCl, 10 mM Tris pH 8.0) and subsequently blocked in 5% nonfat milk (Protifar Plus, Nutricia) in TBS. Captured aggregates were detected by incubation with 1C2 antibody and further treated like western blots. Alternatively, GFP fluorescence of trapped aggregates was analysed by LAS3000.

Acknowledgements

We would like to thank Silvia Coolen and Suzanne van der Horst for assisting experiments, and Derk Amsen, Jacob Aten, Ron van Noorden, Sean Diehl and Dineke Verbeek for carefully reading the manuscript. This study was funded by a grant from the Hereditary Disease Foundation, a VENI grant from NWO-ZonMW, a grant from the Hersenstichting and the Dutch Cancer Foundation KWF.

Supplementary Figures

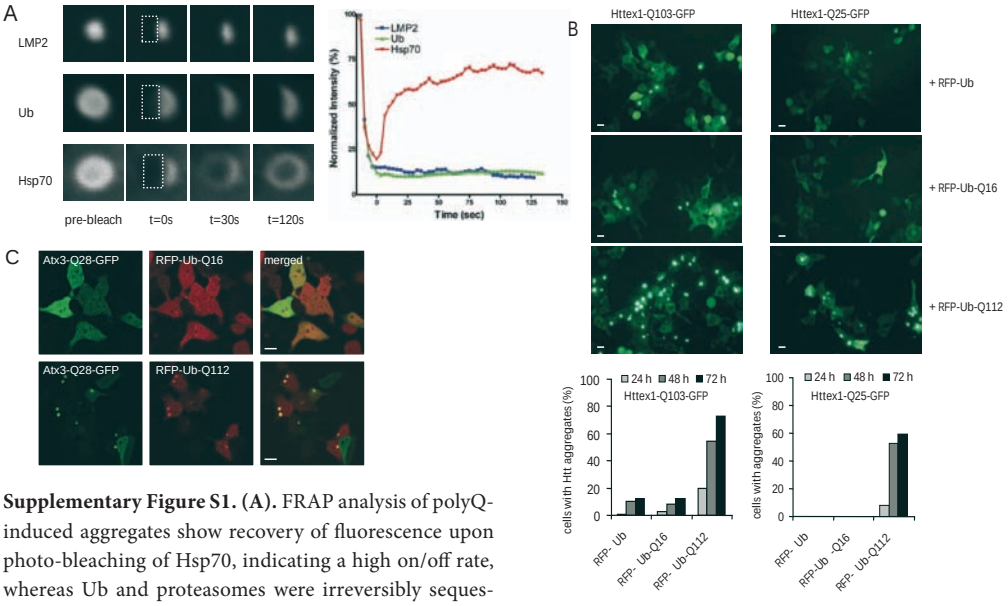

Supplementary Figure S1. (A). FRAP analysis of polyQ-induced aggregates show recovery of fluorescence upon photo-bleaching of Hsp70, indicating a high on/off rate, whereas Ub and proteasomes were irreversibly sequestered. **(B).** The rate of aggregation of httex1-Q103-GFP was enhanced when co-expressed with RFP-Ub-Q112 (left panel). While httex1-Q25-GFP was freely distributed in cells co-expressing RFP-Ub or RFP-Ub-Q16, httex1-Q25-GFP was redistributed to aggregates initiated by RFP-Ub-Q112 (right panel). A representative graph shows the percentage of cells containing huntingtin-positive aggregates at three time points after transfection. **(C).** Ataxin3-Q28-GFP distribution was affected by the presence of polyQ peptide aggregates, leading to sequestering into aggregates induced by RFP-Ub-Q112. Scalebar ~5 µm.

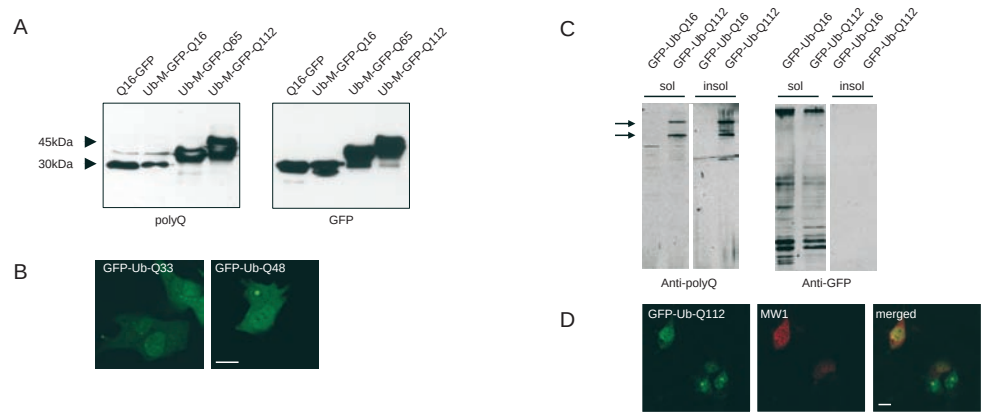

Supplementary Figure S2. **(A)**. The anti-polyQ antibody 1C2 recognized both short (Q16-GFP and GFP-Q16) and expanded (GFP-Q65 and GFP-Q112) polyQ tracts fused to GFP with almost equal efficiencies. **(B).** The expression of GFP-Ub-Q33 did not induce aggregates, but expression of GFP-Ub-Q48 led to aggregate formation in a low percentage of cells after 72 hours of transfection. **(C).** PolyQ peptides derived from GFP-Ub-Q112 were present in both the soluble and insoluble fraction of transfected cells, these peptides were not positive for GFP, indicating efficient cleavage of GFP-UB-Q112. **(D).** Cells transfected with GFP-Ub-Q112 showed only immunostaining with the anti-polyQ antibody MW1 when aggregates were not present, similarly as observed with 1C2 antibody (Fig. 1E). Scalebar ~5 µm.

References

Arrasate M and Finkbeiner S (2005) Automated microscope system for determining factors that predict neuronal fate. *Proc Natl Acad Sci USA* 102: 3840-5.

Bachmair A, Finley D and Varshavsky A (1986) *In vivo* half-life of a protein is a function of its amino-terminal residue. *Science* 234: 79-86.

Bence NF, Sampat RM and Kopito RR (2001) Impairment of the ubiquitin-proteasome system by protein aggregation. *Science* 292: 1552-5.

Bhutani N, Venkatraman P and Goldberg AL (2007) Puromycin-sensitive aminopeptidase is the major peptidase responsible for digesting polyglutamine sequences released by proteasomes during protein degradation. *Embo J* 26: 1385-96.

Busch A, Engemann S, Lurz R, Okazawa H, Lehrach H and Wanker EE (2003) Mutant huntingtin promotes the fibrillogenesis of wild-type huntingtin: a potential mechanism for loss of huntingtin function in Huntington's disease. *J Biol Chem* 278: 41452-61.

Carra S, Seguin SJ, Lambert H and Landry J (2008) HspB8 chaperone activity toward poly(Q)-containing proteins depends on its association with Bag3, a stimulator of macroautophagy. *J Biol Chem* 283: 1437-44.

Cooper JK, Schilling G, Peters MF, Herring WJ, Sharp AH, Kaminsky Z, Masone J, Khan FA, Delanoy M, Borchelt DR et al. (1998) Truncated N-terminal fragments of huntingtin with expanded glutamine repeats form nuclear and cytoplasmic aggregates in cell culture. *Hum Mol Genet* 7: 783-90.

Dantuma NP, Groothuis TA, Salomons FA and Neefjes J (2006) A dynamic ubiquitin equilibrium couples proteasomal activity to chromatin remodeling. *J Cell Biol* 173: 19-26.

DiFiglia M, Sapp E, Chase KO, Davies SW, Bates GP, Vonsattel JP and Aronin N (1997) Aggregation of huntingtin in neuronal intranuclear inclusions and dystrophic neurites in brain. *Science* 277: 1990-3.

Gafni J, Hermel E, Young JE, Wellington CL, Hayden MR and Ellerby LM (2004) Inhibition of calpain cleavage of huntingtin reduces toxicity: accumulation of calpain/caspase fragments in the nucleus. *J Biol Chem* 279: 20211-20.

Goldberg YP, Nicholson DW, Rasper DM, Kalchman MA, Koide HB, Graham RK, Bromm M, Kazemi-Esfarjani P, Thornberry NA, Vaillancourt JP et al. (1996) Cleavage of huntingtin by apopain, a proapoptotic cysteine protease, is modulated by the polyglutamine tract. *Nat Genet* 13, 442-9.

Goti D, Katzen SM, Mez J, Kurtis N, Kiluk J, Ben-Haiem L, Jenkins NA, Copeland NG, Kakizuka A, Sharp AH et al. (2004) A mutant ataxin-3 putative-cleavage fragment in brains of Machado-Joseph disease patients and transgenic mice is cytotoxic above a critical concentration. *J Neurosci* 24: 10266-79.

Graham RK, Deng Y, Slow EJ, Haigh B, Bissada N, Lu G, Pearson J, Shehadeh J, Bertram L, Murphy Z et al. (2006) Cleavage at the caspase-6 site is required for neuronal dysfunction and degeneration due to mutant huntingtin. *Cell* 125: 1179-91.

Haacke A, Broadley SA, Boteva R, Tzvetkov N, Hartl FU and Breuer P (2006) Proteolytic cleavage of polyglutamine-expanded ataxin-3 is critical for aggregation and sequestration of non-expanded ataxin-3. *Hum Mol Genet* 15: 555-68.

Holmberg CI, Staniszewski KE, Mensah KN, Matouschek A and Morimoto RI (2004) Inefficient degradation of truncated polyglutamine proteins by the proteasome. *Embo J* 23: 4307-18.

Ikeda H, Yamaguchi M, Sugai S, Aze Y, Narumiya S and Kakizuka A (1996) Expanded polyglutamine in the Machado-Joseph disease protein induces cell death *in vitro* and *in vivo*. *Nat Genet* 13: 196-202.

Ikeda Y, Daughters RS and Ranum LP (2008) Bidirectional expression of the SCA8 expansion mutation: One mutation, two genes. *Cerebellum* 7: 150-8.

Jana NR, Dikshit P, Goswami A, Kotliarova S, Murata S, Tanaka K and Nukina N (2005) Co-chaperone CHIP associates with expanded polyglutamine protein and promotes their degradation by proteasomes. *J Biol Chem* 280: 11635-40.

Johnson ES, Ma PC, Ota IM and Varshavsky A (1995) A proteolytic pathway that recognizes ubiquitin as a degradation signal. *J Biol Chem* 270: 17442-56.

Kaytor MD, Wilkinson KD and Warren ST (2004) Modulating huntingtin half-life alters polyglutamine-dependent aggregate formation and cell toxicity. *J Neurochem* 89: 962-73.

Kim S, Nollen EA, Kitagawa K, Bindokas VP and Morimoto RI (2002) Polyglutamine protein aggregates are dynamic. *Nat Cell Biol* 4: 826-31.

Ko J, Ou S and Patterson PH (2001) New anti-huntingtin monoclonal antibodies: implications for huntingtin

conformation and its binding proteins. *Brain Res Bull* 56: 319-29.

Li M, Miwa S, Kobayashi Y, Merry DE, Yamamoto M, Tanaka F, Doyu M, Hashizume Y, Fischbeck KH and Sobue G (1998) Nuclear inclusions of the androgen receptor protein in spinal and bulbar muscular atrophy. *Ann Neurol* 44: 249-54.

Li P, Huey-Tubman KE, Gao T, Li X, West AP Jr, Bennett MJ and Bjorkman PJ (2007) The structure of a polyQ-anti-polyQ complex reveals binding according to a linear lattice model. *Nat Struct Mol Biol* 14: 381-7.

Lunkes A, Lindenberg KS, Ben-Haiem L, Weber C, Devys D, Landwehrmeyer GB, Mandel JL and Trottier Y (2002) Proteases acting on mutant huntingtin generate cleaved products that differentially build up cytoplasmic and nuclear inclusions. *Mol Cell* 10: 259-69.

Marsh JL, Walker H, Theisen H, Zhu YZ, Fielder T, Purcell J and Thompson LM (2000) Expanded polyglutamine peptides alone are intrinsically cytotoxic and cause neurodegeneration in Drosophila. *Hum Mol Genet* 9: 13-25.

Matsumoto G, Kim S and Morimoto RI (2006) Huntingtin and mutant SOD1 form aggregate structures with distinct molecular properties in human cells. *J Biol Chem* 281: 4477-85.

Merry DE, Kobayashi Y, Bailey CK, Taye AA and Fischbeck KH (1998) Cleavage, aggregation and toxicity of the expanded androgen receptor in spinal and bulbar muscular atrophy. *Hum Mol Genet* 7: 693-701.

Michalik A and Van Broeckhoven C (2004) Proteasome degrades soluble expanded polyglutamine completely and efficiently. *Neurobiol Dis* 16: 202-11.

Nagai Y, Tucker T, Ren H, Kenan DJ, Henderson BS, Keene JD, Strittmatter WJ and Burke JR (2000) Inhibition of polyglutamine protein aggregation and cell death by novel peptides identified by phage display screening. *J Biol Chem* 275: 10437-42.

Orr HT and Zoghbi HY (2007) Trinucleotide repeat disorders. *Annu Rev Neurosci* 30: 575-621.

Perez MK, Paulson HL, Pendse SJ, Saionz SJ, Bonini NM and Pittman RN (1998) Recruitment and the role of nuclear localization in polyglutamine-mediated aggregation. *J Cell Biol* 143: 1457-70.

Pratt G and Rechsteiner M (2008) Proteasomes cleave at multiple sites within polyglutamine tracts: activation by PA28gamma(K188E). *J Biol Chem* 283: 12919-25.

Qian SB, Ott DE, Schubert U, Bennink JR and Yewdell JW (2002) Fusion proteins with COOH-terminal ubiquitin are stable and maintain dual functionality *in vivo*. *J Biol Chem* 277: 38818-26.

Qin ZH, Wang Y, Sapp E, Cuiffo B, Wanker E, Hayden MR, Kegel KB, Aronin N and DiFiglia M (2004) Huntingtin bodies sequester vesicle-associated proteins by a polyproline-dependent interaction. *J Neurosci* 24: 269-81.

Reits EA, Benham AM, Plougastel B, Neefjes J and Trowsdale J (1997) Dynamics of proteasome distribution in living cells. *Embo J* 16: 6087-94.

Reits EA and Neefjes JJ (2001) From fixed to FRAP: measuring protein mobility and activity in living cells. *Nat Cell Biol* 3: E145-7.

Schmidt T, Landwehrmeyer GB, Schmitt I, Trottier Y, Auburger G, Laccone F, Klockgether T, Volpel M, Epplen JT, Schols L et al. (1998) An isoform of ataxin-3 accumulates in the nucleus of neuronal cells in affected brain regions of SCA3 patients. *Brain Pathol* 8: 669-79.

Servadio A, Koshy B, Armstrong D, Antalffy B, Orr HT and Zoghbi HY (1995) Expression analysis of the ataxin-1 protein in tissues from normal and spinocerebellar ataxia type 1 individuals. *Nat Genet* 10, 94-8.

Trettel F, Rigamonti D, Hilditch-Maguire P, Wheeler VC, Sharp AH, Persichetti F, Cattaneo E and MacDonald ME (2000) Dominant phenotypes produced by the HD mutation in STHdh(Q111) striatal cells. *Hum Mol Genet* 9: 2799-809.

Trottier Y, Lutz Y, Stevanin G, Imbert G, Devys D, Cancel G, Saudou F, Weber C, David G, Tora L et al. (1995) Polyglutamine expansion as a pathological epitope in Huntington's disease and four dominant cerebellar ataxias. *Nature* 378: 403-6.

Venkatraman P, Wetzel R, Tanaka M, Nukina N and Goldberg AL (2004) Eukaryotic proteasomes cannot digest polyglutamine sequences and release them during degradation of polyglutamine-containing proteins. *Mol Cell* 14: 95-104.

Verhoef LG, Lindsten K, Masucci MG and Dantuma NP (2002) Aggregate formation inhibits proteasomal degradation of polyglutamine proteins. *Hum Mol Genet* 11: 2689-700.

Wanker EE, Scherzinger E, Heiser V, Sittler A, Eickhoff

H and Lehrach H (1999) Membrane filter assay for detection of amyloid-like polyglutamine-containing protein aggregates. *Methods Enzymol* 309: 375-86.

Wellington CL, Ellerby LM, Hackam AS, Margolis RL, Trifiro MA, Singaraja R, McCutcheon K, Salvesen GS, Propp SS, Bromm M et al. (1998) Caspase cleavage of gene products associated with triplet expansion disorders generates truncated fragments containing the polyglutamine tract. *J Biol Chem* 273: 9158-67.

Yang W, Dunlap JR, Andrews RB and Wetzel R (2002) Aggregated polyglutamine peptides delivered to nuclei are toxic to mammalian cells. *Hum Mol Genet* 11: 2905-17.

Young JE, Gouw L, Propp S, Sopher BL, Taylor J, Lin A, Hermel E, Logvinova A, Chen SF, Chen S et al. (2007) Proteolytic cleavage of ataxin-7 by caspase-7 modulates cellular toxicity and transcriptional dysregulation. *J Biol Chem* 282: 30150-60.

Chapter 7

Summary / Samenvatting

Summary

Spinocerebellar ataxia type 1 (SCA1) is a neurodegenerative disorder that is caused by a polyglutamine (polyQ) expansion mutation in the protein ataxin-1 of which the functions are largely unknown. The cerebellum is the brain area that is mainly affected with specific loss of the Purkinje cells. Besides SCA1, there are 28 other SCA diseases that have similar clinical and pathological symptoms but are caused by mutations in other seemingly unrelated genes. To understand the biology of SCA1 disease, it is important to unravel the functions of ataxin-1. In the present thesis, we addressed this issue by analyzing ataxin-1 behavior with the use of various visualization techniques in combination with biochemical methods.

As described in Chapter 2, the so-called ataxin-1 polyQ aggregates, initiated when ataxin-1 is overexpressed, appear to be dynamic instead of insoluble aggregates. Since the dynamic structures are induced by both wildtype and mutant ataxin-1, we redefine them as nuclear bodies that may represent functional protein complexes. These nuclear bodies have been found in cells in culture but also *in vivo* in mouse tissues and particularly in cerebellum, and disappear when transcription is blocked, linking ataxin-1 nuclear body formation to ongoing transcription. Instead of slowing down ataxin-1 dynamics, the polyQ expansion mutation increases the dynamics of ataxin-1.

As polyQ expansion did not lead to ataxin-1 sequestration into aggregates, we examined whether the expansion led to altered interactions in localization or dynamics of proteins known to interact with ataxin-1 in a polyQ length-dependent manner. In Chapter 3, we describe that the nuclear proteins LANP, PQBP-1 and RBM17, that were earlier described to interact with ataxin-1, do not colocalize in ataxin-1 nuclear bodies. As the dynamics of these proteins are not affected by mutant ataxin-1, the interaction between ataxin-1 and these proteins does not take place in nuclear bodies, but possibly in the nucleoplasm or cytoplasm without affecting their intracellular dynamics.

To search for a link between the different SCA-related proteins, we next focused on two SCA disorders, SCA1 and SCA14. SCA14 is caused by a missense mutation in the protein PKCγ. In Chapter 4, we describe that PKCγ interacts with ataxin-1 and that the phosphorylation status of ataxin-1 is increased by PKCγ, indicating that PKCγ can also directly phosphorylate ataxin-1 via this interaction. Moreover, PKCγ increases the dynamics of ataxin-1 nuclear bodies. As polyQ expansion of ataxin-1 also affects the localization and autophosphorylation levels of wildtype PKCγ, these data suggest that there is a common underlying mechanism of SCA1 and SCA14 explaining similar symptoms of these two SCAs that are caused by two different mutations.

Although the exact function of ataxin-1 is unknown, there are indications that it is involved in particular stages of transcription and/or translation, such as transcription regulation, mRNA nuclear export, mRNA stability and splicing. Whereas most neurons have ataxin-1 localization restricted to the nucleus, Purkinje cells in the cerebellum have ataxin-1 located in both the nuclear and cytoplasmic compartments. As Purkinje cells are also primarily struck by SCA, we discuss in Chapter 5 how this apparent difference in localizations may play a role in the development of SCA1.

Since all polyQ proteins are finally degraded by proteases like the proteasome, we studied in Chapter 6 whether protea-

some-generated polyQ fragments can initiate aggregation. We show that only expanded polyQ peptide, without the original protein context, are sufficient to cause aggregation and toxicity. These aggregates sequester heat-shock proteins, proteasomal subunits and ubiquitin resembling the aggregation of other polyQ-expanded proteins such as huntingtin involved in Huntington's disease.

In summary, the ataxin-1 protein does not behave like other polyglutamine proteins, and we suggest that aggregation is not the primary cause of SCA1 disease. More likely, the mutant ataxin-1 protein participates in multiple pathways that include other SCA-related proteins including the SCA14-related protein, PKCγ. This suggests that there is an underlying pathway that interconnects the proteins involved in the 29 different SCAs. Since Purkinje cells in the cerebellum are the major cell type that is affected by SCAs and the only cell type that has ataxin-1 expression in the cytoplasm, identification of the functions of cytoplasmic ataxin-1 may provide novel insights of SCA1 disease.

Samenvatting

Spinocerebellaire ataxie type 1 (SCA1) is een neurodegeneratieve ziekte, die wordt veroorzaakt door een verlenging van een reeks glutamine (Q) aminozuren in het ziekte-gerelateerde eiwit ataxine-1, een eiwit waarvan de functie grotendeels onbekend is. Bij gezonde personen is deze reeks maximaal 40 glutamines, terwijl SCA1 patiënten een langere reeks glutamines hebben. Deze lange reeks glutamines wordt aangeduid met polyQ, en leidt bij de meeste polyQ ziektes zoals de ziekte van Huntington tot eiwit aggregatie. In deze neurodegeneratieve ziekte is voornamelijk het cerebellum aangetast. Dit uit zich vooral in een specifiek verlies van de Purkinje cellen. Deze neuronen zijn van essentieel belang voor een belangrijke functie van het cerebellum, namelijk de motorcoördinatie. Naast SCA1 zijn er nog 28 andere SCA-ziektes, die klinische en pathologische symptomen hebben die lijken op SCA1. Deze ziekten worden echter veroorzaakt door mutaties in andere, ogenschijnlijk niet-gerelateerde eiwitten. Om de biologie van de ziekte SCA1 beter te kunnen begrijpen, is het belangrijk om de normale functie van ataxine-1 te ontrafelen, en hoe ataxine-1 mogelijk interacteert met eiwitten gemuteerd in andere SCA-ziektes. In dit proefschrift hebben wij dit gedaan door het analyseren van het gedrag van ataxine-1 met behulp van verschillende visualisatietechnieken in zowel levende cellen als in hersenweefsel, in combinatie met biochemische methoden.

In Hoofdstuk 2 beschrijven wij dat de zo genoemde ataxine-1 polyQ-aggregaten, die worden geïnitieerd door de (over)expressie van ataxin-1, juist dynamische structuren blijken te zijn in plaats van onoplosbare aggregaten. Omdat deze dynamische structuren worden geïnduceerd door zowel gezond, wildtype maar ook mutant polyQ ataxine-1, herdefiniëren wij ze als "nuclear bodies". Deze structuren representeren waarschijnlijk functionele eiwitcomplexen. De "nuclear bodies" zijn gevonden in gekweekte cellen maar ook *in vivo* in hersenen van muizen, in het bijzonder in het cerebellum. Deze "nuclear bodies" verdwijnen wanneer het transcriptieproces geblokkeerd wordt. Dit duidt op een verband tussen het ontstaan van deze "nuclear bodies" en het proces van transcriptie. In plaats van de verwachte vermindering van de dynamiek van de ataxine-1 eiwitten bij SCA1, zorgt de polyQ expansie er juist voor dat de dynamiek van ataxine-1 toeneemt wat vervolgens effect kan hebben op DNA transcriptie.

Aangezien een polyQ expansie niet leidt tot de vorming van aggregaten, hebben wij vervolgens bestudeerd of de expansiemutatie een veranderde interactie of dynamiek tot gevolg heeft van eiwitten, die met ataxine-1 interacteren op een polyQ-afhankelijke manier. In Hoofdstuk 3 beschrijven wij dat de kerneiwitten LANP, PQBP-1 en RBM17, waarvan al eerder beschreven is dat ze interacteren met ataxine-1, niet colocaliseren in de ataxine-1 "nuclear bodies". Ook de dynamiek van deze eiwitten in de kern, of hun transport tussen kern en cytoplasma, is niet veranderd door de aanwezigheid van mutant ataxine-1. Onze resultaten laten zien dat deze kerneiwitten niet interacteren met ataxine-1 in de "nuclear bodies", maar dit waarschijnlijk doen in het nucleoplasma of mogelijk zelfs in het cytoplasma. De polyQ expansie van ataxine-1 heeft echter geen invloed op de intracellulaire dynamiek van de bestudeerde interacterende eiwitten.

Om een link te vinden tussen de verschillende SCA-gerelateerde eiwitten, hebben wij in onze volgende studie de aandacht gericht op SCA1 en SCA14. SCA14 wordt

veroorzaakt door een mutatie in het eiwit PKCγ. In Hoofdstuk 4 beschrijven wij dat PKCγ met ataxine-1 kan interacteren en dat de fosforylering van ataxine-1 toeneemt als PKCγ aanwezig is. Dit wijst erop dat PKCγ direct het ataxine-1 kan fosforyleren door een interactie aan te gaan met ataxine-1. Bovendien zorgt PKCγ voor een verhoogde dynamiek van de ataxine-1 bevattende "nuclear bodies". Omgekeerd veroorzaakt polyQ ataxine-1 een veranderde lokalisatie en (auto)fosforylatie van het wildtype PKCγ. Kennelijk beïnvloedt in SCA1 patiënten het gemuteerde ataxin-1 het gezonde PKCγ, en in SCA14 patiënten het gemuteerde PKCγ het gezonde ataxine-1, duidend op een gemeenschappelijk onderliggend mechanisme. Deze interactie is een mogelijke verklaring voor de soortgelijke klinische symptomen van deze twee neurodegeneratieve ziektes, die worden veroorzaakt door mutaties in verschillende genen.

Ondanks dat de exacte functie van het ataxine-1 niet bekend is, zijn er verschillende indicaties dat ataxine-1 betrokken is bij bepaalde stappen in het transcriptie- en/of translatieproces, zoals de regulatie van transcriptie, de export van mRNA vanuit de kern naar het cytoplasma, de stabiliteit en de "splicing" van het RNA. Terwijl ataxine-1 in de meeste neuronen met name in de kern tot expressie komt, bevindt ataxine-1 zich in Purkinje cellen zowel in de kern als in het cytoplasma. De cytoplasmatische localisatie is mogelijk een reden, waarom juist de Purkinje cellen het meest zijn aangetast in SCA. In Hoofdstuk 2 laten we zien dat, in tegenstelling tot wat werd verondersteld, de polyQ expansie niet verhindert dat ataxine-1 de kern kan verlaten. Deze bevinding ondersteunt ook onze hypothese dat juist het cytoplasmatische polyQ ataxine-1 belangrijk is voor het ontstaan van SCA1. Het belang van de exacte intracellulaire ataxine-1 lokalisatie en hoe dat een rol kan spelen in het ontwikkelen van SCA1 bediscussiëren we in Hoofdstuk 5.

Omdat alle eiwitten inclusief polyQ eiwitten uiteindelijk worden afgebroken door proteases, zoals het proteasoom, bestudeerden wij in Hoofdstuk 6 of juist de polyQ fragmenten die door het proteasoom zijn gegenereerd aggregatie kunnen veroorzaken. Hier laten wij zien dat een polyQ peptide langer dan 40 glutamines, dus zonder eiwitcontext, voldoende is om aggregatie en toxiciteit te veroorzaken. Deze aggregaten trekken ook heatshock eiwitten, proteasomale eiwitten en ubiquitine aan. Daarmee zijn deze aggregaten vergelijkbaar met die van andere eiwitten met een polyQ expansie, en mogelijk de initiators van aggregatie bij verschillende polyQ ziektes.

Zoals beschreven in dit proefschrift gedraagt het ataxine-1 eiwit zich niet zoals andere polyglutamine-eiwitten en onze data laten zien dat aggregatie niet de primaire oorzaak is van SCA1. Meer aannemelijk is het dat mutant ataxine-1 participeert in meerdere cellulaire signaleringsroutes, waarin ook andere SCA-gerelateerde eiwitten een rol kunnen spelen, zoals het SCA14 eiwit PKCγ. Dit suggereert dat er een onderliggend mechanisme kan zijn, dat de mutante eiwitten, betrokken bij de 29 verschillende SCAs, verbindt. Omdat de Purkinje cellen in het cerebellum het meest zijn aangetast in SCA-patiënten, en het de enige neuronen zijn die ataxine-1 tot expressie brengen in het cytoplasma, zouden inzichten in de functies van cytoplasmatisch ataxine-1 kunnen leiden tot nieuwe inzichten in de ziekte SCA1.

Dankwoord/Acknowledgments

Graag wil ik de volgende mensen bedanken die hebben bijgedragen aan het tot stand komen van mijn proefschrift:

Beste Ron, jij bent tijdens mijn promotie mijn achtervang en houvast geweest. Als ik het niet meer zag zitten dan stond jij voor mij klaar niet alleen als promotor maar ook als mens. Deze manier van samenwerken heb ik als heel prettig ervaren. Het vertrouwen dat jij in mij had was een motivatie om door te gaan. Mijn dank hiervoor.

Beste Eric, mijn onderzoek is niet verlopen zoals wij beiden hadden gehoopt. Ik heb hier heel veel van geleerd en wil je bedanken voor de vrijheid die je mij als begeleider hebt gegeven om mijn eigen pad te bewandelen.

Beste Elly, jouw kritische vragen en doelgerichtheid hebben mij geholpen om meer focus te krijgen tijdens mijn project en vooruit te komen. Ik vond het heel fijn om met jou samen te werken.

Lieve Dineke, jij hebt voor een hoop inhoudelijke en praktische feedback gezorgd toen je bij ons in de groep kwam werken. Je was eigenlijk een beetje mijn dagelijkse coach op het werk. De ervaring die jij al had opgedaan als beginnende post-doc was precies wat ik op dat moment nodig had. Bovendien wist jij een hoop over SCA en daar heb ik veel uit kunnen putten. Ik vond het erg leuk om met jouw samen het SCA1-SCA14 project te doen. Daarin kwamen onze beide interesses samen.

Lieve Judith, wat hebben wij een hoop ervaring van onze projecten met elkaar gedeeld. Teleurstellingen werden afgewisseld met euforische momenten. Wij hebben elkaar steeds gemotiveerd om door te gaan, van elkaar te leren en tot het einde toe vol te houden. Het contact met jou heb ik als heel open ervaren. Nooit was er competitie maar juist een sterk gevoel van samenwerken.

Beste Marcel, een rode kleur das en lid van een verkeerde studentenvereniging, ik had wel wat vooroordelen. Toch is het goed gekomen tussen ons. Je bent een echte Groninger en die droge humor kan ik als Fries wel waarderen. Ik hoop dat je veel succes en vlotheid zult ervaren met afronden van je promotie.

Beste Przemek, heel veel dank dat je mij hebt geholpen met de lay-out van dit proefschrift. Ik zou niet weten hoe ik dat alleen had moeten doen. Dank voor al jouw hulp maar bovenal natuurlijk dank voor de prettige samenwerking met het Plos One artikel.

Dear Harry, thanks for all your support. Our meeting at Cold Spring Harbor laboratories was at exactly the right moment. The collaboration with you has been my biggest source of inspiration. Many thanks.

Beste Klazien, dank voor al jouw ondersteuning in het lab. Je bent echt de beste in het uitvoeren van kleuringen.

Beste Hessel, enorme blije student die je bent. Dank voor de 6 maanden dat je mij hebt geholpen en ondersteund om verder te komen in mijn project.

Dear Alicia, thanks for all your support during the last few months. You made it possible for

me to do most of the writing at home.

Beste Jan Stap, dank voor het 100 keer uitleggen hoe de life cell microscoop werkt. Ik ben het nu alweer vergeten.

Beste Trees, dank voor al jouw hulp bij het afronden van mijn proefschrift.

Lieve papa en mama, jullie hebben mij geleerd het dicht bij mij zelf te houden. Afgaan op je gevoel met je verstand erbij. Dank voor al jullie coaching, advies en hulp. Jullie zijn mijn solide basis waar ik altijd een beroep op kan doen.

Lieve Bas, jij bent mij altijd blijven motiveren en inspireren en gaf mij alle ruimte om mijn promotie af te maken. Daarin heb jij veel geduld gehad, in het bijzonder de laatste maanden. 24 uur per dag heb jij altijd voor mij klaar gestaan om mij te coachen en feedback te geven.

Lieve Olivier, heerlijk klein ventje dat je bent. Jouw geboorte heeft van mij een moeder gemaakt en iets nieuws in mij opgeroepen. Jij hebt mij doen relativeren en van elke dag leren genieten. In mijn werk werd ik daardoor efficiënter omdat ik snel weer met jou wilde knuffelen. Ik hou zielsveel van jou en Bas, jullie zijn mijn allergrootste geluk, de rest is allemaal bijzaak.

Hilde